ACTA UNIVERSITATIS SZEGEDIENSIS

ACTA MINERALOGICA-PETROGRAPHICA

TOMUS XXV, FASC. 1

SZEGED, HUNGARIA
1981

ACTA UNIVERSITATIS SZEGEDIENSIS

ACTA MINERALOGICA-PETROGRAPHICA

TOMUS XXV

SZEGED, HUNGARIA
1981—1982

HU ISSN 0365 — 8066

Adjuvantibus

BÉLA MOLNÁR et TIBOR SZEDERKÉNYI

Redigit

GYULA GRASSELLY

Edit

Institutum Mineralogicum, Geochimicum et Petrographicum
Universitatis Szegediensis de Attila József nominatae
Egyetem u. 2—6., H-6722 Szeged, Hungary

Nota

Acta Miner. Petr., Szeged

Szerkeszti

GRASSELLY GYULA

a szerkesztőbizottság tagjai

MOLNÁR BÉLA és SZEDERKÉNYI TIBOR

Kiadja

a József Attila Tudományegyetem Ásványtani, Geokémiai és Kőzettani Tanszéke
H-6722 Szeged, Egyetem u. 2—6.

Kiadványunk címének röviditése

Acta Miner. Petr., Szeged

CONTENTS

ACTA UNIVERSITATIS SZEGEDIENSIS

ACTA MINERALOGICA-PETROGRAPHICA

TOMUS XXV, FASC. 1

SZEGED, HUNGARIA
1981

HU ISSN 0365 — 8066

Adjuvantibus

BÉLA MOLNÁR et TIBOR SZEDERKÉNYI

Redigit

GYULA GRASSELLY

Edit

Institutum Mineralogicum, Geochimicum et Petrographicum
Universitatis Szegediensis de Attila József nominatae
Egyetem u. 2—6., H-6722 Szeged, Hungary

Nota

Acta Miner. Petr., Szeged

Szerkeszti

GRASSELLY GYULA

a szerkesztőbizottság tagjai

MOLNÁR BÉLA és SZEDERKÉNYI TIBOR

Kiadja

a József Attila Tudományegyetem Ásványtani, Geokémiai és Kőzettani Tanszéke
H-6722 Szeged, Egyetem u. 2—6.

Kiadványunk címének rövidítése
Acta Miner. Petr., Szeged

Acta Mineralogica-Petrographica, Szeged XXV/1, 3—24, 1981

PLATE TECTONICS INTERPRETATION OF THE SOUTH TRANSDANUBIAN ULTRAMAFICS

Z. BALLA

ABSTRACT

Original rock of the South Transdanubian serpentine was oceanic harzburgite according to chemical composition. In country metamorphic rocks and granites, serpentines lie with steep tectonic contacts. They must have got in this position from above trough obduction. Consequently, these bodies wedge out downwards and do not have any „roots". Serpentines underwent multiphase and partly very strong metamorphism, and their present lizardite—chrysotile composition has been developed probably in last phases. Regional granitization seems to be connected with the obductional origin of the peridotite bodies. Accordingly, the following geological history appears to have taken place: oceanic spreading — about Silurian; island arc development through subduction — about Devonian; collision of Precambrian continent having located on the coast of former ocean, with island arc — Upper Devonian to Lower Carboniferous; postcollisional thermic—isostatic equalization („orogeny") — Lower (and Middle?) Carboniferous. The Upper Carboniferous to Lower Permian molasse is probably a product of the denudation and peneplanation after this „orogeny".

INTRODUCTION

In Southern Transdanubia ultramafics are known near Ófalu on the surface and near Helesfa and Gyód from drilling data *(Fig. 1.)*. The occurrence of serpentine near Ófalu was stated long ago (for review see: SZEDERKÉNYI [1977b]) but it has been investigated in details only through artificial section [SZEDERKÉNYI, 1977c, 1977d; GHONEIM and SZEDERKÉNYI, 1979]. Near Helesfa and Gyód, boreholes drilled by the Mecsek Ore and Mining Company for the control of geomagnetic anomalies, penetrated serpentines [BARABÁS *et al.*, 1964]; their ultramafic origin was established by the first analyses [ERDÉLYI, 1970, 1971, 1974].

1. OUTLINES OF SERPENTINE BODIES

Three South Transdanubian serpentine bodies will be discussed separately first of all on the basis of newest data.

1.1. The Ófalu serpentine body

Near Ófalu serpentine was known in outcrops of about 10×10 m on the eastern slope of Goldgrund valley *(Fig. 2.)* and was traced by geomagnetic measurements not far to the west (JANTSKY, 1979]. According to GHANEM and RAVASZ—BARANYAI [1969] and GHONEIM and SZEDERKÉNYI [1977], country rocks are represented by tuffaceous shale belonging to a volcanogenic-sedimentary sequence of intermediate-basic composition affected by metamorphism in the greenschist-facies. In the natural outcrops, the serpentine body was regarded as a sill [GHANEM and RAVASZ—BARANYAI, 1969; SZEDERKÉNYI, 1974), then as a sill or lavaflow [SZEDERKÉNYI, 1977a].

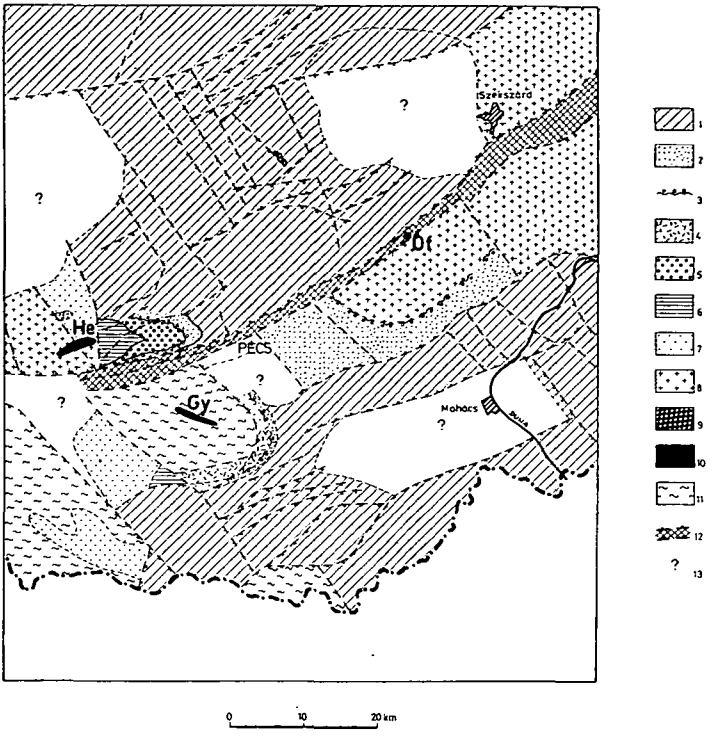

Fig. 1. Position of serpentines within the pre-Cenozoic complexes of Southern Transdanubia

Basic map: according to KASSAI, [1980], simplified

Legend:

1 — Mesozoic (simplified)
2 — Upper Permian — Lower Triassic Jakabhegy red sandstone
3 — the Jakabhegy chief conglomerate in discordant overlying
4 — Upper Permian quartz porphyry
5 — Upper Permian sandstone
6 — Lower Permian red sandstone and siltstone
7 — Upper Carboniferous sandstone
8 — granite
9 — Silurian siliceous shale
10 — serpentine: He — Helesfa, Gy — Gyód, Óf — Ófalu
11 — metamorphic rocks
12 — the Mecsekalja dislocation zone
13 — uninvestigated area

Artificial section has confirmed concordant position of the body and its thickness about 10 m but contacts have been proved to be of tectonic type *(Fig. 3)* without any traces of thermal affects [SZEDERKÉNYI, 1977c, 1977d; GHONEIM and SZEDERKÉNYI, 1979]. Metamorphism in country rocks has affected also the serpentine body manifesting in shearing of outer zones, in appearance of antigorite in the same zones and in occurrence of reaction rims on chromite grains [GHONEIM and SZEDERKÉNYI, 1979].

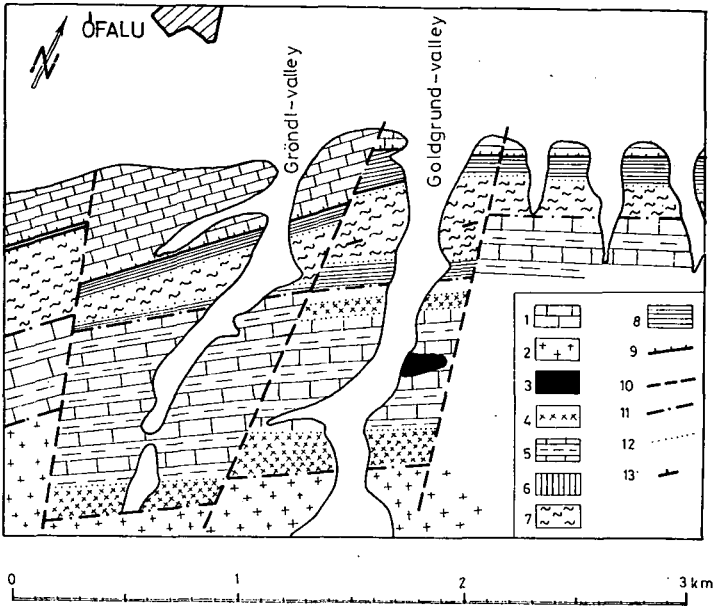

Fig. 2. Geological sketch map of the area Ófalu serpentine

Compiled by GHONEIM [1977] (see in GHONEIM and SZEDERKÉNYI, [1979])
Legend:
1 — Jurassic limestone
2 — anatectic granite
3 — serpentine and associated rocks
4 — albite porphyry
5 — marble and phyllitic tuff
6 — amphibolite
7 — mica schist
8 — andesitic basalt and its metasomatized varieties
9 — intra-Pannonian overthrusting zone
10 — fault
11 — approximate formation contact
12 — gradational contact
13 — strike and dip

1.2 The Helesfa serpentine body

Near Helesfa serpentine buried by Pannonian sediments was marked by a geomagnetic anomaly of about 5 km long *(Fig. 4)*. The anomaly pattern and two boreholes showed that serpentine was of about 600 m in thickness, of about 150/82 dipping, with sharp contacts of tectonic character and was represented by a wedge-like body in cataclastic-mylonitic granite *(Fig. 5;* see also SZEDERKÉNYI [1970*)*. The lower tectonic contact was penetrated by the borehole Helesfa—2 in 381,2—289,0 m [JANTSKY, 1979]. The bulk of serpentine minerals (lizardite and chrysotile) marks 1T metamorphism but sporadically diaspore occurs [ERDÉLYI, 19271] probably because of a later thermal effect. Talc-schists [SZEDERKÉNYI, 1976b; JANTSKY, 1979] originated from the serpentine, perhaps are related to the same effect. Serpentines are crossed by aplite-microgranite veins with traces of strong Mg metasomatism [SZEDERKÉNYI, 1970, 1974; JANTSKY, 1979].

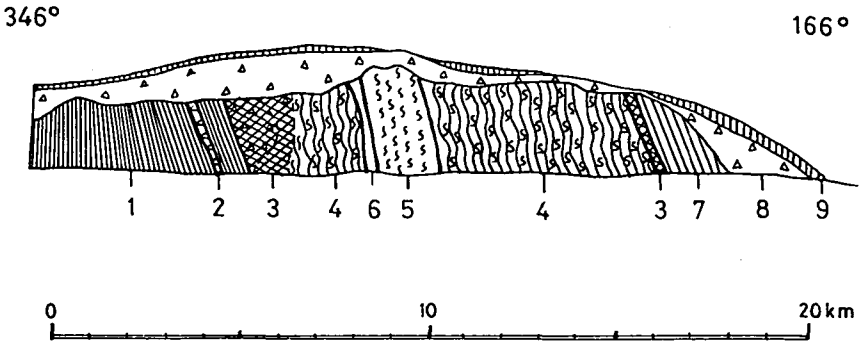

Fig. 3. Profile of the opencast Ófalu serpentine mass, compiled by GHONEIM and SZEDERKÉNYI, [1979]

Legend:
1 — serizite-phyllite
2 — serizite-phyllite breccia
3 — tectonic zone
4 — sheared serpentine
5 — massive serpentine
6 — chlorite schist
7 — siliceous shale
8 — talus
9 — loess

1.3 The Gyód serpentine body

Near Gyód serpentine buried by Pannonian sediments was marked by a geomagnetic anomaly of about 5 km long *(Fig. 6)*. This anomaly pattern and three boreholes showed that the serpentine body was of about 200 m in thickness, of about SSW 80—82° dipping in approximate concordance with the country gneiss [SZEDERKÉNYI, 1970, 1974, 1976a, 1977a]. Concerning the type of contact there are no data. *(Fig. 7)*. Clinoenstatite, secondary forsterite and diaspore occurring beside

---

Fig. 4. Geological and geophysical maps of the Helesfa serpentine body

A. Geomagnetic ΔZ-map [HAÁZ and KOMÁROMY, 1964]

Legend:
1 — scale of vertical component of the geomagnetic field
2 — boreholes on the magnetic anomaly with serial numbers

B. Geological map [BARABÁS, *et. al.* 1964]

Legend:
1 — topography of the pre-Cenozoic basement
2 — boreholes on the magnetic anomaly with serial numbers
3 — other boreholes
4—11 — rocks on the surface
4 — Lower Cretaceous diabase
5 — Middle Triassic limestone and dolomite
6 — Lower Triassic sandstone, shale, dolomite and anhydrite
7 — Upper Permian red sandstone and conglomerate
8 — Upper Permian variegated sandstone
9 — Lower Permian siltstone
10 — Lower Permian sandstone and conglomerate
11 — granite

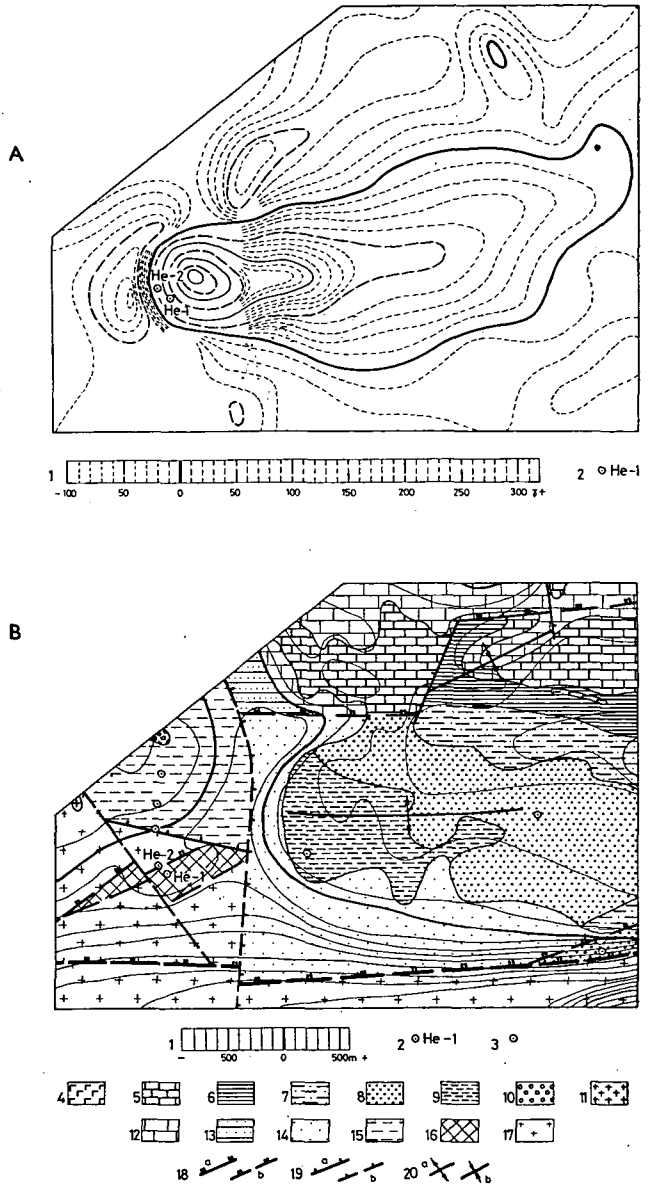

12—17 — rocks buried by Neogene sediments
12 — Middle and Upper Triassic
13 — Permian and Lower Triassic
14 — Permian
15 — Lower Permian
15 — serpentine
17 — granite
18 — reverse fault: a — on surface, b — buried
19 — normal fault: a — on surface, b — buried
20 — fold axis: a — anticlinal, b — synclinal

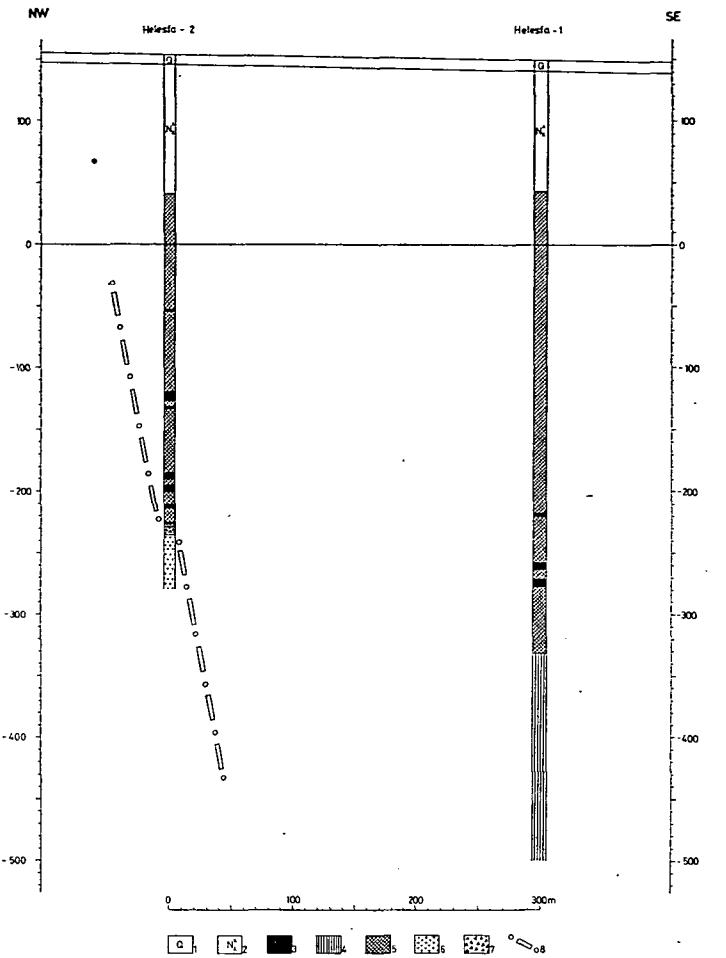

Fig. 5. Position of the Helesfa boreholes in vertical section
Source of columns: JANTSKY [1979] (simplified)
Horizontal distances: from the map scale 1:100.000 *(Fig. 4-B)*

Legend:
1 — Quaternary sediments
2 — Middle Pliocene sediments
3 — aplite-microgranite vein
4 — talc schist
5 — serpentine
6 — cataclastic-mylonitic granite
7 — tectonic breccia
8 — assumed contact of the serpentine body

the dominant lizardite and chrysotile gives evidence of a strong later thermal affect [ERDÉLYI, 1971]. Serpentines are crossed by aplite-microgranite veins with a strong Mg metasomatism [SZEDERKÉNYI, 1970, 1974; JANTSKY, 1979].

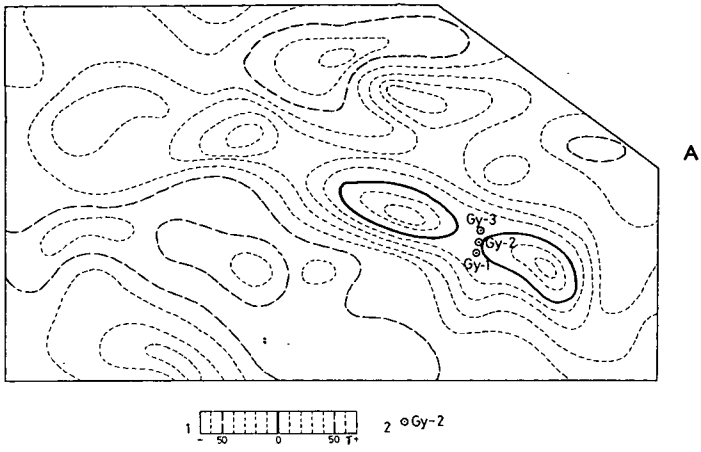

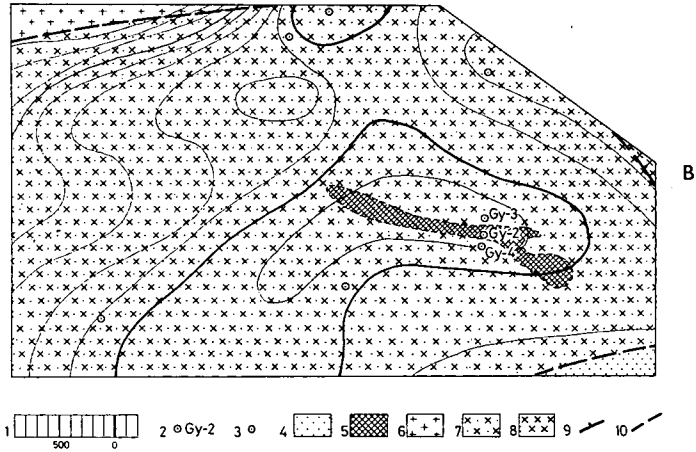

Fig. 6. Geological and geophysical maps of the Gyód serpentine body
A. Geomagnetic ΔZ-map (HAÁZ and KOMÁROMY, 1964]

Legend:
1 — scale of vertical component of the geomagnetic field
2 — boreholes on the magnetic anomaly with serial numbers

B. Geological map (BARABÁS *et. al.*, 1964]

Legend:
1 — topography of the pre-Cenozoic basement
2 — boreholes on the magnetic anomaly with serial numbers
3 — other boreholes
4 — 8 — rocks buried by Neogene sediments
4 — Permian
5 — serpentine
6 — granite
7 — metamoprhis rocks and Upper carboniferous sandstone and sericite schist
8 — metamoprhic rocks
9 — normal fault
10 — fault of unclear type

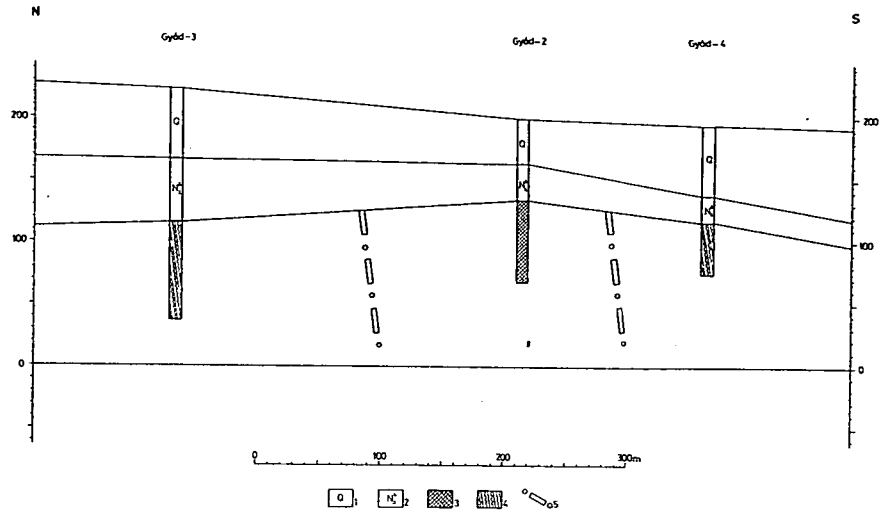

Fig. 7. Position of the Gyód boreholes in vertical section

Source of columns: JANTSKY [1979] (simplified)
Horizontal distances — from SZEDERKÉNYI [1976a] and from the map scale 1:100.000 [BARABÁS *et al.* 1964]

Legend:
1 — Quaternary sediments
2 — Middle Pliocene sediments
3 — serpentine
4 — migmatic amphibolite
5 — assumed contacts of the serpentine body

1.4 Summary

Main geological peculiarities of three serpentine bodies are practically identical. They are steep dipping sheet- or lens-like bodies with tectonic contacts concordant with the schistosity. Serpentinization took place at comparatively low temperature according to dominance of lizardite and chrysotile. Serpentine was affected by thermal influences of variegated intensity.

2. ORIGINAL ROCKS OF SERPENTINES

Original rocks of the Helesfa and the Gyód serpentine were considered by ERDÉLYI [1970, 1971] to be peridotite. According to his opinion, magnetite (5—6% of rock) originated from olivine through its serpentinization. SZEDERKÉNYI [1974, 1976a, 1977a] qualified the same rocks to be pyroxenite on the basis of their characteristic "mush" structure and of occurrence of clinoenstatite in the Gyód serpentine. Later he considered original rock of the Ófalu serpentine with the same "mush" structure to be peridotite [GHONEIM and SZEDERKÉNYI, 1979], therefore structural criteria seem to be uncertain. According to ERDÉLYI [1971], clinoenstatite occurs on the cleavage planes and is originated only through a strong thermal influence. According to DEER *et al.* [1963], clinoenstatite does not occur in rocks. According to DOBRETSOV *et al.* [1980], clinoenstatite is known from two points on the whole Earth

(Papua and Mariana) and in specific rocks (marianites) only. Therefore clinoenstatite is not a suitable basis for the diagnostic of pyroxenites and ERDÉLYI' s opinion on the peridotite origin of the Helesfa and Gyód serpentines seems to be more convictive. On the basis of the petrochemistry and the Ni—Cr contents, GHONEIM and SZEDERKÉNYI [1979] considered original rock of the Ófalu serpentine to be Alpine type peridotite with MgO/SiO_2 ratio near to that in lherzolites.

Several investigations including statistic evaluation of 3500 ultramafic analyses from 160 regions of the Earth [ABRAMOVICH and KLUSHIN, 1978] show that chemical composition of dunites and peridotites remains statistically unchanged during serpentinization except for increase of the water content and the Fe_2O_3/FeO ratio. Therefore serpentine analyses calculated on the water-free basis are expected to reflect composition of the original ultramafics realistically. The South Transdanubian serpentines, however, contain CO_2 beside H_2O, in the largest amount near Ófalu (Table 1). Relationship between the CO_2 and other rock-components has been examined in the Ófalu serpentine. Good correlation occurs with the SiO_2, MgO and CaO contents *(Fig. 8)*. On the plots SiO_2 against CO_2 and MgO *versus* CO_2, two groups with independent correlations are delineated. Differences in the CaO—CO_2 correlation between these two groups are insignificant (Table 2). Other components do not show any coherence with the CO_2.

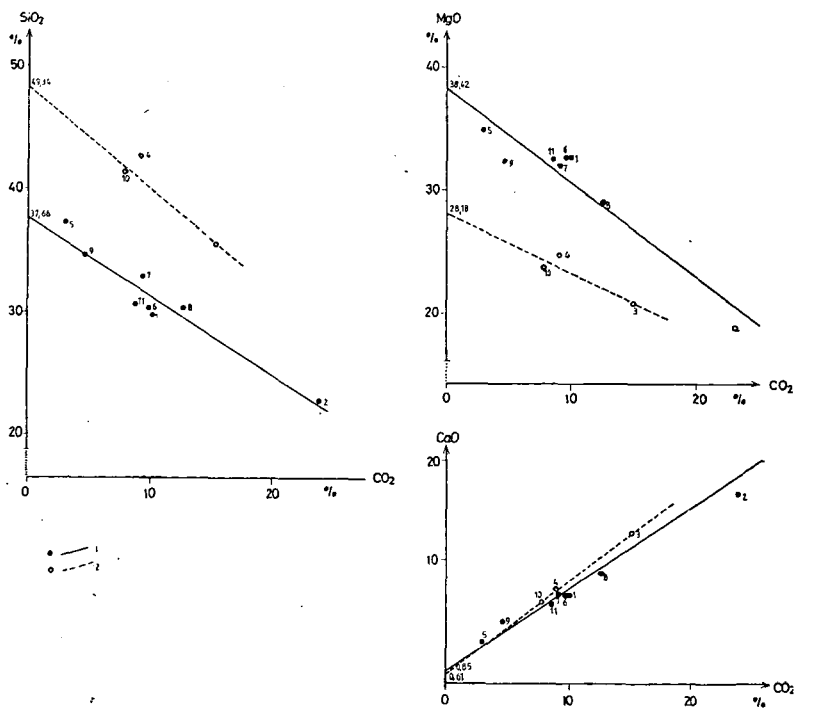

Fig. 8. Correlation between the CO_2 and the SiO_2, MgO and CaO in the Ófalu serpentine
Source of data: Table 1

Legend:
1 — sample and regression line of I group
2 — sample and regression line of II group

TABLE 2

Regression coefficients of linear correlations between CO_2 and main components of serpentines

	Ófalu—I (8)	Ófalu—II (3)	Helesfa (5)	Gyód (4)	Perkupa (5)
SiO_2	0.92	0.87	0.78	0.02	0.80
Al_2O_3	0.12	0.99	0.17	0.01	0.18
Fe_2O_3	0.01	0.30	0.16	0.26	0.80
FeO	0.21	0.33	0.03	1.00	0.91
MnO	0.41	0.99	0.01	1.00	0.06
MgO	0.90	0.84	0.52	0.97	0.90
CaO	0.98	1.00	0.30	0.93	0.06
Na_2O	0.02	0.99	0.43	0.02	0.97
K_2O	0.00	0.98	0.04	0.28	0.03

Source of data: Table 1
in brackets: numbers of employed data (*i.e.* of CO_2 determinations)

TABLE 3

Average serpentine composition in volatile-free form

	Ófalu—I [8]	Ófalu—II [3]	Helesfa [6]	Gyód [3]	Perkupa [5]	Pyrox.	Perid.	Lherz. [69]	Harzb. [71]
SiO_2	42.85+	55.85+	53.72+	45.05	43.75	44.64	50.78	43.90	45.7	45.0
TiO_2	0.01	0.00	0.00	0.01	0.00	0.00	0.53	0.82	0.2	0.1
Al_2O_3	2.24	1.35	4.42+	2.03	2.45	2.21	4.12	4.02	3.7	1.7
Cr_2O_3	—	—	—	—	—	0.43	—	—	0.3	0.3
Fe_2O_3	7.57	7.67	7.38	6.72	6.28	5.19	2.45	2.53	5.1	6.8
FeO	2.24	2.16	2.08	2.41	0.59+	0.82+	7.41	9.92	3.6	2.2
MnO	0.16	0.11	0.37+	0.13	0.09	0.14	0.13	0.21	0.1	0.1
MgO	43.72+	31.90+	30.68+	43.21	46.51+	46.01+	21.83	34.29	38.4	42.6
CaO	0.97+	0.69+	0.66+	0.31	0.18+	0.50	12.07	3.49	2.3	0.7
Na_2O	0.11	0.08	0.25+	0.07	0.06	0.04+	0.45	0.56	0.3	0.2
K_2O	0.03	0.11	0.36+	0.07	0.08	0.01	0.21	0.25	0.1	0.1
P_2P_5	0.09	0.08	0.08	0.01	0.01	0.00	—	—	—	—

+— calculated from the correlation with CO_2
in brackets: number of data
source of Hungarian data: Table 1
Pyrox. — NOCKOLDS' pyroxenite average [HUANG. 1962]
Perid. — NOCKOLDS' peridotite average [HUANG. 1962]
Lherz. — oceanic lherzolite average [KASHINTSEV *et. al.*, 1979]
Harzb. — oceanic harzburgite average [KASHINTSEV *et. al.*, 1979]

Since the SiO_2, MgO and CaO vary to a large extent with the CO_2 content and relative deviations from the regression lines get at 10% there is no reason for all data to be corrected separately. Therefore corrections are made for the groups only and average compositions are calculated. The SiO_2, MgO and CaO contents are extrapolated by the regression lines to 0,00 % CO_2 and other components are determined arithmetically. Results are calculated on the volatile-free basis (Table 3). A control calculation shows that practically the same data can be got if first all samples to be calculated on the water-free basis and then correlation with CO_2 to be estimated.

TABLE 4

Composition of serpentines in volatile-free form

	Helesfa—1			Helesfa—2			Gyód—2			Perkupa—mine				
	121,0	300,0	400,0	134,6	143,0	300,0	82,0	90,5	125,0	4	5	6	7	11
SiO_2	45.74	43.81	44.89	45.15	45.65	45.03	43.95	44.08	43.76	44.56	43.96	44.96	44.87	44.34
TiO_2	0.03	0.00	0.00	0.01	0.00	0.00	0.00	0.00	0.00	0.00	0.00	0.00	0.00	0.00
Al_2O_3	1.85	2.81	1.74	2.00	2.32	1.45	2.45	2.52	2.39	3.38	1.25	2.17	2.34	1.89
Cr_2O_3	—	—	—	—	—	—	—	—	—	0.37	0.56	0.41	0.48	0.34
Fe_2O_3	6.68	6.78	6.97	6.92	6.37	6.58	6.49	5.88	6.53	5.15	6.98	5.29	5.47	7.60
FeO	2.40	2.12	2.29	2.47	2.78	2.39	1.72	0.95	0.93	0.91	1.56	1.30	0.87	2.63
MnO	0.16	0.18	0.13	0.09	0.09	0.11	0.10	0.09	0.09	0.12	0.12	0.13	0.16	0.17
MgO	42.83	43.97	43.51	42.60	42.27	44.05	43.08	45.45	45.53	44.95	44.61	45.00	44.99	41.29
CaO	0.12	0.21	0.37	0.58	0.35	0.26	2.05	0.94	0.58	0.35	0.41	0.54	0.70	0.55
Na_2O	0.08	0.05	0.05	0.09	0.09	0.03	0.06	0.02	0.08	0.19	0.55	0.21	0.12	1.20
K_2O	0.09	0.06	0.05	0.08	0.08	0.07	0.09	0.06	0.09	0.01	0.00	0.00	0.00	0.00
P_2O_5	0.00	0.01	0.01	0.00	0.00	0.01	0.01	0.01	0.01	0.00	0.00	0.00	0.00	0.00

Source of data: Table 1

On the basis of experiences from the calculations given above a further investigation has been made to determine relationship between the CO_2 and other rock-components in the Helesfa and the Gyód serpentines as well as in the Perkupa ones (North Hungary) included in analysis for the comparison. The regression coefficient values (Table 2) show no clear correlation ($r^2 \geqq 0{,}90$) in the Helesfa serpentine but FeO, MgO and CaO in the Gyód serpentine and FeO, MgO and Na_2O in the Perkupa one change in close relationship with CO_2. Since the low CO_2 the analyses calculated on the volatile-free basis without any corrections (Table 4), reflect the petrochemistry about realistically. Corrections are made only for average composition (Table 3) calculations.

Chemical composition of the Ófalu, Helesfa, Gyód and Perkupa serpentine (without H_2O and CO_2) is comparatively constant and differences between samples are insignificant. Average compositions of different bodies are also similar. The Ófalu II group is the only exception. Similarly to other groups, SiO_2 and MgO are dominant but in a very unusual ratio: beside about 56% SiO_2 the MgO is of 32%. Among magmatic rocks of such acidity, even the marianites and boninites (52—57% SiO_2) extreme enriched of MgO, contain only 12—24% MgO (DOBRETSOV *et al.*, 1980). Therefore the analytical data of the Ófalu II group do not reflect any real magmatic rock composition and will be not discussed below. In further discussion the "Ófalu serpentine" will mean average composition of the I group.

Original magmatic rocks of four Hungarian serpentine bodies are very similar to each other petrochemically. On the one hand, the Ófalu and Helesfa, and on the other hand, the Gyód and Perkupa serpentines correspond in particular well. In the first pair there is of 2% more FeO and less MgO than in the second one. At the same time, the Ófalu and Gyód serpentines on the one hand, and the Helesfa and Perkupa ones on the other hand are similar in their SiO_2 contents and more acidic rocks of Helesfa and Perkupa contain less Al_2O_3 and Fe_2O_3 than more basic ones of Ófalu and Gyód.

Concerning original magmatic rocks, two alternatives were born: the peridotite [ERDÉLYI, 1970, 1971, 1974; GHONEIM and SZEDERKÉNYI, 1979] and the pyroxenite

[SZEDERKÉNYI, 1974, 1976a, 1977a] ones. Through comparison with the NOCKOLDS' averages [HUANG, 1962] (see Table 3), pyroxenite is to be excluded: they contain much more SiO_2, Al_2O_3 and particularly CaO and much less MgO. The "peridotite average" is nearer to the discussed rocks and shows a deviation of the same direction as the "pyroxenite average". This "peridotite average" presents sum of various continental rocks named "peridotite".

Peridotites occur on continents in various magmatic complexes [KUZNETSOV, 1964]. In most of them, peridotites play a subordinate role and form layer- or band-like derivatives of dominant basic or alkalic magmatic rocks, for example, in gabbro—pyroxenite—dunite complexes of folded area or in differenciated gabbro—norite complexes of cratons occurring, as a rule, in lopoliths. Alkalic—ultramafic—carbonatite complexes are found also in cratonic area as pillar-form intrusion of vertical position and concentric structure. Last two cases can be excluded on the basis of their tectonic position (craton) and the first one is not suitable because of its metallogenetic character (Ti—Fe—V).

Analogues of the South Transdanubian serpentines are to be found first of all among rocks of dunite—harzburgite complexes (i.e. "Alpine type ultramafics"). This complex is the lower member of ophiolitic series which latter, in turn, is a fragment of oceanic lithosphere overthrusted on continent. That is why analogues of the South Transdanubian serpentines have to be looked for among oceanic rocks (Table 3).

Identity of chemical composition of the Ófalu and Helesfa serpentine with the oceanic harzburgite average is doubtless and similarity of the Gyód and Perkupa serpentine is also very high. At the same time, deviation from the oceanic lherzolite average is also clear. In their Al_2O_3 contents, the South Transdanubian rocks are much nearer to harzburgite, and considering the trend of differences between the oceanic lherzolite and harzburgite in SiO_2, MgO and CaO, the South Transdanubian serpentines get beyond harzburgite, perhaps trending to dunite. Consequently, the *South Transdanubian serpentines have been originated from rocks being very similar to present oceanic harzburgite.*

3. ORIGIN AND POSITION OF PERIDOTITES

The South Transdanubian serpentines are located in uppermost levels of continental lithosphere. According to principles of the classic geology, their intrusive origin seemed to be obvious. There are two possibilities: to assume either upward rise of ultramafic material direct from the mantle or origin through differentiation of other magmas. Upward rise of magmas is always caused first of all by hydrostatic forces. Magma of basic or alkalic composition can rise into the upper levels of continental crust if it has originated from the deeper horizons of mantle, and the density excess compared to the continental crust is overcompensated by the density deficit compared to the mantle material. Peridotites originated from these magmas through intracrustal differentiation, are commonly subordinated and characterized first of all by clinopyroxene (*CPx*) beside olivine (*Ol*) with scarcity of orthopyroxene (*OPx*). Therefore these peridotites are dominantly of wehrlite (*Ol+CPx*) composition and even lherzolite (*Ol+CPx+OPx*) are rare and harzburgite (*Ol+OPx*) are practically absent. As seen, relationships with these intrusive complexes have been excluded also on the basis of other data.

Material of dunite—harzburgite complexes originates from mantle. Density of these ultramafics is much more as compared to continental crust and approximate-

ly coincides with the mantle density. Such a material in mantle surrounding cannot become bouyant and rise into the upper levels of continental crust and form intrusive or effusive bodies there. The same density excess excludes also tectonic rise upward from mantle independently from plasticity of serpentines.

Therefore, the South Transdanubian serpentines cannot be originated from under continental crust. According to petrochemistry, they are analogues of the oceanic harzburgites. Accounting this analogy for a proof of the *oceanic origin,* the only realistic explanation can be got. Two kinds of mechanism for explanation of the peridotite appearance in continental surrounding exist. Both of them are related to subduction processes.

First mechanismus is the so-called *obduction,* i.e. overthrusting of oceanic lithosphere on continental crust. Obduction takes place during the continent — island arc collision when a continental slab subduces beneath an island arc [ZONENSHAIN et al., 1976]. The island arc itself is generated by subduction of an oceanic slab. *Collision* takes place if the oceanic part of the subducing slab has consumed and the continent being located on the contrary coast of the former ocean, arrives at the island arc (for example, as Australia at the Indosenian arc). It is a substantial thing that subducing slab descends with a sharp break. Continental lithosphere cannot be broken such a way that is why it can subduce up to former break only, i.e. about 100—150 km from the oceanic border of the island arc *(Fig. 9).*

Island arcs often are generated on oceanic lithosphere (*i.e.* through subduction of ocean—ocean type). Thus, in the basement of island arcs oceanic lithospheric elements can exist. That has been proved by sampling of oceanic tholeiites, gabbro and peridotites on the inner (i.e. island arc) slope of oceanic trenches [KASHINTSEV *et al.,* 1979; SHARASKIN *et al,* 1980]. All these rocks get above the continental slab subduced: that is the obduction.

After the collision finishing, the cooling effect illustrated in general by geoisotherm bending *(Fig. 10),* stops and *thermic equalization* takes place. It results in partial melting of the subduced continental slab. Melted material is of less density and becomes bouyant and rises upward like a diapir being intruded into the oceanic — island arc complex. In this process, the deepest subduced crustal sections, *i.e.* the former edge of the continent only participate. Further from this edge, the oceanic-island arc complex covers the subduced continental crust as a nappe system.

Subducing oceanic slab drags the continental one which is in rigid connection with it. Density of oceanic slab is higher than that of underlying astenosphere that is why it sinks in astenosphere and drags continental slab not only forwards but also down. After the collision finishing, the dragging effect stops and an *isostatic equalization* takes place: continental lithosphere of less density emergences. Anatexis and granite intrusion mentioned above can be considered also as elements of this process.

The assemblage of thermic and isostatic equalization is the process named by classic geology "orogeny". During this process, the obduced oceanic-island arc complex suffers a deep erosion and its fragments only may be preserved. These fragments originated from the lowermost horizons of obduced oceanic lithosphere consist mostly of peridotite. These fragments are of two main types: the first in the granitization zone and the second before it. Structural position of peridotites in general depends on these types and is of two varieties, the first of them can be named "disjuncted" and the second one "plicated".

Peridotite of *disjuncted position* has got at present site from side or from above through tectonic movements dismembering obduced nappes. The same density excess

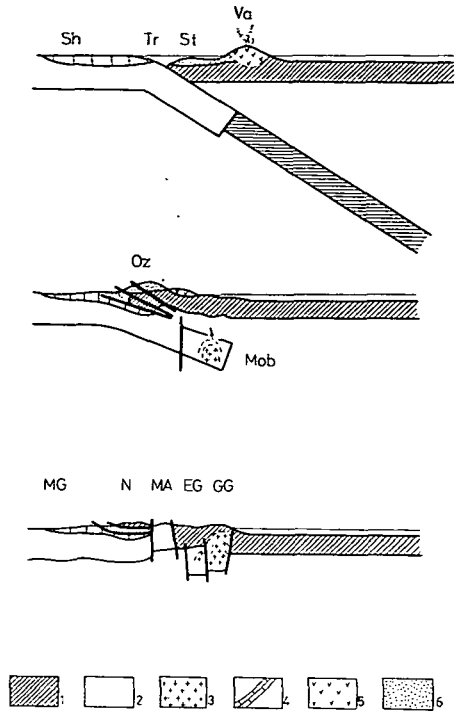

Fig. 9. Principal scheme of continent — island arc collision according to ZONENSHAIN *et al.* [1976] modified

Legend:
Sh — shelf
Tr — oceanic trench
St — sedimentary terrace
Va — volcanic arc
Oz — obduction zone
MG — "miogeosynclinal zone"
N — nappes
MA — "marginal anticlinorium"
EG — "eugeosynclinal zone"
GG — granite — gneiss doming zone
Mob — mobilization of subduced continental crust
1 — oceanic lithosphere
2 — continental lithosphere
3 — palyngenetic granite mobilized (accompanied by hT metamorphism)
4 — carbonate shallow-marine sediments
5 — island arc volcanites
6 — continental rise sediments (mostly turbidites)

which excludes rise upward of peridotites through continental crust, helps for its sinking into fracture zone generated during emergence due to isostatic equalization. Therefore, the origin from above is more probable even in lateral-slip faults. Disjuncted position probably is characteristic for areas far from the granitization zone.

Plicated position comes into being through folding of an obduced nappe system together with its continental basement. In the granitization zone, both can become so plastic as to undergo isoclinial and multiple folding. In a deep eroded state, syncline

hinges of lowermost position only are preserved as peridotite bodies of lens-like form in a horizontal plane and of wedging out downward form in a vertical cross-section.

Form of the South Transdanubian serpentine bodies corresponds to both alternatives. According to thermal effects and to country rock folding, the Gyód and the Ófalu serpentines may be of syncline position. The Helesfa serpentine within granite is rather of disjuncted position. The only certain consequence, however, is that all South Transdanubian serpentine bodies wedge out downward and don't have any "roots".

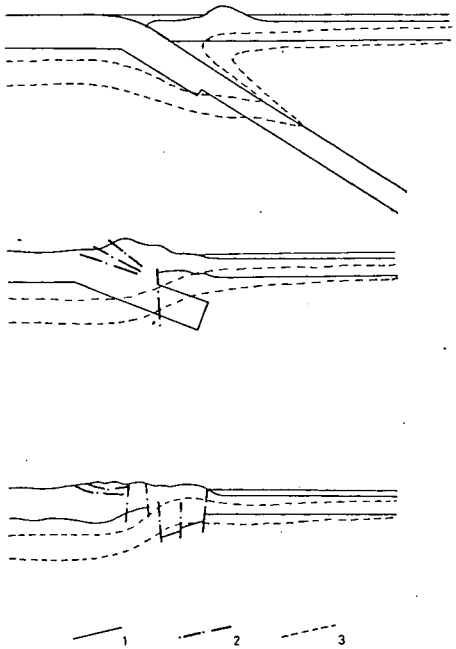

Fig. 10. Geoisotherms in the continent — island arc collision according to ZONENSHAIN *et. al.*, [1976] modified

Legend:
1 — contours of lithospheric slabs (from the *Fig. 9)*
2 — main faults (from the *Fig. 9)*
3 — geoisotherms (schematically)

Another mechanism of the peridotite appearance in continental surrounding is related to mélanges or olistostromes. In a mature state of subduction an *accretionary wedge* develops on oceanic side of island arcs from sediments being scraped off the descending oceanic slab and folded—thrusted before the wedge-like edge of the island arc lithosphere *(Fig. 11)*. Between volcanic arc and oceanic trench, undersea terraces appear then a non-magmatic high comes into being as a second island row (for example, Andaman or Mentawai Islands in front of the Indonesian volcanic arc). Along the overthrusting plane within fan-like structure of accretionary wedges *(Fig. 12)*, *mélange* can be formed. On the rim of the shallow-marine area, on one hand, and on the inner trench slope, on the other hand, rocks outcrop which roll down along

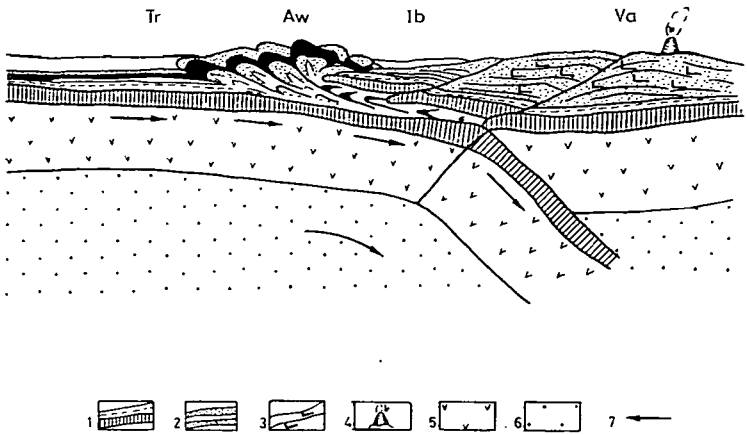

Fig. 11. Crustal structure model of an active island arc according to SOROKHTIN, [1979] modified

Legend:
Tr — oceanic trench
Aw — accretionary wedge
Ib — interarc basin
Va — volcanic arc
1 — oceanic crust with sedimentary cover
2 — sediments of the continental slope and continental rise
3 — sedimentary—volcanogenic sequence
4 — active volcano
5 — upper mantle part of the oceanic lithosphere
6 — asthenosphere
7 — motion

the steep slope of terraces or of non-magmatic high, and are buried in lower position as olistolithes. Sediments rich in olistolithes are called *olistostromes.* Consequently, mélange and olistostrome mark practically identical geodynamic conditions and differ in forming mechanismus only. Both can contain peridotite blocks. Their amount is significant mostly in mélanges.

During obduction in a late phase of the continent — island arc collision, mélange and olistostrome get above the continental slab subduced. During nappe forming, new mélange zones are coming into being and olistostrome-lenses are occurring in the molasse complexes of foredeeps developed from oceanic trenches. Therefore, appearance of peridotite blocks in mélanges or olistostromes marks the same geodynamic situation as fragments of obduced nappes. In South Transdanubia the only Ófalu serpentine can be supposed to be of such origin according to proportions and form.

In any case, the South Transdanubian serpentines give evidence of a continent — island arc collision and postcollisional thermic—isostatic equalization. Possibilities of their position are as follows: for Helesfa—disjuncted, for Gyód — syncline-like or disjuncted, for Ófalu — olistolithe, block in mélange, disjuncted or syncline-like.

4. METAMORPHISM OF SERPENTINES

The first serpentinization was taking place as late as during subduction, and the peridotite bodies are getting at obduced position having been serpentinized. Lizardite—chrysotile composition would correspond to this metamorphism but in the same

way, it could be a product of any latest 1T metamorphism. Concerning the postcollisional metamorphism, numerous problems are raised:

a) The borehole Helesfa—1 penetrated talc schists beneath serpentine with serpentine "intercalations". Talc can develop in serpentines in consequence of both hydrothermal ifluence and metamorphism in greenschist facies [DEER *et al.*, 1963]. ERDÉLYI [1974] that talc had originated from olivine and/or orthopyroxene at 700—800 °C in hydrous conditions. Thus, talc may be originated either from serpentine or from olivine and enstatite showing a higher temperature metamorphism in any case.

b) In serpentine of the borehole Gyód—2 clinoenstatite and forsterite was determined by ERDÉLYI [1971]. According to him [ERDÉLYI, 1974], serpentine minerals decompose over 800 °C to produce forsterite and partly enstatite which latter at 1140 °C turns into clinoenstatite. By the study of 2—3 cm clinoenstatite crystals were first chloritized (at about 500—600 °C) then substituted by lizardite (under 400 °C), therefore progressive metamorphism was followed by retrograde one, raising a question on existence of several generations of 1T serpentine minerals.

c) The Helesfa and the Gyód serpentines are crossed by aplite-microgranite veins. I suppose that the source of Mg during their strong metasomatism was the serpentine rock itself. Hydrothermal origin of this metasomatism does not seem to be probable because there are no traces of hydrothermal effects in country granites. This metasomatism can be regarded rather as a metamorphic feature, i.e. as a result

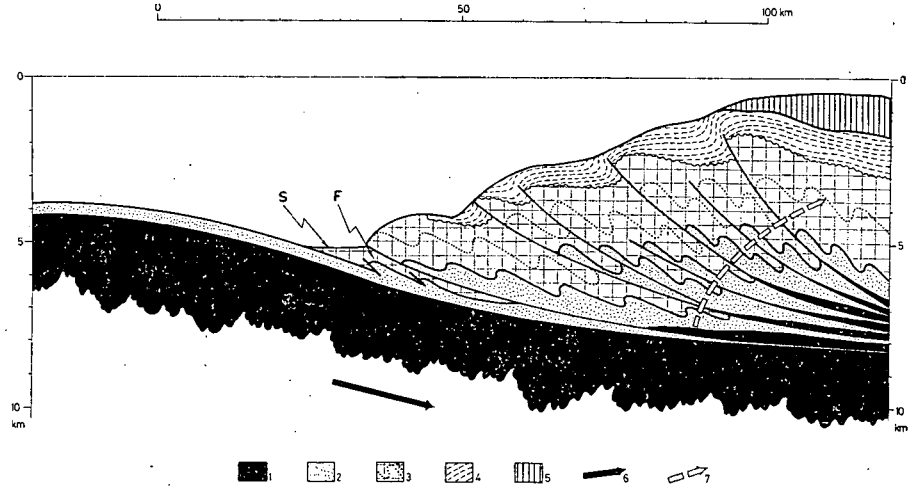

Fig. 12. Accretionary wedge model according to SEELEY *et al.*, [1974] modified

Legend:
S — sedimentation level
F — folding zone
1 — oceanic crust
2 — pelagic sediment
3 — trench sediment (also in folded state)
4 — continental slope sediment
5 — shallow-marine sediment
6 — motion
7 — folding and imbrication oldering

of reactions between acidic magma and ultramafic rocks at *hT—hP* conditions. Identity of this metamorphism with that resulted in appearance of aplite-microgranite magma through partial melting seems to be the simplest assumption. It would mean, however, a quite high temperature (min. 700—800 °C) what should be reflected also in alteration of serpentine minerals. Clinoenstatite and forsterite in the Gyód serpentine and talc in the Helesfa one and chlorite in both of them may reflect this thermal effect, and the later rise of lizardite and chrysotile bulk should be resulted from that. Since the lack of acceptable textural analysis it is not proved. It is also difficult to understand why clinoenstatite and forsterite occur in the Gyód serpentine and talc appears in the Helesfa one only while aplite-microgranite veins undergone Mg metasomatism, are known in both sites.

d) According to GHONEIM and SZEDERKÉNYI [1979], antigorite appears in the outer zones of the Ófalu serpentine body. That would reflect a later thermal influence. Thickness of about several meters of these outer zones and the lizardite — chrysotile composition of central part of the body would show weakness of this thermal influence. According to ERDÉLYI [1974], antigorite is absent in the Ófalu serpentine but his two samples may have been taken from the central part. He describes a large amount of forsterite, enstatite and clinoenstatite of contact origin and presence of monoclinic chlorite and of the γ-Al_2O_3 originated from böhmite at 800—1000 °C. That would be understable only assuming the later origin of lizardite and chrysotile. If antigorite really is limited to outern zones, it can be product of a more later metamorphism.

e) Garnet was mentioned from the Helesfa serpentine by SZEDERKÉNYI [1970] and from the Ófalu one by JANTSKY [1979]. If this garnet is of metamorphic origin, it reflects pressure corresponding with about 15—20 km depth [LUTS, 1974]. Even if the heat-flow was normal, that means a temperature of about upper existence limit of antigorite or higher, therefore both the Helesfa and Ófalu serpentinization could take place after garnetic metamorphism only. Higher more temperature is shown by the Görcsöny eclogite in several km west of Gyód [RAVASZ—BARANYAI, 1969]. This eclogite, perhaps, is originated from basic magmatic rock associated with the Gyód peridotite, and its mineral composition and texture give evidences of multiphase retrograde metamorphism [RAVASZ—BARANYAI, 1969] what supports the idea of late rise of serpentine mineral bulk.

Thus the South Transdanubian serpentines were affected by complicated multiphase metamorphism which is not analysed and cannot be interpreted. Lizardite and chrysotile in the Helesfa and Gyód serpentines are expected to be products of the last low-grade metamorphism while antigorite of the Ófalu serpentine fixes a stronger thermal effect as the last metamorphic event.

5. GEOLOGICAL HISTORY AND AGE

For reconstruction of geological history, two sure objects only exist: peridotite and granite. First of them marks a continent — island arc collision and the second one marks a postcollisional thermic — isostatic equalization. Supposition of causal relations between them seems to be the simplest concept resulted in several statements as follows:

a) Aplite-microgranite veins occurring in both the Gyód and Helesfa serpentine as well as the thermal metamorphism affected these bodies, are products of a postcollisional granitization taken place immediately after obduction of peridotites above continental crust.

b) On the basis of real dimensions of the Earth and of observable plate motion rates, a concrete piece of oceanic crust can exist maximally for 150—200 m. yr. Since granitization was produced by a process finishing total disappearance of oceanic crust in a concrete area, peridotite can be older than granite maximally of 150—200 m. yr.

c) Granitization begins in deep horizons of continental crust. These deep horizons are everywhere on the Earth of Middle Proterozoic or older age [DOBRETSOV, 1980]. Therefore presence of such metamorphics in granitized complexes of any age is natural. Melted granite together with fragments of their original country rocks is intruded into oceanic — island arc complex which forms the bulk present country rocks. Through purposeful investigations only, it can be established which part of metamorphic rocks are originated from the subduced continental slab and which one are generated from the oceanic basement and volcanogenic—sedimentary cover of the island arc.

d) Peridotite and granite fixes the following events: normal oceanic spreading, subduction (island arc), continent — island arc collision and postcollisional thermic—isostatic equalization.

Age of these events can be determined only going backward in the time. Upper age boundary of granitization and metamorphism connected with postcollisional equalization, is fixed by presence of detrital material of related rocks in Upper Carboniferous — Lower Permian sediments [SZEDERKÉNYI, 1974]. These sediments are of molasse type and are supposed to have been accumulated in depressions of a mountain system. Origin of this mountains can be related most simple to postcollisional emergence what fixes age of granitization and metamorphism in Lower Carboniferous. Collision can be finished maximally 10 m.yr before this date and can be started maximally 15—20 m.yr before the second date. Thus collision can begin only as early as in Upper Devonian. Subduction time interval cannot be estimated but according to the age of collision, oceanic lithosphere cannot be formed earlier as in Ordovician, corresponding with conclusions based on analogies that the Ófalu complex seems to be of Silurian [SZEDERKÉNYI, 1970], partly perhaps of Ordovician [SZEDERKÉNYI, 1977a] or of Devonian [Szederkény, 1977d] age.

CONCLUSIONS

Therefore, the South Transdanubian sequences mark the following events *(Fig. 13)*:

1. Ocean generation with ancient (Precambrian) continents on the coasts — (Ordovician?) — Silurian—(Devonian?).
2. Subduction: island arc coming into being chiefly on oceanic crust — Devonian.
3. Collision: subduction of the ancient continent being scarred with the former oceanic lithosphere, under island arc — (Upper Devonian?) — Lower Carboniferous.
4. Postcollisional equalization: partial mobilization and emergence of the subduced ancient continent — Lower (and Middle?) Carboniferous.
5. Denudation and peneplanation: Upper Carboniferous — Lower Permian.

Conclusions given above are based on an assumption of causal relationship between appearance of peridotite and granitization. In reality, radiometric and paleomagnetic data [MÁRTON—SZALAY, 1979] give evidences of Upper Carboniferous age of granite. Relative direction of subduction as well as present position of the collisional suture could be determined on the basis of investigation of structural zonality. Now, this zonality cannot be reconstructed because many problems of metamorphic

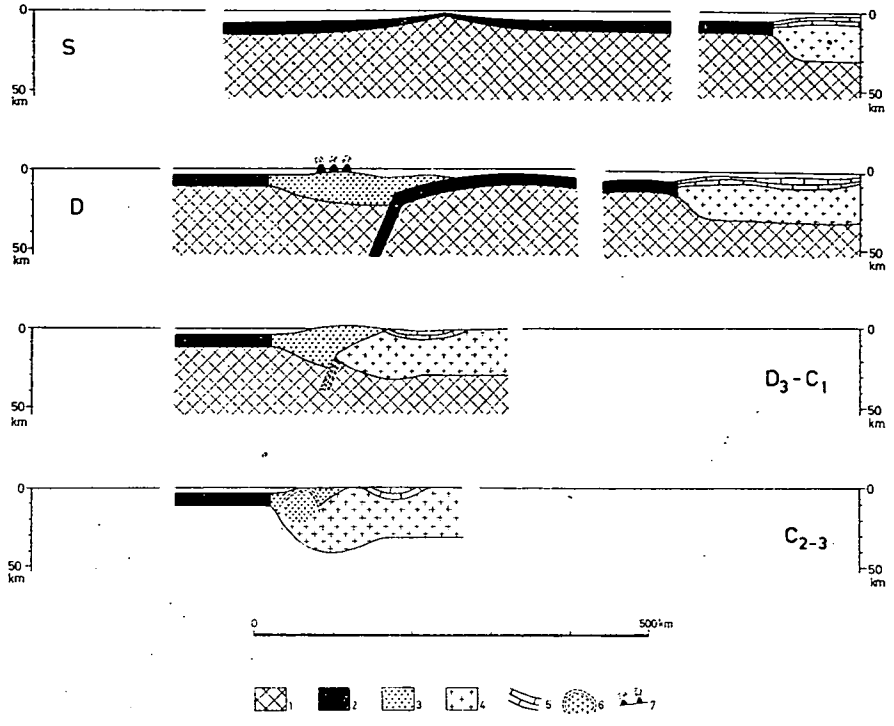

Fig. 13. Scheme of development of the South Transdanubian Paleozoic (todays orientation of the cross-section is unknown)

Legend:
1 — upper mantle
2 — oceanic crust
3 — island arc crust
4 — continental crust
5 — shallow-marine sediments
6 — zone of granitization and metamorphism
7 — active calc-alkalic volcanoes

rocks are unsolved and a later (Alpine) rearrangement must have taken place. For example, the Ófalu complex bearing serpentine coincides with an obvious young (Cretaceous or Cenozoic) tectonic zone which seems to lay between the Helesfa and the Gyód bodies *(Fig. 1)*. On the basis of the plate tectonics concept, cataclastic rocks should be expected in this zone instead of metamorphic ones, although these cataclastic rocks might be originated also from metamorphic ones.

ACKNOWLEDGEMENTS

Principal ideas for plate tectonics interpretation of the South Transdanubian serpentines were given by L. P. ZONENSHAIN (USSR Academy of Sciences, P. P. Shirshov Institute of Oceanology, Moscow) and by N. L. DOBRETSOV (USSR Academy of Sciences, Siberian Department, Buriat Branch, Geological Institute, Ulan-Ude) during a common excursion "Ultramafics and basic rocks of Bohemian Massif"

(Sept. 1980). Hungarian Geological Institute gave permission for the employment of unpublished data. A very helpful consultation to the interpretation of metamorphic events in general and in South Transdanubia in particular was given by GY. LELKES—FELVÁRI (Hungarian Geological Institute).

REFERENCES

ABRAMOVICH, I. I., KLUSHIN, Y. G. [1978]: Petrochemistry and structure of the Earths depth-(in Russian). — "Nedra", Leningrad, p. 375.

BARABÁS, A., BARANYI, I., JÁMBOR Á. [1964]: Map of the Pretertiary basement of the Mecsek and Villány Mountains, scale 1:100.000.
— Results of the geophysical exploration of the Mecsek and Villány Mountains, Ann. Hung. Geophys. Inst., 1, Budapest, Suppl.

DEER, W. A., HOWIE, R. A., ZUSSMAN, J. [1963]; Rock-forming minerals. — Longmans, London.

DOBRETSOV, N. L. [1980]: Introduction to global petrology (in Russian). — "Nauka", Novosibirsk, p. 200.

DOBRETSOV, N. L., SHARASKIN, A. YA., LAVRENTJEV, YU. G., SOBOLEV, A. V., SOBOLEV, N. V., KOMATSU, M., TAZAKI, K., DIETRICH, V., OBERHÄNSLI, R. [1980]: Marianite—boninite series of volcanic rocks (in Russian). — Chapter 5, Geology of the Philippine Sea floor, „Nauka", Moscow, pp. 149—179.

ERDÉLYI, J. [1969]: Micromineralogical examination of the Hungarian serpentines; the Perkupa serpentine (in Hungarian). — Manu script, Hung. Geol. Inst., Budapest.

ERDÉLYI, J. [1970]: Report on first group of the Mecsekian (Helesfa) serpentine in frame of the topic "Examination of Hungarian serpentines" (in Hungarian). — Manuscript, Hung. Geol. Inst,. Budapest.

ERDÉLYI, J. [1971]: Report on the micromineralogical examination of the Mecsekian serpentines (in Hungarian). — Manuscript, Hung. Geol. Inst. Budapest.

ERDÉLYI, J.: [1974] Mineralogical investigation of the Hungarian serpentines (in Hungarian with Russian abstract). Földtani Kutatás, 17, 1—2, Budapest, pp. 97—100.

GHANEM, E. A. RAVASZ—BARANYAI, L. [1969]: Petrographic study of the crystalline basement rocks, Mecsek Mountains, Hungary. — Acta Geol. Acad. Sci. Hung., 13, 1—4. Budapest, pp. 191—219.

GHONEIM, M. F., SZEDERKÉNYI, T. [1977]: Preliminary petrological and geochemical studies of the area Ófalu, Mecsek Mountains, Hungary. — Acta Miner. Petrogr., 23, 1, Szeged, pp. 15—28.

GHONEIM, M. F., SZEDERKÉNYI, T. [1979]: Petrological review of the Ófalu serpentinite, Mecsek Mountains, Hungary. — Acta Miner. Petrogr., **24** 1, Szeged, pp. 5—18.

HAÁZ, I., KOMÁROMY, I. [1964]: Magnetic map of the Mecsek and Villány Mountains. Anomalies of the vertical intensity of the Earth's magnetic field. 1:100 000. — Results of the geophysical exploration of the Mecsek and Villány Mountains, Ann. Hung. Geophys. Inst., **1**, Budapest, Suppl.

HUANG, W. T. [1962]: Petrology. — McGraw-Hill, New York — San Francisco — London—Toronto.

JANTSKY, B. [1979]: Géologie de socle cristallin granitisé de la Montagne Mecsek. — Ann. Inst. Géol. Hung., **60**, Budapest, pp. 195—294.

KASHINTSEV, G. L., RUDNIK, G. B., FROLOVA, T. I. [1979]: Magmatic and metamorphic rocks of the ocean floor (in Russian). — Chapter I, Oceanology, Geology of the Ocean, Sedimentology and magmatism of the Ocean, „Nauka, "Moscow, pp. 9—87.

KASSAI, M. [1980]: Distribution of the Upper Carboniferous formations as outlined upon seismic and telluric measurements in SE Transdanubia (in Hungarian with English abstract). — Annual Rep. Hung. Geol. Inst. of 1978, pp. 301—307.

KUZNETSOV, YU. A. [1964]: Main types of magmatic formations (in Russian). — „Nedra" Moscow, p. 387.

LUTS, B. G. [1974]: Petrology of the deep zones of the continental crust (in Russian). — „Nauka", Moscow, p. 304.

MÁRTON—SZALAY, E. [1979]: Paleomagnetism of the granitoids from the Mecsek Mountains, SE-Transdanubia, Hungary (in Hungarian, with English abstract). — Gener. Geol. Rev. **13**, Budapest, pp. 71—94.

RAVASZ—BARANYAI, L. [1969]: Eclogite from the Mecsek Mountains, Hungary. — Acta Geol. Acad. Sci. Hung., **13**, 1—4, Budapest, pp. 315—322.

SAVELYEVA, G. N., DOBRETSOV, N. L., LAVRENTJEV, YU. G., LUTS, B. G., DIETRICH, V., COLEMAN, R. [1980]: Petrology of ultrabasic rocks, gabbro and metamorphic rocks. (in Russian). — Chapter 6, Geology of the Phillippine Sea floor, „Nauka", Moscow, pp. 180—236.
SEELEY, D. R., VAIL. P. R., WALTON, G. G. [1974]: Trench slope model. — The geology of continental margins, Springer—Verlag, Berlin—Heidelberg—New York, pp. 249—260.
SZEDERKÉNYI, T. [1970]: Geochemical examination of Lower Paleozoic formations of SE-Transdanubia (in Hungarian). — Manuscript, Hung. Geol. Inst., Budapest.
SZEDERKÉNYI, T. [1974]: Paleozoic magmatism and tectogenesis in Southeast Transdanubia. — Acta Geol. Acad. Sci. Hung., **18**, 3—4, Budapest, pp. 305—313.
SZEDERKÉNYI, T. [1976a]: Barrow type metamorphism in the crystalline basement of Southeast Transdanubia. — Acta Geol. Acad. Sci. Hung., **20**, 1—2, Budapest, pp. 47—61.
SZEDERKÉNYI, T. [1976b]: The Cr, Ni, As, Pt, Os, Ir and Au contents in the ultramafic rocks and their derivats from South Trandsdanubia (in Hungarian). — Manuscript, Hung. Geol. Inst., Budapest.
SZEDERKÉNYI, T. [1977a]: Geological evolution of South Transdanubia (Hungary) in Paleozoic time. — Acta Miner. Petrogr., **23**, 1, Szeged, pp. 3—14.
SZEDERÉNYI, T. [1977b]: Historical review of investigation of Precambrian and Lower Paleozoic formations of South Transdanubia (in Hungarian). — Manuscript, Hung. Geol. Inst., Budapest.
SZEDERKÉNYI, T. [1977c]: Documents of the Paleozoic Key Sections Programme, Mórágy Monuntains, 1976—1977. (in Hungarian). — Manuscript, Hung. Geol. Inst., Budapest.
SZEDERKÉNYI, T., [1977d]: Complex geological working up of the Mecsekian Precambrian—Lower Paleozoic key sections (in Hungarian). — Manuscript, Hung. Geol. Inst., Budapest.
ZONENSHAIN, L. P., KUZMIN, M. I. MORALEV, V. M. [1976: Global tectonics, magmatism and metallogenesis (in Russian). — "Nedra", Moscov, p. 231.

Manuscript received, April 10, 1981

ZOLTÁN BALLA
Hungarian Geophysical Institute
Kolumbusz u. 19—23
H—1145 Budapest
Hungary

Acta Mineralogica-Petrographica, Szeged, XXV/1, 25 — 39, 1981

NILE DELTA BEACH PEBBLES I: GRAIN SIZE AND ORIGIN

N. M. EL-FISHAWI and B. MOLNÁR

ABSTRACT

In the present paper a study of beach pebble size has been used to establish the source and movement of pebbles along a 75 km stretch of Nile Delta coast. A total number of 5200 pebble size measurements was done along 26 locations. Characteristic features of grain size distribution and probable origin are discussed on the basis of approaching hydrodynamic factors and old topographic features of Nile Delta continental shelf.

The average pebble size shows a general decrease and sorting improves with increasing distance of transport. It is believed that size-sorting plays an important part on pebble distribution along the coast. Three locations are considered to be secondary sources because eastwards of each there is a directional gradations in pebble size and sorting, this is with the agreement of west-east littoral current. The locations of secondary sources are closely related to the position of old submarine banks located off Nile Delta coast. Nile Delta beach pebbles are derived mainly from these banks due to onshore movement by the action of stormy waves.

INTRODUCTION

Wide consideration has been given to beach pebbles. Many authors studied pebble size and shape parameters. Early studies of beach pebbles were made by WENTWORTH, C. K. [1919], MARSHALL, P. [1928], and LANDON, R. E. [1930]. More recent works have been published by KRUMBEIN, W. C. [1941], CAILLEUX, A. [1945, 1947], KEUNEN, PH. H. [1964], BLUCK, B. J. [1967, 1969], CARR, A. P. [1971], and SPALLETTI, L. A. [1976]. Considerable attention has been given to the problem of whether size or shape is the dominant factor in the sorting of pebbles along and across a beach.

Nile Delta beach pebbles have the greatest continuity and largest areal extent between west of Burullus outlet and 12 km east of Gamasa *(Fig. 1)*. West of Burullus, the continuity becomes rare and pebbles can be observed in some restricted areas. On the other hand, as far as 12 km east of Gamasa, they have disappeared.

The pebbles are of fair size, their long, intermediate, and short diameter ranges between 300—200, 200—12, and 32—2 mm respectively. The short diameter is very small regarding to the other two diameters, for this reason, Nile Delta beach pebbles are named "flat stones".

Beach pebbles consist mostly of mudstones and silty sandstones, the later are less abundant. Many surfaces have conspicous niks and pits while the other are stained by iron oxides to various shades of brown to a depth of a few millimeters. Pebbles containing shell fragments and other fossils are common. They are characterized, especially the large pebbles, by the presence of encrusting organisms and animal borings.

SAMPLING

The area under investigation lies between longitudes 30° 55′—31° 45′ E, and extends for about 75 km along the coast. Beach, backshore plains, and coastal dune belts are the main geomorphological unites of the area *(Fig. 1)*. The pebbles tend to distribute on the surface of the beach and backshore area. They cover a wide variety of grain size. Pebbles of five size classes were abundant; 300—256 mm, 256—128 mm, 128—64 mm, 64—32 mm and 32—16 mm (—8 ∅ to —4 ∅). The location and sample site used in this study are illustrated in *Fig. 1.*

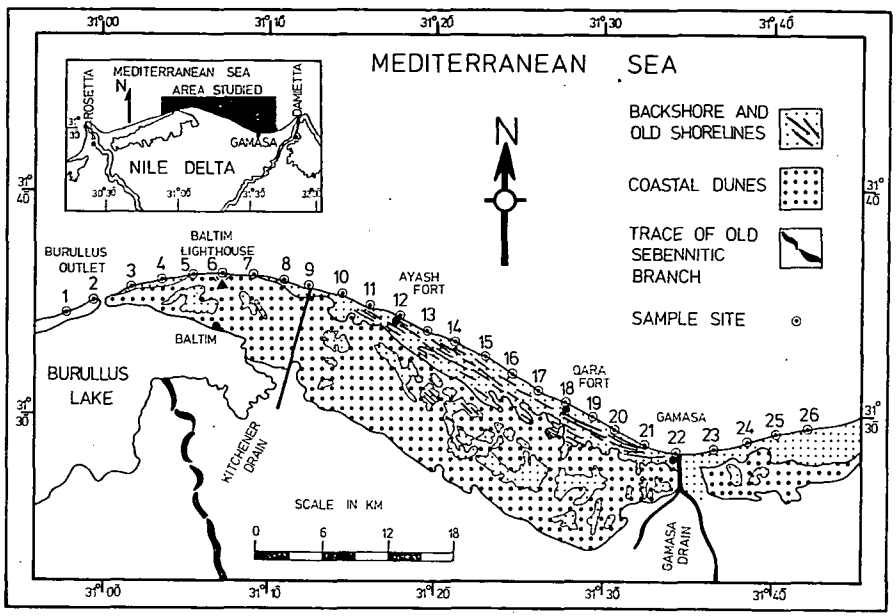

Fig. 1. Location map showing sampling sites for beach pebbles and geomorphology of coast for area studied.

During April, 1980, Nile Delta coast was surveyed and sample sites were chosen at 3 km intervals. The aim of sampling is to represent the populations of pebble size on each location along the coast. A total number of 5200 size measurements was obtained along 26 locations. At each location, a set of pebbles was collected by taking all pebbles within an area of 4 square meters to obtain a number of pebbles ranges from 60—75. Pebbles of five size classes were separated and counted. This technique was repeated for three times within the location and the average of occurrence of each size class was calculated. At some locations, it was necessary to collect some pebbles outside the considerable area in order to cover all size classes occurred within the location. Only 20 pebbles were collected from the eastern end location because pebbles were rare and absent eastward.

In the laboratory, cumulative percentages of number of occurence were plotted on probability paper and grain size parameters were calculated using formulae of FOLK, R. L. and WARD, W. C. [1957].

According to the studies of Institute of Coastal Research [1973], QUÉLENNEC, R. E. [1976], and MANOHAR, M. [1976], two types of waves are predominant. Storm waves of winter season rarely exceed 3.5 m in height, and summer swells are generally 40—70 cm high. The wave period 7—10 sec. predominates over all other periods for all class intervals of wave heights. The predominat direction of wawes is NNW and NW, but this is somewhat changed during stormy period when waves from N, NNE and NE are dominating. The direction of energy flux are the same as those of waves. *Fig. 2A* shows the average wave-rose of Nile Delta.

The interaction of the wave stresses with the beach induces a net boundary current flowing in the direction of wave travel. Along Nile Delta coast, the net result littoral current feeds from west to east. Measurements indicate that over 50% of the readings, the eastward current is up to 80 cm/sec. [MANOHAR, M., 1976].

In the present study, littoral current has been measured 6 times during 1976—1977, it was intended to make a measurement every 2 km. The results are shown in *Fig. 2B*. Due to the wide variation of the wave breaker angle and beach orientation, the net results are strong variations of the direction, occurrence and velocity of littoral current along Nile Delta coast. Moreover, the irregular form of some shorelines cause relative convergence and divergence of current. Thus, depending upon direction, percentage of occurrence, and corresponding average velocity, littoral current can be divided into three groups. Eastward littoral current predominates with percentage of occurrence >50% and average velocity of 36 cm/sec. Westward current occurs with lesser degree (20—50%) and velocity of 33 cm/sec. At some stretches, the current is often reversed causing convergence and divergence current with lesser occurrence (<20%) and velocity (27 cm/sec.). It is worthy to say that eastward current plays an important role in the movement of beach materials along Nile Delta coast.

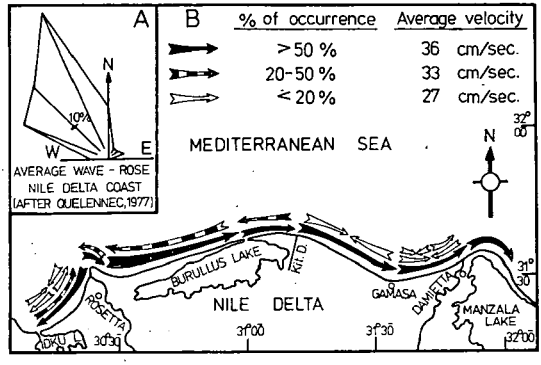

Fig. 2. Littoral currents along Nile Delta coast and average wave-rose.

LONG-AXIS ORIENTATION OF PEBBLES

The up-and-down motion of beach materials with the action of wave produces a net drifting of pebbles to beach surface. It thought that the orientation of long-axis is perpendicular to the direction of incoming waves.

Several readings of long-axis orientation were made only for elongated pebbles of each location (26—37 readings), and a total number of 781 readings were tabulated.

Brunton compass was used for measurements and each pebble was laid flat on its maximum projection face. Percentage of reading for 30° intervals, arithmetic mean, standard deviation, and coefficient of variance were calculated (Table 1). Rose diagrams were plotted on a map of the area *(Fig. 3)*.

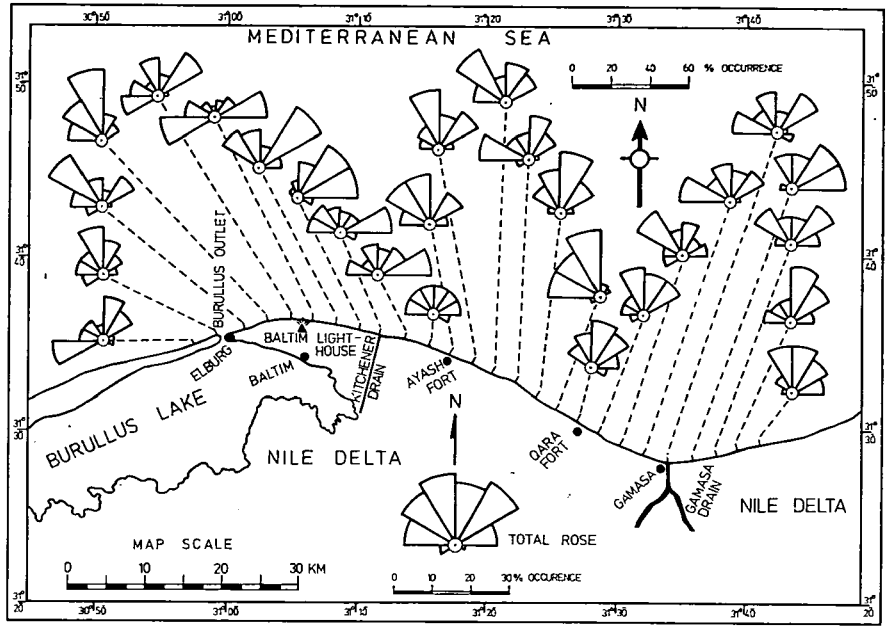

Fig. 3. Rose diagrams of long-axis orientation of beach pebbles.

Rose diagram figures give an idea about the changes in long-axis orientation along the coast. Such variation is a function to the directional effect dynamic forces and beach orientation. Rose diagrams show that 9 locations have a unimodal pattern and 12 ones have essentially a bimodal pattern, while 5 locations have a polymodal pattern.

The determination of actual direction of dynamic forces affecting each location is one definite aim of these measurements. But, how well do long-axis orientation correlate with the direction of dynamic factors? Indeed, it is so difficult to say because waves with different heights and directions, and littoral current with different velocities and directions are acting together to drift and orient pebbles on beach surface. But, however, by tracing the changes in long-axis orientation on each site along the coast, and as is evident from rose diagrams, it can be concluded that there is a gradual significant trend. From west of Burullus outlet to Baltim the orientation changes gradually from W to NW and then to N. Baltim coast characterized by E—W orientation and towards west of Ayash it tends to be from NE to E. Between Ayash and Gamasa, high percentage of occurrence are oriented again from NW to N, and eastwards it becomes from NE at the eastern end. In fact, the final rose diagram of long-axis orientation well represent all types and directions of dynamic factors affecting any location at a certain period.

TABLE 1

Long-axis orientation for beach pebbles along Nile Delta coast

Sample site	Percentage of reading								Ar. m.	St. dev.	Cof. var.
	0°—30°	30°—60°	60°—90°	90°—120°	240°—270°	270°—300°	330°—330°	330°—360°			
1	23.07	11.53	3.84	3.84	26.92	11.53	11.53	7.69	180	±129	0.72
2	17.85	10.71	7.14	—	10.71	14.28	14.28	25.00	212	137	0.64
3	8.10	18.91	2.70	—	8.10	16.21	32.43	13.51	227	126	0.56
4	13.33	10.00	—	—	—	16.66	23.33	36.66	254	129	0.51
5	11.11	25.92	3.70	—	18.51	14.81	7.40	18.51	193	133	0.69
6	7.69	11.53	26.92	—	26.92	15.38	7.69	3.84	178	114	0.64
7	11.11	37.03	11.11	—	—	—	22.22	18.51	161	143	0.89
8	19.23	30.76	30.76	7.69	—	—	3.84	7.69	87	95	1.09
9	10.00	10.00	26.66	6.66	—	16.66	16.66	13.33	179	130	0.73
10	12.90	16.12	29.03	—	—	16.12	9.67	16.12	163	134	0.82
11	15.15	15.15	15.15	9.09	—	15.15	15.15	15.15	173	135	0.78
12	3.22	19.35	9.67	—	—	16.12	25.80	20.80	233	129	0.55
13	16.66	23.33	6.66	—	—	10.00	13.33	30.00	192	148	0.77
14	20.00	16.66	3.33	—	—	16.66	30.00	13.33	201	142	0.71
15	22.58	16.12	3.22	—	6.45	25.80	12.90	12,90	188	138	0.73
16	31.25	18.75	6.25	—	—	6.25	15.62	21.87	160	150	0.94
17	5.88	2.94	—	—	2.94	26.47	26.47	35.29	290	88	0.30
18	25.00	21.42	14.28	7.14	—	—	14.28	17.85	138	138	1.00
19	21.42	21.42	3.57	—	7.14	10.71	16.71	25.00	184	146	0.79
20	16.66	10.00	13.33	—	10.00	10.00	26.66	13.33	201	135	0.67
21	16.12	19.35	3.22	—	3.22	25.80	12.90	19.35	203	138	0.68
22	10.00	23.33	3.33	6.66	—	23.33	13.33	20.00	199	155	0.78
23	18.18	27.27	27.27	3.03	—	6.06	—	18.18	119	124	1.04
24	13.88	25.00	13.88	—	2.77	8.33	22.22	13.88	173	139	0.80
25	27.27	22.22	11.11	—	2.77	13.88	11.11	11.11	143	137	0.96
26	25.00	20.00	15.00	—	—	5.00	10.00	25.00	156	148	0.95
Mean	16.13	18.56	11.01	1.66	4.60	13.44	16.13	18.43	185	137	0.74

Ar. m. = Arithmetic mean, St. dev. = Standard deviation, Cof. var. = Coefficient of variance

RESULTS

The distribution of Nile Delta beach pebbles along the coast shows a directional gradation in size with the presence of three major fluctuations. Results of the study are summarized in Table 2 and illustrated in *Figs. 4* through *9*.

Distribution of size classes

The distribution of particle size of beach pebbles is unimodal. *Fig. 4* illustrates the average histogram and cumulative curve for all pebbles. Pebbles greater than 256 mm constitute the smallest percentage with an average of 2.22%. Particles of size 128—64 and 64—32 mm constitute the main bulk of beach pebbles (36.70 and 37.17% respectively). Nile Delta beach pebbles characterize by an average median of —6.12 ∅ (64 mm). Pebbles are moderately well sorted (0.64 ∅), negatively skewed (—0.10), and mesokurtic kurtosis (0.99).

Twenty six sample sites were investigated for lateral variation of particle size analysis along the coast. Lateral variations of pebble size are graphically shown in *Fig. 5*.

TABLE 2

Particle size variation and statistical parameters for beach pebbles along Nile Delta coast

Sample site	% of size classes					Statistical Parameter			
	256 mm	256—128 mm	128—64 mm	64—32 mm	32—16 mm	D_{50}	σI	SK_1	K_G
1	7.69	42.31	34.62	15.38	—	—7.00	0.78	0.12	0.87
2	21.43	50.00	21.43	7.14	—	—7.40	0.80	0.11	1.05
3	—	30.30	39.39	27.27	3.03	—6.50	0.92	—.05	0.94
4	—	30.30	36.67	30.30	3.33	—6.45	0.94	—.10	0.94
5	—	18.52	44.44	29.63	7.41	—6.25	0.81	—.16	0.94
6	—	7.69	50.00	30.77	11.54	—6.10	0,71	0.16	0.94
7	—	14.81	51.85	33.33	—	—6.30	0.53	—.19	1.02
8	—	11.54	69.23	19.23	—	—6.45	0.44	0.01	1.08
9	—	33.33	46.67	20.00	—	—6.65	0.70	—.08	0.87
10	9.68	19.35	51.61	19.35	—	—6.60	0.80	—.25	1.05
11	6.06	18.18	66.67	9.09	—	—6.65	0.63	—.23	1.29
12	6.25	31.25	43.75	18.75	—	—6.75	0.73	—.09	0.91
13	6.67	33.33	46.67	13.33	—	—6.80	0.71	—.13	0.94
14	—	10.00	46.67	43.33	—	—6.10	0.51	—.33	0.97
15	—	6.45	54.85	38.71	—	—6.15	0.43	—.23	0.99
16	—	3.13	43.75	46.88	6.25	—5.59	0.59	0.05	0.94
17	—	—	43.45	45.45	9.09	—5.90	0.68	—.02	1.00
18	—	—	42.86	39.29	17.86	—5.80	0.81	—.09	0.87
19	—	—	17.86	60.71	21.43	—5.45	0.53	—.07	0.87
20	—	—	30.00	53.33	16.67	—5.65	0.62	—.08	0.91
21	—	—	6.45	70.97	22.58	—5.30	0.42	—.05	1.04
22	—	—	6.67	63.33	30.00	—5.20	0.42	—.09	0.88
23	—	0.09	21.21	60.61	0.09	—5.75	0.73	—.22	1.20
24	—	5.56	22.22	61.11	11.11	—5.65	0.66	—.17	1.17
25	—	—	8.33	69.44	22.22	—5.35	0.43	—.05	0.95
26	—	—	5.00	40.00	55.00	—4.95	0.43	—.40	1.02
Mean	2.22	14.42	36.70	37.17	4.49	—6.12	0.64	—.10	0.99

The largest beach pebbles (>256 mm) are found in two restricted areas; just astride the Burullus outlet and between 27—36 km to the east. The percentage of largest pebbles ranges between 21.43 and 6.06% from west to east. It is believed that littoral current is often insufficient to move the larger pebbles along the coast, therefore, they concentrated in the two mentioned areas.

Pebbles range between 256—128 mm are well distributed than the other pebbles. Their percentage attain the maximum value (50%) near Burullus outlet. There is a steady decrease in the percentage of these particles to Kitchener drain where it reaches to 11.54%. Eastward, the percentage increases more or less gradually and attains the value of 33.33% in the location 36 km. It appears to decrease again rapidly where the percentage is reduced to 3.13% (location 45 km). Eastward of this location, such particles have disappeared, however, a small amount are only present near Gamasa.

Beach pebbles whith size 128—64 mm are dominantly found along the coast and characterized by a higher percentage of occurrence. There is a trend to a regular increase in the percentage from 21.43% near Burullus outlet to the maximum value of 69.23% near Kitchener drain. Toward the east, the percentage of particles decreases slowly with some fluctuations, then it decreases rapidly to Gamasa (6.67%). East

of Gamasa, the percentage increases again and then decreases to the minimum value (5%) because they are replaced by an abundance in finer pebbles.

Pebbles with size 64—32 mm are well distributed and behave in different way rather than the other populations. Between Burullus outlet and 3 km east of Ayash

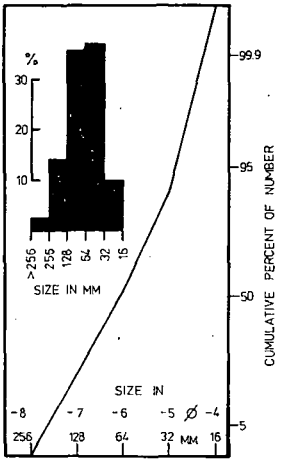

Fig. 4. Average histogram and cumulative curve for all beach pebbles.

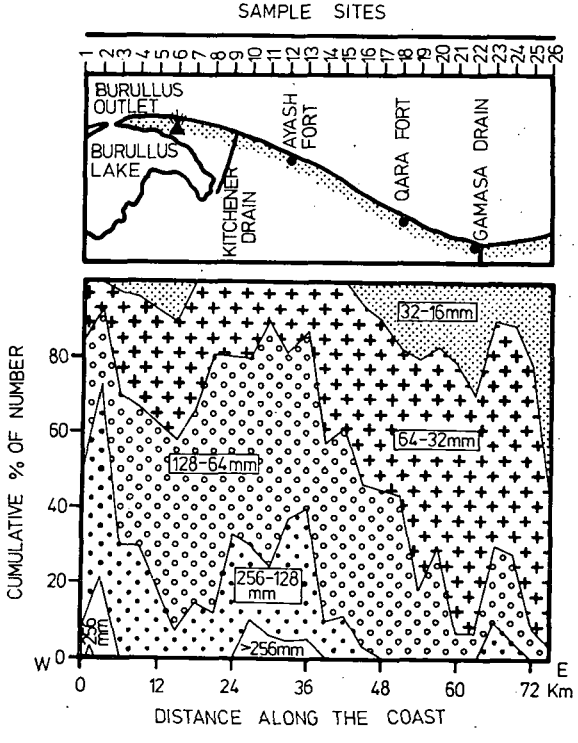

Fig. 5. Lateral variation of particle size of pebbles along Nile Delta coast.

Fort, the percentage ranges between 7.14 and 33.33%. Eastwards, it observed that the percentage increases rapidly with some fluctuations and attains the maximum abundance (70.97%) east of Gamasa.

The smallest beach pebbles (32—16 mm) does not occur dominantly along the coast, but they are only found in two areas *(Fig. 5)*. Between the locations 6—15 km, the percentage ranges from 3.03 to 11.54%. The pebbles appear again from the location 45 km, the percentage becomes higher and attains its maximum value (55%) in the eastern end.

It is observed from the lateral variation of beach pebbles size *(Fig. 5)* along the coast that:

1. The largest pebbles are distributed in limited areas while the smaller ones are well distributed and dominantly occurred with increasing trend. It is believed that the ordinary hydrodynamic factors (littoral current and waves) are often insufficient to move the larger pebbles along the coast. On the other hand, the smaller pebbles were washed out laterally by littoral current and shifted to the beach with ease by waves.
2. In such progressive decrease in pebble size, fluctuations might also result. With fluctuations, the largest pebbles will be moved only occasionally, whereas the smallest ones may be carried even when the transporting agent is at a minimum competency [PETTIJOHN, F. J., 1949].
3. The lateral variation of pebble size along the coast reflects a decreasing trend with the presence of three main peaks in the locations 3,36, and 66 km.

Distribution curves and grain size parameters

Pebble size distribution curves, plotted on probability paper, are illustrated in *Fig. 6*. It is clearly observed from the last figure that the cumulative curves are shifted gradually from the coarse to the fine area of the figure; *i.e.* there is a fining cycle median size from Burullus toward the east. It is also noticed that the three groups of curves commonly show a truncation with certain trend. Moreover, the angle of central part of curves shows a significant trend reflecting an improvement in sorting eastwards. Table 3 summarizes the last results.

Table 2 shows the statistical parameters (median, sorting, skewness, and kurtosis) for pebbles. They are illustrated graphically in *Fig. 7* where visual analysis of data can be made by plotting these parameters against distance along the coast.

Median tends to decrease gradually from west to east. At first, it decreases slowly from Burullus outlet (—7.4 ∅) to the location 36 km (—6.8 ∅). Eastwards, the decreasing trend in median became quick until it reaches to the minimum value (—4.95 ∅) in the eastern end of the investigated area. This is may be an indication for the active motion of pebbles during transport which is certainly responsible for the quick decreasing trend.

There is a general improvement in the standard deviation (sorting) from west to east with some fluctuations. It ranges between 0.94 ∅ (moderately sorted) east of Burullus outlet and 0.42 ∅ (well sorted) in the eastern end. *Fig.* 7 shows that both median and sorting follow each other in many locations.

Inclusive graphic skewness ranges between +0.16 and —0.40. The pebbles become more negatively skewed from west to the location 39 km. Eastwards, they tend to be more symmetrical and then again high negatively skewed near the end (—0.40).

The variation of graphic kurtosis behaves differently along the coast. It ranges between 0.87 (platykurtic) to 1.29 (leptokurtic). Kurtosis values tend to increase

TABLE 3

Characteristic features of cumulative curves

Features \ Location	Burullus to Kitchener	Kitchener to Gamasa	East of Gamasa
Median	—6.70 ∅	—6.00 ∅	—5.40 ∅
Truncation	90—80 %	80—60 %	45—30 %
Angle of slope	70°	75°	79°

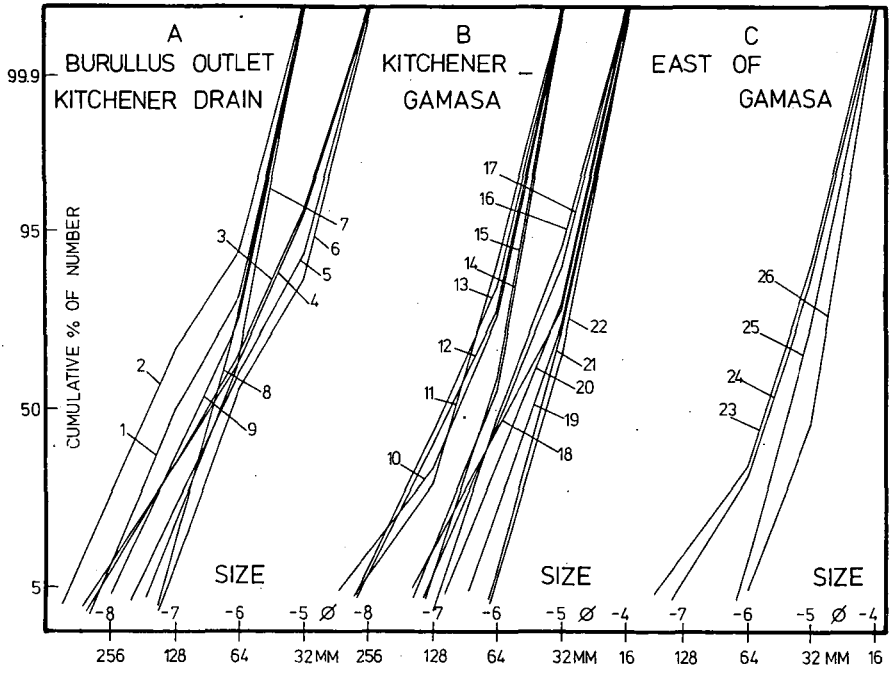

Fig. 6. Particle size distribution curves for beach pebbles. Numbers indicate sample sites.

generally from west to the location 30 km and then decrease with some higher values east of Gamasa.

The marked variations of median along the coast did not correspond to any change in other parameters, with the exception of sorting. Actually, these relationships can not be properly interpreted.

Size-sorting of pebbles

During lateral movement of sediment along the coast, hydrodynamic factors tend to sort particles according to their size and shape. Great attention has been given to the problem of whether size or shape is the dominant factor in the sorting of pebbles. Recent studies mentioned that waves sorted pebbles by shape on a beach and sorting, not abrasion, is the cause of the presence of discs pebbles high on the beach [KRUMBEIN, W. C. and GRIFFITH, J. S., 1938; VAN ANDEL, TJ. H. *et al.*, 1954; BLUCK, B. J., 1967; HUMBERT, F. L., 1968].

Along Nile Delta coast, beach pebbles show a progressive decrease in cumulative

percentage of larger pebbles, increase of smaller ones, decrease of median size and improvement of sorting *(Figs. 5* and *7)*. Such decreasing trend is caused, with the direction of eastward current, by decreasing availability of larger pebbles. There is also a significant correlation for the relationship between the standard deviation and the size of pebbles *(Fig. 8)*. The positive correlation shows that the larger pebbles are ill sorted, and the sorting improves when the pebbles becoming more smaller.

During the course of transport, the ability of pebbles to be abraded is high due to their clay-silt-sand components. There are also some instances where larger peb-

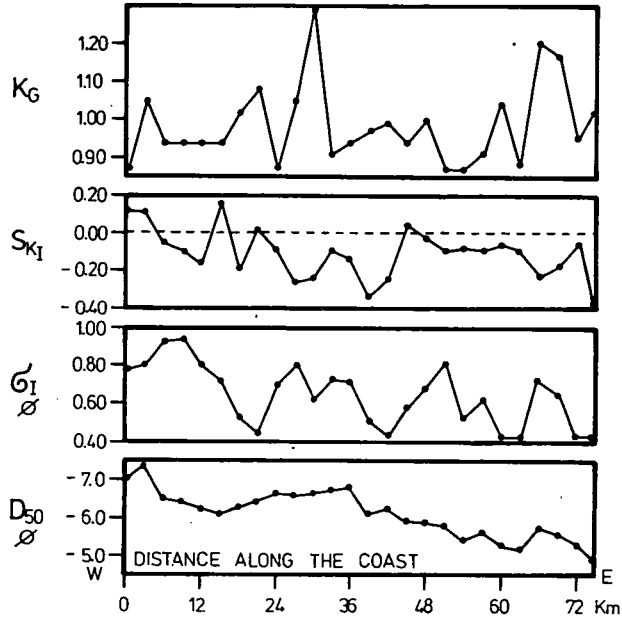

Fig. 7. Lateral variation of statistical parameters for beach pebbles.

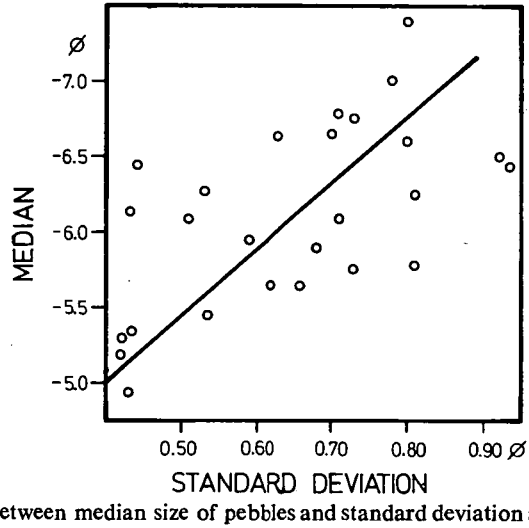

Fig. 8. Relationship between median size of pebbles and standard deviation along Nile Delta coast.

bles can be broken due to splitting and crushig (BLUCK, B. J., 1967]. By sorting processes, pebbles displaying a similarity of size are naturally separated by the action of waves because wave energy may be high enough to move all the different shape of pebbles. This is with the agreement of the relationship between size and sorting of pebbles. For these reasons, size-sorting plays a major role on beaches and is the dominant factor in the sorting of pebbles along Nile Delta coast.

Size-sorting processes due to littoral current drift may be responsible to the pebble size decreasing trend. Such trend is caused by either a current of decreasing strength or by the decreasing availability of larger pebble size away from west to east.

Peaks pattern

The study of the distribution of beach pebbles along the coast can be truly significant when it can related its distribution to the probable source area. In fact, pebble size variations reveal a progressive decrease of median size and an improvement of sorting along the coast. There has been, however, a pattern of peaks. They are marked by a higher percentage of large pebbles, higher median size and badly sorted than in neighbouring sites of sampling. These peaks can be seen in three locations and *Figs 5, 6* and *7* reflect them clearly. The first peak occurs just east of Burullus outlet and it is the sharpest one. The second peak can be found in the location 36 km, and it is smaller than the first one. The third peak is the smallest one and can be seen east of Gamasa drain. Eastwards of each peak, there is a directional gradiations in size of pebbles and sorting along with a considerable increase in the percentage of finer pebbles *(Fig. 9)*. Such trend may serve to indicate the sources supplied the pebbles.

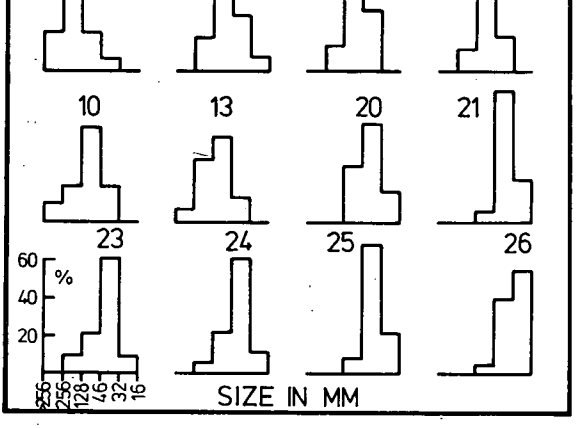

Fig. 9. Histograms for size classes distribution of beach pebbles. Observe the directional gradations in size and sorting from left to right within each peak. Numbers indicate sample sites.

Logically, the three major peaks are considered to be the secondary sources for pebbles, this is with the agreement of the eastward littoral current.

Whereas for the distribution of beach pebbles along the coast, it is observed that they are periodically added to the coast during winter storms. So, a primary source of these pebbles is not available in the coast itself and these pebbles should come from outside.

Primary source areas: a discussion

The aim of the present surveying and discussion would be identify the probable sources, the general path of pebbles from these sources and then along Nile Delta coast.

EMERY, K. O. [1955] mentioned that there are four main possible sources of beach pebbles: sea-cliff erosion, stream discharge, sea-floor erosion, and longshore transport from one or more of the first three primary sources. In fact, Nile Delta coast is sandy without any cliffs, and the main Nile branches do not discharge any sort of pebbles like that which are seen along the coast. But, the occurrence of large pebbles astride Burullus outlet, Kitchener and Gamasa drains can be assumed that the outlet discharge and the present drains may be the sources for pebbles formation. These drains discharge fine sand, silt and clay which are lithologically similar to pebble components. Coagulation between these components and salt water may be occurred. But it is difficult to relate the origin of pebbles to the load of channels due to lacking of pebbles near the other branches.

The stretch of pebbles coincides with a part of the coast where Nile branches discharged in ancient times (Sebennitic, Saitic, and Atribic). Offshore of this stretch, there are old lagoonal deposits which were formed during the low stands of sea level. So, some ideas related the origin of pebbles to these old lagoonal clays (personal communication with PROF. DR. M. G. BARAKAT, Geology Dept., Cairo Univ.).

Nile Delta beach pebbles do not come from the local erosion of sub-beach layers, nor do they seem to be formed by diagenesis in place [EL-FISHAWI, N. M. *et al.*, 1976]. On the other hand, at the top of Rosetta Submarine Banks, the CHAIN (an American Vessel) dredged lagoonal mudstone and sandstone which are lithologically similar to the beach pebbles along the coast [MISDORP, R. and SESTINI, G., 1976]. For these reasons, sea-flower erosion from the old banks is the probable source for Nile Delta beach pebbles.

A map of physiographic units of the Nile Delta continental shelf (after Coastal Erosion Studies, 1976) gives some ideas about the old topographic banks *(Fig. 10)*.

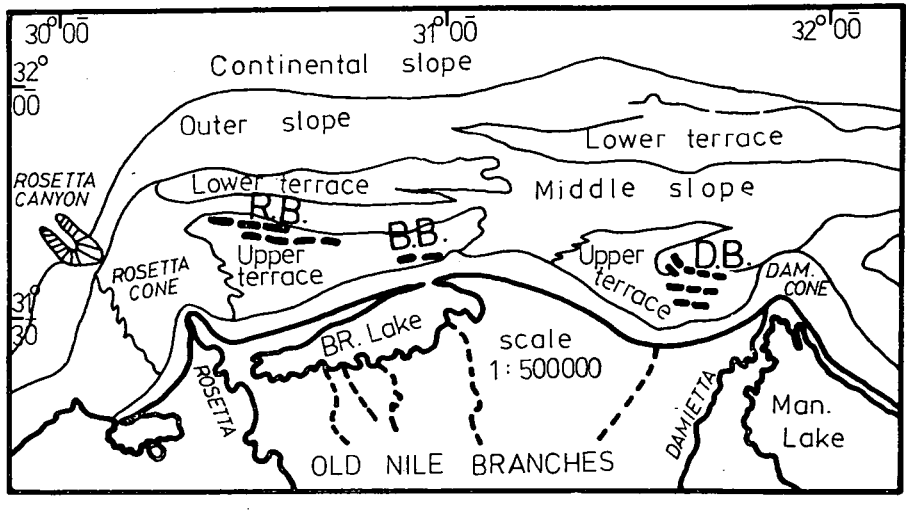

Fig. 10. Physiographic units of the Nile Delta continental shelf (after Coastal Erosion Studies, 1976), R. B. = Rosetta Banks, B. B. = Burullus Banks, D. B. = Damietta Banks.

These banks appear to be remnants of erosional surfaces, made of indurated sands with lagoonal muds, which may consider to be the primary sources for beach pebbles. Analyses of submarine morphology carried out by MISDORP, R. and SESTINI, G. [1976] illustrated that three old banks are occurred, they are Rosetta, Burullus, and Damietta *(Fig. 10)*.

Rosetta Banks located between long. 30° 23′ and 30° 42′ E (60—30 km NW off Burullus outlet) and marked by a line of small ridges and hills elongated NW—SE. Burullus Banks located 4—6 km north off Burullus outlet between long. 30° 53′ and 31° 00′. These hills parallel with coast and less elongated. Damietta Banks are a group of E—W hills, 10—20 km off Gamasa. They are three parallel ridges lie between long. 31° 35′ and 31° 43′, and 5—13 km long.

Now, the analysis made of beach pebbles suggests that the three peaks of size (secondary sources) are closely related to the locations of Rosetta, Burullus, and Damietta Banks (primary sources). Rosetta Banks appear to feed west Burullus outlet stretch with pebbles, while Burullus Banks feed the eastern stretch. Waves and swells approaching the coast from NNW and NW play an important role in onshore movement from primary sources to the coast. On the other hand, Damietta Banks seem to be responsible for feeding Gamasa coast with pebbles. However, the location of these banks (NE off Gamasa) does not agree with the approaching NNW waves. But in fact, winter waves coming from N and NE may throw a light on the processes of pebbles movement.

During storms, a lot of material is in suspension, and due to onshore movement, coarse sand is periodically added to the accretional areas of Burullus coast [Coastal Erosion Studies, 1976; EL-FISHAWI, N. M. *et al.*, 1976; EL-FISHAWI, N. M., 1977]. It is possible also that the pebbles appear to have come in the same way especially there are many evidences of large pebbles reaching the coast from known places even many km away from the shore [JOHNSON, D. W., 1919; EMERY, K. O. and TSCHUDY, R. H., 1941; SHEPARD, F. P., 1963; BASCOM, W., 1964].

To sum up, Nile Delta beach pebbles can be derived from the submarine banks. Materials from offshore reach the beach under the influence of wave action. Long waves move sediment in greater depth than short waves [KING, C. A. M., 1972]. So, during winter storms and summer swells waves are coming from NNW, NW, N and NE. Owing to their enough energy flux, they play an effective role in carrying sediments in suspension, the pebbles are then moved shorewards. The eastward littoral current is predominant and pebbles can be shifted sideway by ease to complete the processes of transport with directional gradation along the coast.

CONCLUSION

The distribution of beach pebbles along the eastern Nile Delta coast of Burullus is a function to the source area and sediment movement. Beach pebbles are periodically added to the coast during winter storms so that primary source is not available in the coast itself. The average pebble size generally decreases and sorting improves along the coast in the direction of littoral current from west to east. The decreasing trend of pebble size is mostly related to abrasion and size-sorting processes during transport. Lateral decreasing of median size results mainly from abrasion of particles. The ability of pebbles to abrasion is high owing to their clay-silt-sand components. Also, by size-sorting processes, pebbles displaying a similarity of size are naturally separated from associated by a decreasing trend of current, then waves with enough energy can shifted them easily to the coast.

Three beaches along the coast are characterized by presence of higher percentage of pebbles than the other beaches. This is do not agree with the eastward littoral drift and it have to be explained in the assumption that there are three secondary sources, derived from primary sources, because eastward of each peak there is a tendency to decrease the median size and improve the sorting.

Beach pebbles are considered remnants of old alluvial banks related to old Nile branches in classical times. During winter storms and summer swells, waves approaching the coast from NNW, NW, N and NE owing to their enough energy flux, pebbles are moved shorewards. The littoral current feeding from west to east complete the processes of transport by shifting the pebbles sideway with decreasing trend along the coast.

REFERENCES

BASCOM, W. [1964]: Waves and beaches. Anchor Books, Doubledy & Co., New York, 267 p.

BLUCK, B. J. [1967]: Sedimentation of beach gravels: Examples from South Wales. Jour. Sed. Pet., **37**, No. 1, p. 128—156.

BLUCK, B. J. [1969]: Particle rounding in beach gravels. Geol. Mag., **106**, p. 1—14.

CAILLEUX, A. [1945]: Distinction des Galets Marins et Fluviatiles. Soc. Geol. France Bul., 5th. serie, t. 15, p. 375—404.

CAILLEUX, A. [1947]: L'indice demousse: Definition et Premiere Application. C. R. S., Soc. Geol. de France, p. 250—252.

CARR, A. P. [1971]: Experiments on longshore transport and sorting of pebbles: Chesil Beach, England. Jour. Sed. Pet., **41**, No. 4, p. 1084—1104.

COASTAL EROSION STUDIES, [1973]: Detailed Technical Report. Project Egy. 70/581, UNESCO /ASRT/ UNDP, Alex., 259 p.

COASTAL EROSION STUDIES, [1976]: Detailed Technical Report on Coastal Geomorphology and Marine Geology, Nile Delta. Project Egy. 73/063, UNESCO /ASRT/ UNDP, Alex., 175 p.

EL-FISHAWI, N. M. [1977]: Sedimentological studies of the present Nile Delta sediments on some accretional and erosional areas between Burullus and Gamasa. M. Sc. thesis, Alex. Univ.

EL-FISHAWI, N. M., SESTINI, G., FAHMY, M., SHAWKY, A. [1976]: Grain size of Nile Delta beach sands. In: UNESCO /ASRT/ UNDP-Proceedings of seminar on Nile Delta Sedimentology, Alex., Oct. 1975, p. 79—94.

EMERY, K. O. [1955]: Grain size of marine gravels. Jour. Geology **63**, p. 39—49.

EMERY, K. O. and TSCHUDY, R. H. [1941]: Transportation of rock by kelp. Geol. Soc. America. Bull., **52**, p. 855—862.

FOLK, R. L. and WARD, W. C. [1957]: Brazos River bar, a study in the significance of grain size parameters. Jour. Sed. Pet., **27**, No. 1, p. 3—27.

HUMBERT, F. L. [1968]: Selection and wear of pebbles on gravel beaches. Univ. Groningen. Geol. Inst. Publ., **190**, 144 p.

JOHNSON, D. W. [1919]: Shore processes and shoreline development. Wiley and Sons, New York, 584 p.

KING, C. A. M. [1972]: Beaches and coasts. London, Edward Arnold Ltd. 570 p.

KRUMBEIN, W. C. [1941]: Measurement and geological significance of shape and roundness of sedimentary particles. Jour. Sed. Pet., **11**, p. 64—72.

KRUMBEIN, W. C. and GRIFFITH, J. S. [1938]: Beach environment in Little Sister Bay, Wisconsin. Geol. Soc. Amer. Bull., **49**, p. 629—652.

KUENEN, PH. H. [1964]: Experimental abrasion: 6. Surf action. Sedimentology **3**, p. 29—43.

LANDON, R. E. [1930]: An analysis of beach pebble abrasion and transportation. Jour. Geology **38** p. 437—446.

MANOHAR, M. [1976]: Dynamic factors affecting the Nile Delta coast. In UNESCO /ASRT/ UNDP-Proceedings of seminar on Nile Delta sedimentology, Alex., Oct. 1975, p. 104—129.

MARSHALL, P. [1928]: The wearing of beach gravels. Tran 8. & Proc., New Zealand Inst., **58**, p. 507—532.

MISDORP, R. and SESTINI, G. [1976]: Main features of the continental shelf topography of the Nile Delta. In: UNESCO /ASRT/ UNDP-Proceedings of seminar on Nile Delta sedimentology. Alex., Oct. 1975, p. 145—161.

PETTIJOHN, F. J. [1949]: Sedimentary rocks. Harper & Brothers Publishers, New York, p. 419—420.

QUÉLENNEC, R. E. [1977]: Eastern Mediterranean stormy weather and wave climatology off Nile Delta. In: UNESCO /ASRT/ UNDP-Proceedings of seminar on Nile Delta coastal processes. Alex., Oct. 1976, p. 81—115.
SHEPARD, F. P. [1963]: Submarine geology. Harper & Row, New York, 557 p.
SPALLETTI, L. A. [1976]: The axial ratio C/B as an indicator of Shape selective transportation. Jour. Sed. Pet., **46**, No. 1, p. 243—248.
VAN ANDEL, TJ. H., WIGGERS, A. J. and MAARLEVELD, G. [1954]: Roundness and shape of marine gravels from Urk (Netherlands), A comparison of several methods of investigation. Jour. Sed. Pet., **24**, No. 2, p. 100—116.
WENTWORTH, C. K. [1919]: A laboratory and field study of cobble abrasion. Jour. Geology **27**, p. 506—521.
Manuscript received, May 5, 1981

B. MOLNÁR
József Attila University
Department of Geology and
Paleontology
6722 Szeged, Egyetem u. 2.
Hungary

NABIL M. EL-FISHAWI
Institute of Coastal Research
Alexandria, Egypt.
Present adress:
József Attila University
Department of Geology and
Paleontology
6722 Szeged, Egyetem u. 2.
Hungary

Acta Mineralogica-Petrographica, Szeged, XXV/1, 41—61, 1981

NILE DELTA BEACH PEBBLES II: ROUNDNESS AND SHAPE PARAMETERS AS INDICATORS OF MOVEMENT

N. M. EL-FISHAWI and B. MOLNÁR

ABSTRACT

This paper discusses roundness, sphericity, flatness index, flatness ratio and elongation parameters of Nile Delta beach pebbles. Generally 1365 pebbles were analysed and a total of 12 285 measurements was done. Beach pebbles were measured for the main diameters, large inscribing circle and diameters of corners. Several indices was used to study the variations in the roundness and shape of pebbles. Three principal methods of evaluating roundness and two methods for sphericity are correlated in relation to their results.

Flatness index is more close to being the inverse of the maximum projection sphericity of SNEED, E. D. and FOLK, R. L. [1958] than the KRUMBEIN, W. C. [1941] measure. Beach pebbles show a significant change with decreasing size, they become well rounded, more spherical, less elongate and more flattened in shape.

On light of roundness, sphericity and other shape parameters, the relations to distance of transport along the coast are analysed. The increasing in roundness which accompanies the decreasing in sphericity and flatness paints to beach pebbles abrasion as a main cause for movement along the coast. The increasing in flatness index and decreasing in elongation index of beach pebbles from the points of supply towards the east was so marked. Geometrically, this modification should take place by abrasion chiefly of both short and long axes with slightly different rates.

INTRODUCTION

Beach pebble is an unconsolidated, natural accumulation of rounded rock fragments resulting from erosion and consisting predominantly of particles larger than sand.

Early studies of beach pebbles were done by many authors. DUNN, E. J. [1911] observed that slate pebbles were discoidal and uniform-wearing rocks developed spherical forms. WENTWORTH, C. K. [1922] found that massive igneous rocks yielded flat pebbles on New England beaches. MARSHALL, P. [1928, 1930] concluded that beach pebbles were abraded flat by the sliding action of the surf or by the swash of finer material over them. LANDON, R. E. [1930] experimentally concluded that discs should accumulate high on the beach while the spheres should lie at the foot.

More recent works has been published and gave a great advance to the pebbles studies. CAILLEUX, A. [1945, 1947, 1952] studied the flatness of beach pebbles on varied rock types and related it to marine wear. SNEED, E. D. and FOLK, R. L. [1958] showed that sphericity depends most importantly on the inherent abrasional properties of the different rock types. On the basis of particle shape, BLUCK, B. J. [1967] subdivided the gravels of South Wales beaches into four zones and related these features to different settling velocities of different shape particles. KING, C. A. M., and BUCKLEY, J. T. [1968] succeeded to differentiate between Arctic environments by using flatness, roundness and sphericity. DOBKINS, J. E. and FOLK, R. L. [1970] mentioned

that roundness increases from river to beaches while sphericity decreases. They found also that wave height is crudely related to mean beach pebble roundness.

CARR, A. P. [1971] concluded that lateral movement of individual pebbles is not necessarily greater under storm conditions, and added that there is a relationship between pebble size and longshore movement. GOEDE, A. [1975] related the downstream changes in shape of pebbles of rhyodacite and sandstone in Tambo River to four main processes: abrasion, shape-sorting, dilution and breakage. ORFORD, J. D. [1975] concluded that the degree of shape zonation appears to be a function of wave energy conditions, with maximum pebble zonation appearing as a product of swell wave action. By using the axial ratio C/B of Sarmiento River and Pellegrini Lake, SPALLETTI, L. A. [1976] found that their values tend to increase with transport distance when the movement of particles is in traction, and to diminish in suspension.

This paper is a continuation to the previous studies of beach pebbles morphology along the coast. The main part includes the study of pebble roundness, sphericity and shape analysis to provide a body of basic data to be used in the study of sediment movement.

SAMPLING

Nile Delta beach pebbles located between 3 km west of Burullus outlet and 12 km east of Gamasa drain. They are continous over distance of 75 km. To study the lateral variation in pebbles moprhology, sampling sites were chosen at 3 km intervals *(Fig. 1)*.

A total number of 1365 pebbles was measured along 26 localities. At each locality, a set of pebbles was collected by taking all pebbles within an area of 4 square meters to obtain a number of pebbles ranges from 62 to 75. At some localities, it

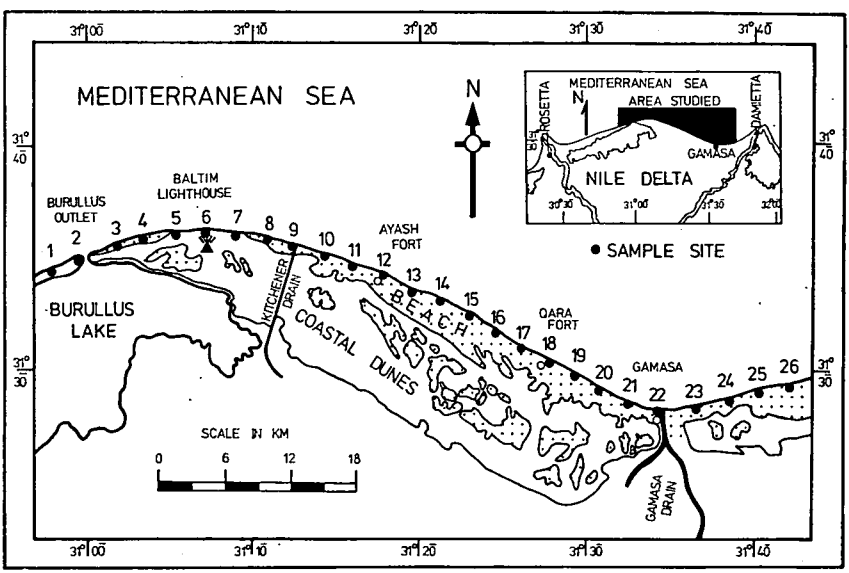

Fig. 1. Locality map showing sampling sites for Nile Delta beach pebbles.

was necessary to collect a few pebbles outside the considerable area to cover the occured size classes within the locality.

Size classes, defined on the basis of the long dimension of the pebble were >256 mm, 256—128 mm, 128—64 mm, 64—32 mm, and 32—16 mm(>—8∅, —8 to —7 ∅, —7 to —6 ∅, —6 to —5 ∅, and —5 to —4 ∅). In each size class, 10—25 pebbles were measured.

METHODS OF STUDY

Roundness: According to several authorities, roundness would be as follows:

WENTWORTH, C. K. [1922a]: $D_k/0.5(L+I)$

CAILLEUX, A. [1947]: D_k/L

WADELL, H. [1933]: $\Sigma D_c/ND_i$

KUENEN, PH. H. [1956]: D_k/I

DOBKINS, J. E. and FOLK, R. L. [1970]: D_k/D_i

where: L: long axis of the pebble, I: intermediate axis, D_k: diameter of the sharpest corner, D_c: diameter of curvature of corners, D_i: diameter of the largest inscribed circle, N: number of corners.

Diameter of corners and largest inscribed circles are measured with a nest of concentric coloured circles duplicated on transparent plastic film. Circles are spaced logarithmically at the equivalent of quarter phi unit intervals. To measure the diameter of the corners, the largest inscribed circle and the axes, the pebble is laid flat on its maximum projection face. The last five measures for roundness are computed.

Sphericity: It is quantitative parameter measuring the departure of a body from equidimensionality. In other terms it measures the ratio between the three major dimensions of a particle. The three axes (L, I, S) of each pebble were measured according to the method suggested by KRUMBEIN, W. C. [1941]. In this paper, it was decided to use the following two famous sphericity methods:

KRUMBEIN, W. C. [1941]: $\sqrt[3]{IS/L^2}$

SNEED, E. D., and FOLK, R. L. [1958]: $\sqrt[3]{S^2/LI}$

In his evaluation of several sphericity indices, HUMBERT, F. L. [1968] found that the maximum projection sphericity of SNEED and FOLK [1958] was the most satisfactory in beach pebble studies.

Flatness ratio and flatness index: These two pebble shape parameters introduced by WENTWORTH, C. K. [1919, 1922a] in one of the first attempts to quantify pebble shape. They are given as:

Flatness ratio $=(L+I+S)/3$

Flatness index $=(L+I)/2S$

CAILLEUX, A. [1947, 1952] adopted the last measure change and is incorrectly called the Cailleux Index.

Elongation index: It was described by SCHNEIDERHÖHN, P. [1954] as the ratio of the greatest width to the greatest length (I/L). FOLK, R. L. [1968] suggested the least projection widths and lengths to be used. I/L and S/I are parameters used also by ZINGG, TH. [1935] to differentiate spherical and rods clasts from those of discoidal and bladed form.

(L—I)/(L—S) ratio: This measure was used by SNEED, E. D., and FOLK, R. L. [1958] in the sphericity-form diagram. The value (L—I)/(L—S) defines whether the intermediate axis is closer in size to the short or to the long axis and as a result it gives three different shapes (platy, bladed and elongated).

Comparison of various roundness and sphericity measures:

Five measures for roundness have been computed; the roundness of WENTWORTH, C. K. [1922a], WADELL, H. [1933], CAILLEUX, A. [1947], KUENEN, PH. H. [1956], and DOBKINS, J. E. and FOLK, R. L. [1970]. Some of the last measures show great varieties while the others varying within a small range. For Nile Delta beach pebbles, it was found that the long axis (L) is generally larger than both the intermediate axis (I) and the diameter of the largest inscribing circle (D_i). On the other hand, (D_i) is close to (I) in most of pebbles. Logically, the roundness of WADELL, H. [1933] is the highest value because it depends on the average diameter of all corners. When the diameter of the sharpest corner (D_k) is dividing by the D_i, I, L, and (L+I)/2, it can be found that the roundness of DOBKINS and FOLK (the modern measure) is closely related to KUENEN measure, has small differences with WENTWORTH measure, and it is much higher than CAILLEUX measure. Table 1 shows the results of various measures related to DOBKINS and FOLK measure.

TABLE 1

Various roundness measures related to DOBKINS *and* FOLK *[1970]*

Measures	WENTWORTH (1922b)	WADELL (1933)	CAILLEUX (1947)	KUENEN (1956)	DOBKINS & FOLK (1970)
Average roundness	0.304	0.470	0.265	0.362	0.393
Percentage	77%	120%	67%	92%	100%

The roundness of DOBKINS and FOLK runs about 8—23% higher than both of WENTWORTH and KUENEN, but 33% higher than that of CAILLEUX and it is big difference. It averages also 20% lower than that of WADELL. For this reason, the correlation may be made between the roundness of DOBKINS and FOLK, CAILLEUX (the owlest value) and WADELL (the highest value).

Two famous measures of sphericity were computed; KRUMBEIN, W. C. [1941] sphericity which modified from WADELL, H. [1934] and SNEED, E. D., and FOLK, R. L. [1958] sphericity. The maximum projection sphericity of SNEED and FOLK takes into consideration the hydraulic behaviour of the particle and therefore is a more actualistic concept of sphericity and preferred measure. The average sphericity for all pebbles according to SNEED and FOLK measure is 0.265, while it is 0.433 in the measure of KRUMBEIN. Thus, the maximum projection sphericity runs about 40% lower than that of KRUMBEIN measure.

Fig. 2 shows the mean roundness and sphericity for various measures along Nile Delta coast pebble beaches. Regarding the roundness, it is found that the three measures of WADELL, CAILLEUX, and DOBKINS and FOLK follow each other along the coast. With the direction of movement from west to east, the difference between WADELL and DOBKINS and FOLK roundness reduces gradually from 0.20 to 0.05. Such decreasing trend is due to the effect of abrasion which tends to reduce the corners of pebbles from four or more to two and the pebbles become more rounded. Nearly, CAILLEUX roundness keeping the same difference with the other two measures.

Considering the sphericity along the coast, it is observed that the maximum projection sphericity of SNEED and FOLK follows quite closely that of KRUMBEIN.

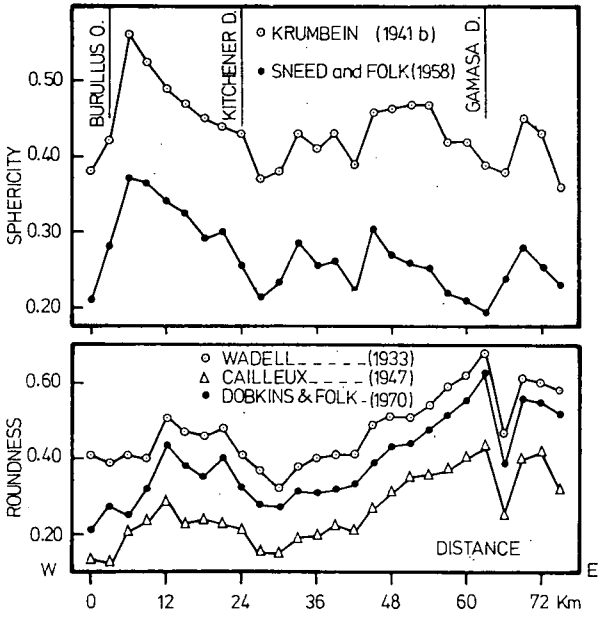

Fig. 2. Mean sphericity and roundness for various measures along Nile Delta pebble beaches.

(Fig. 2). The two measures show a wide difference which reflect the ratio between the main axes of pebble. Nile Delta beach pebbles are so flat because the short diameter is very small (32—2 mm) regarding to the other two diameters (300—12 mm). As a result of this, the maximum projection sphericity shows a high difference comparing to KRUMBEIN measure. But, however, by tracing the sphericity along the coast from west to east *(Fig. 2)*, it is found that the difference between the two measures gradually increases from 0.15 to 0.20. This is because the pebbles become more flattend in shape near the eastern end of movement.

Correlation between couples of roundness and sphericity

The relations between couples of roundness for various measures [WADELL, H., 1933; CAILLEUX, A., 1947; DOBKINS, J. E., and FOLK, R. L., 1970] usually follow a positive correlations *(Fig. 3A)*. In each relation the axes "X" and "Y" represent the mentioned first and second measure successively. *Fig. 3A* depends on both the mean roundness in each pebble class and the mean roundness for all pebbles on each locality. It is clearly seen in *Fig. 3A* that the relation couple of roundness follow a slight curved line and each couple keeps the same difference to the other. In other ways, it is reflecting the features of axes and mentioned that various measures of roundness are dependable populations. The same result could be seen in *Fig. 3B* where the relation between KRUMBEIN and SNEED and FOLK sphericities is drawn. In fact, such relationships can be used to convert both roundness and sphericity from one measure to the other depending upon the last two Figs.

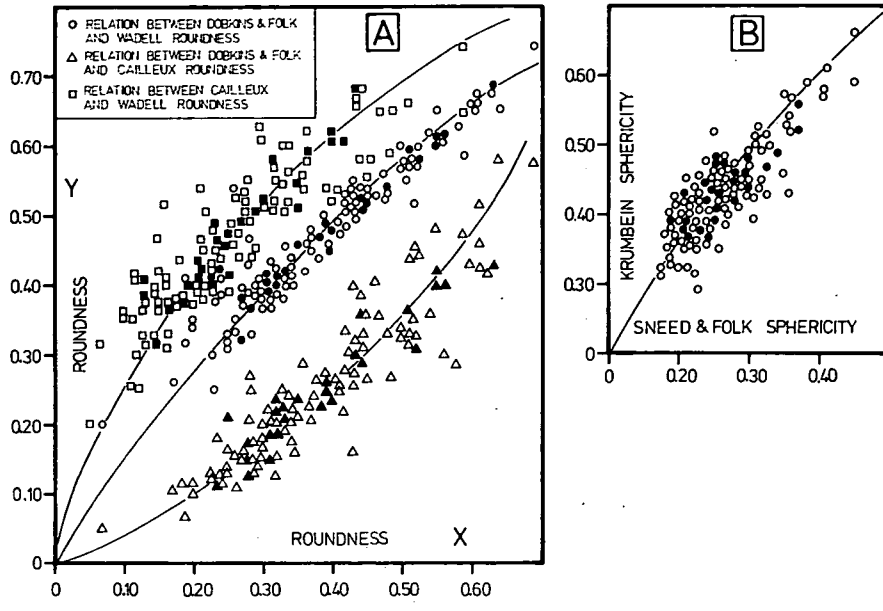

Fig. 3. Relation between couples of roundness *(A)* and couples of sphericity *(B)* .White symbol represents the mean value in each pebble class while the black one represents the mean in each location.

Correlation between flatness index and sphericity

A plot was made of sphericity on each locality (using both measures of KRUMBEIN, W. C. [1941]; SNEED, E. D., and FOLK, R. L., [1958] *versus* flatness index of WENTWORTH, C. K. [1922 a]. The association between the values is shown in *Fig. 4.* The available data plot as curved line which means that the function is of the type $Y = bX^a$ where Y is the sphericity, X is the flatness index, a is coefficient

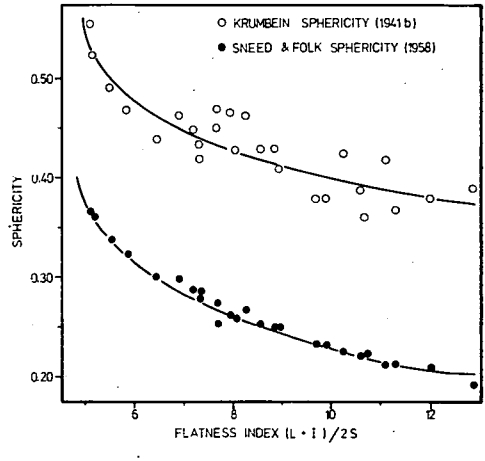

Fig. 4. Correlation between flatness index and sphericity measures.

and b is a constant. It is apparent that as the flatness index increases the sphericity decreases and the two values stood in inverse relations to each other. HUMBERT, F. L. [1968] and KING, C. A. M. and BUCKLEY, J. T. [1968] also noted the same relationship.

The negative correlation between KRUMBEIN sphericity and flatness index shows more individual deviation of values from the mean curved line *(Fig. 4)*. On the other hand, the relation of SNEED and FOLK sphericity to flatness index represents a smooth curved line without deviations and the individual values are well spreaded along the curved line. The proposed measure of SNEED and FOLK "the maximum projection sphericity" takes into consideration the hydraulic behaviour of the particles. Therefore, this measure seems to te be closely related to the flatness index which reflects the actual settling velocities of irregular particles in water. Thus, the flatness index came more close to the maximum projection sphericity than the KRUMBEIN measure which least reflects the hydraulic behaviour.

Sphericity-form diagram

Sphericity-form diagram was used to determine the form of Nile Delta beach pebbles. In order to make comparison between form and size of pebbles, *Fig. 5* shows data distribution area for each size class. Beach pebbles larger than 256 mm are very significantly bladed to slightly elongated with lowest sphericity values. Pebbles with size 256—128 mm are completely bladed with higher sphericity values

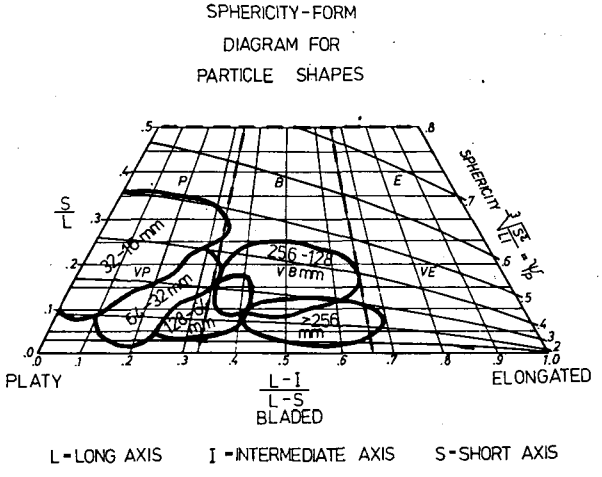

Fig. 5. Sphericity — form diagram for particle shapes. This triangle graph shows data distribution area for each mean pebble class in all localities.

than the largest size. All pebbles within the 128—64 mm range from slightly bladed to slightly platy but with sphericity values lower than the last size class. Smaller pebbles with size classes 64—32 mm and 32—16 mm show a distinct tendency to be more platy with an increasing in sphericity to attain the maximum values. Thus, the form changes are shown well in *Fig. 5*. With decreasing size, pebbles tend to change from slightly elongate or bladed to platy. In the same trend, pebbles become more spherical. Therefore, the form of Nile Celta beach pebbles is significantly a function of size.

Pebble size as a function to roundness and shape parameters

Nile Delta beach pebbles show a significant change of roundness, sphericity, flatness index, flatness ratio, elongation index and the platy — bladed — elongated ratio with size of pebbles. The results are illustrated in Table 2 and *Figs 6* and *7*.

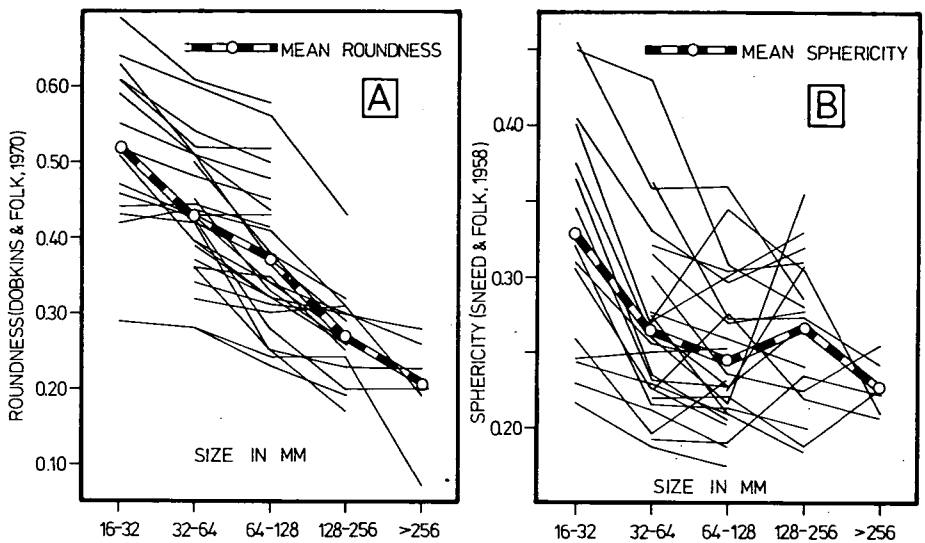

Fig. 6. Relation of roundness *(A)* and sphericity *(B)* to size of Nile Delta beach pebbles in each locality. Pebbles markedly increase in roundness with decreasing size. Smaller sizes tend to be more spherical than the larger ones.

TABLE 2

Mean roundness and shape parameters compared with size classes of beach pebbles

Size class in mm	Roundness	Sphericity	Flattness index	Flatness ratio (mm)	Elongation index	(L—I)/(L—S)
>256	0.21	0.227	9.93	149	0.58	0.46
256—128	0.27	0.268	8.34	85	0.61	0.44
128— 64	0.37	0.247	9.39	52	0.69	0.35
64— 32	0.43	0.265	8.56	31	0.78	0.25
32— 16	0.52	0.329	6.00	19	0.88	0.15

Size and roundness

Simply stated, the beach pebble populations markedly increase in roundness with decreasing size. Among the five size classes, beach pebbles larger than 256 mm show the worst rounding. As illustrated in Table 2 and shown in *Fig 6A*, the roundness of largest size ranges between 0.07 and 0.28 with an average of 0.21. With decreasing size, the roundness tends to increase gradually. The smallest pebbles 32—

16 mm show the best rounding. Their roundness value ranges between 0.29 and 0.69 with an average of 0.52. The majority of the individual lines, representing the change in roundness, behave with a lesser degree than the average line. In other words, the roundness increases very slowly but in some cases remains nearly constant.

Due to the action of approaching waves, pebbles according to their size show a certain tendency level of sliding and moving. As a result, each size attains a certain roundness value. The nearly straight line of mean roundness connected between size classes *(Fig. 6A)* may support such tendency. Small pebbles are easily sliding and for them the abrasion during movement is enough to produce well rounding corners and to reduce its number from four or more to one or two. The difference in roundness values within the size classes may represent also up-and-down drift pebbles and was assigned to the distance of transport.

Incomplete data from PETTIJOHN, F. J. [1957] suggest that the coarsest fraction of outwash gravels (64—8 mm) was better rounded than the smallest size. But, in fact, the difference in roundness value between the gravel classes ranges between 0.06—0.09. Moreover, his roundness value for 32—16 mm compares closely with the mean value of smallest *Nile Delta beach pebbles* (0.52). In casual examination of Colorado River pebbles, SNEED, E. D. and FOLK, R. L. [1958] found an increase of roundness with increasing size. There exists a middle grain size of pebbles which shows the best rounding [KUENEN, PH. H., 1964; FÜCHTBAUER, H., and MÜLLER, G., 1970]. In Tahiti-Nui, DOBKINS, J. E., and FOLK, R. L. [1970] found that the smallest pebbles on sandy beaches are well rounded than that on a gravelly beaches, and generally the largest and smallest pebbles are less rounded.

Size and sphericity

Nile Delta beach pebbles show a sort of change of sphericity with size over the range from larger than 256 mm to 16 mm *(Fig. 6B,* Table 2*)*. However, the difference between the average lowest and highest sphericity values of size classes is about 0.102, but the relation shows an increase in sphericity with decreasing size with the exception of size class 256—128 mm. Beach pebbles larger than 256 mm have the lowest mean sphericity value of 0.227 and range between 0.208 and 0.254. The smallest pebble size 32—16 mm ranges between 0.216 and 0.453 with an average of 0.329. Generally, Nile Delta beach pebbles show small size-to-size sphericity variation but greater pebble-to-pebble variation within each size class. So, regarding the relation between Nile Delta pebble size and both roundness and sphericity, it can be said that roundness well represent this relation and serves better than sphericity.

Little extensive study has been carried out in the relation between size and sphericity. PLUMLEY, W. J. [1948] found that 64—32 mm pebbles of limestone had higher sphericities than did 32—16 mm pebbles. CARROLL, D. [1951] found no significant change of sphericity with three size classes of sandstone pebbles. PETTIJOHN, F. J. [1957] cites many examples of a sphericity increase with size, but they are examples taken from sand range. SNEED, E. D., and FOLK, R. L. [1958] noted the tendency for small pebbles to have higher sphericity than larger ones in Colorado River. DOBKINS, J. E., and FOLK, R. L. [1970] observed that the largest beach and river pebbles have the lowest sphericities. It now appears probable that the maximum of the sphericity *versus* size curve occurs in the coarse sand to granule range and that particles both coarser and finer than this have continually decreasing sphericity.

Flatness index, the first sphericity measure which suggested by WENTWORTH, C. K. [1922a], shows the same behaviour of maximum projection sphericity with relation to size. Flatness index decreases with decreasing size as shown in *Fig. 7A.*

A drop in flatness index is observed for the pebble size 256—128 mm, this drop is reflected also by the sphericity measure. Flatness index and sphericity stood in inverse relations to each other as shown in *Fig. 7A*; as the flatness index decreases sphericity increases.

Flatness ratio is one of the first attempts to quantify pebble shape and was introduced by WENTWORTH, C. K. [1919]. The relation between flatness ratio and size shows a fantastic decreasing trend *(Fig. 7B)*. A smooth curved line connected between size classes can be shown. Flatness ratio decreases gradually with decreasing size without any drop. The individual curves also show the same picture and there is no overlapping in the flatness values for the different size classes. Thus, flatness ratio can be used to differentiate well between size classes of Nile Delta beach pebbles.

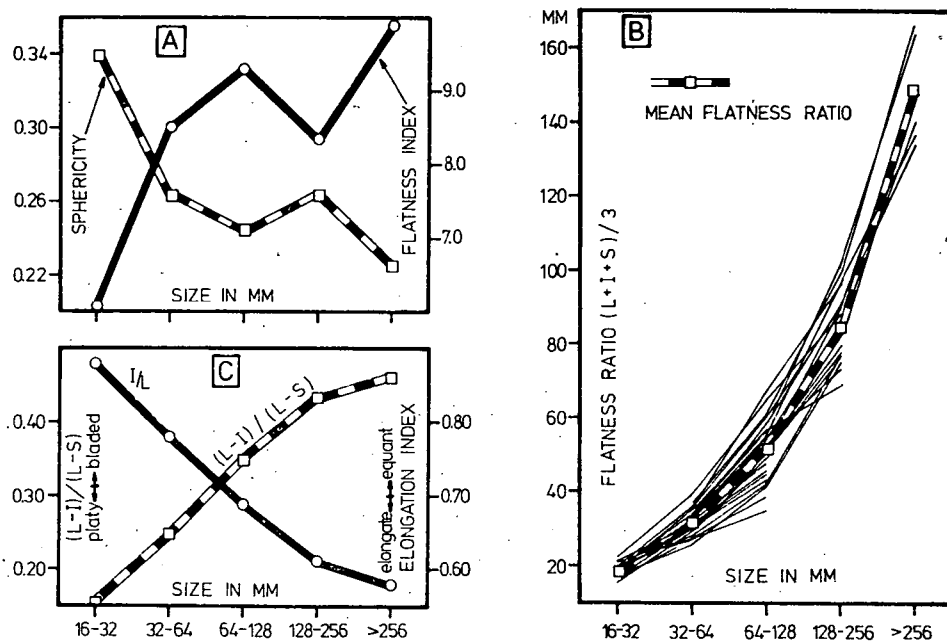

Fig. 7. Relations of shape parameters to size of Nile Delta beach pebbles. *A* — Sphericity and flatness index. *B* — Flatness ratio. *C* — Elongation index (I/L) and (L—I)/(L—S) value.

Size and pebble elongation

Two formulae can be used to describe the elongation of beach pebbles. The first formula is (L-I)/(L-S) value which classifies the form of pebbles to platy, bladed and elongated. The second formula is the elongated index (I/L) which gives three main classes: equant, intermediate and elongate.

Nile Delta beach pebbles show marked difference in the (L-I)/(L-S) value with size as shown in *Fig. 7C*. There is a great tendency for the pebbles to change from bladed to platy with decreasing size. However, the difference between the two larger classes is small, but the mean value decreases directly with constant rate toward the smallest pebble size.

The same relation is observed between the elongation index (I/L) and size.

There is a regular increasing in the elongation index with decreasing size. In other words, larger pebbles tend to be elongated while the smaller ones tend to be equant or less elongated *(Fig. 7C)*.

A scatter plot between (L—I)/(L—S) value and (I/L) shows that there is a linear relationship between the two parameters and they are inversely reflected the same description of elongation trend of beach pebbles. Although elongation index is independent upon the short axis of pebbles, it gives also the same features regarding to (L—I)/(L—S) value. In fact, this is an indication to the highly flatness of Nile Delta beach pebbles.

Characteristic features of beach pebbles

The relation between pebble size and roundness, sphericity and other shape parameters is not usually random, but it follows a sort of decreasing or increasing trend. Such change is shown as a function of selective abrasion effect among different size population and depends on the distance of transport.

Nile Delta beach pebbles are generally flattened in shape, nearly with the same composition (sand+silt+clay) without any tendency to partings. On the other hand, they show a wide variety in size (>256—16 mm). So, the selective abrasion of beach pebbles depends on size and hydrodynamic factors affecting the movement of pebbles. Wave heights of about 80 cm are average for Nile Delta coast. During the storm season, the average wave heights are 130 cm with maxima never exceed 300 cm. Littoral current generally feeds from west to east with an average velocity of 80 cm/sec [MANOHAR, M. 1976]. Thus, the significant change of pebble parameters with size can be related directly to the effect of hydrodynamic factors. Due to the action of approaching waves, the beach pebbles show some varieties according to their effect. It is thought that wave heights have not the ability to move all sizes with the same degree. Therefore, for each pebble size there is a certain tendency level of moving and as a result certain features.

For the smallest beach pebbles, they have the highest mean roundness and sphericity, lowest flatness ratio, and highest elongation index. Of course, small pebbles are easily washed by current and gentle waves which can apparently slide and bounce them randomly to obtain their characteristic feautres. On the other hand, larger pebbles show the lowest mean roundness and sphericity, highest flatness ratio, and lowest elongation index. PETTIJOHN, F. J. [1957] mentioned that the larger pieces are most readily rounded. But local materials of coarse grain may not be as well rounded as the finer far-travelled materials. Of course, these differences were assigned to differences in distance of transport. It was observed that larger beach pebbles were concentrated only in three restricted areas along Nile Delta coast. So, the larger pebbles are not always in motion because hydrodynamic factors are often insufficient to move then enough up-and-down the beach face and also to a long distance. Thus, larger pebbles do not well rounded.

Pebles movement and its relation to roundness, sphericity, flatness and elongation index

An investigation has been made to analyse the movement direction of pebbles along 75 km strecth of Nile Delta coast. What started out as a simple study of roundness and shape parameters of beach pebbles has become very complex. This is largely due to the presence of three secondary sources, variable influence of hydrodynamic factors affecting the coast and the influence of pebble size. The results are illustrated in Table 3 and *Figs 8* through *10*.

TABLE 3

Mean roundness, sphericity and other shape parameters along the coast

Localities	Sampling site no.	Roundness	Sphericity	Flatness index	Flatness ratio (cm)	Elongation index	(L—I)/(L—S)
0.0 km	1	0.21	0.210	11.98	7.99	0.69	0.32
3.0	2	0.28	0.282	7.28	10.20	0.61	0.44
6.0	3	0.25	0.368	5.08	5.31	0.85	0.18
9.0	4	0.32	0.364	5.14	5.26	0.77	0.29
12.0	5	0.44	0.338	5.50	4.67	0.73	0.32
15.0	6	0.38	0.326	5.85	4.53	0.69	0.37
18.0	7	0.35	0.290	7.20	5.64	0.72	0.33
21.0	8	0.40	0.303	6.46	5.47	0.65	0.40
24.0	9	0.32	0.255	8.54	6.28	0.74	0.30
27.0	10	0.28	0.214	11.30	7.67	0.65	0.38
30.0	11	0.27	0.234	9.67	8.35	0.63	0.40
33.0	12	0.31	0.285	7.29	7.65	0.67	0.38
36.0	13	0.31	0.254	8.95	8.25	0.67	0.37
39.0	14	0.32	0.261	8.01	5.39	0.74	0.30
42.0	15	0.33	0.223	10.63	5.25	0.70	0.34
45.0	16	0.39	0.303	6.91	4.51	0.74	0.31
48.0	17	0.43	0.269	8.25	3.47	0.82	0.21
51.0	18	0.44	0.262	7.97	3.30	0.85	0.18
54.0	19	0.48	0.252	7.64	3.25	0.83	0.19
57.0	20	0.51	0.226	10.25	3.17	0.80	0.22
60.0	21	0.55	0.209	11.12	3.14	0.85	0.17
63.0	22	0.63	0.193	12.83	2.88	0.80	0.21
66.0	23	0.39	0.237	9.88	4.05	0.62	0.42
69.0	24	0.56	0.278	7.67	4.22	0.77	0.25
72.0	25	0.55	0.249	8.91	3.15	0.75	0.28
75.0	26	0.52	0.227	10.70	2.68	0.59	0.44

Roundness and movement

All size classes of Nile Delta beach pebbles show a definite though fluctuating increase in both mean and individual roundness for each class. *Fig. 8A* shows the lateral variation of roundness along 26 sampling sites.

East of Burullus outlet, the initial mean roundness is 0.21, it increases laterally eastwards and rapidly attains its maximum value of 0.44 at locality 12 km. The area east and west of Kitchener drain characterized by decreasing of roundness. Eastward of locality 27 km *(Fig. 8A)*, there is a significant increasing in roundness. It tends to increase gradually and attains its maximum value of 0.63 at Gamasa coast. A drop of roundness was observed for all pebble sizes just east of Gamasa but it tends to increase again eastwards. Theoreticaly, by progressive abrasion, pebbles would be more rounded with a value of 1.0, but actually such value is never reached. The maximum roundness value was found to be 0.69 for the smallest size class 32—16 mm. PETTIJOHN, F. J. [1957] related this phenomenon to the inhomogeneities in the material and to the rigor of the abrasive process. Between Burullus outlet and Kitchener drain,

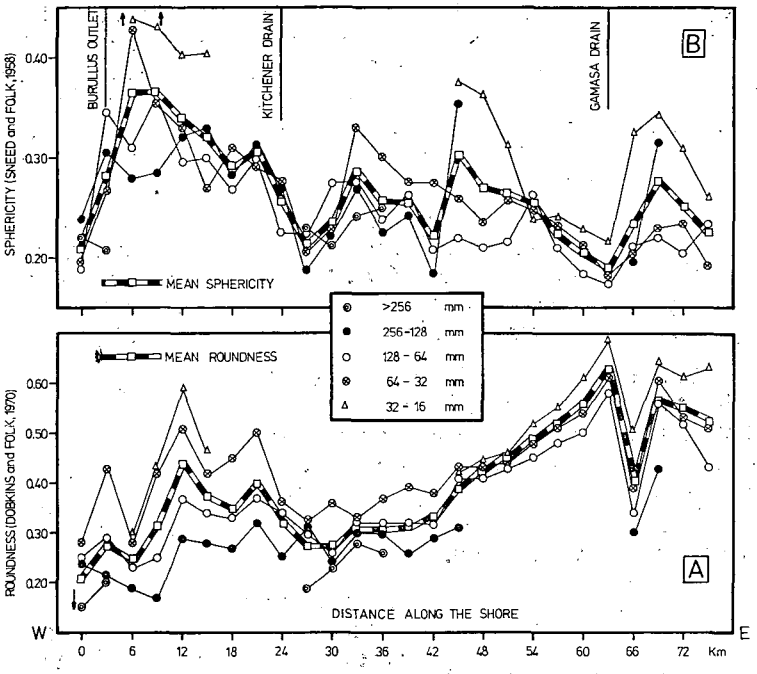

Fig. 8. Lateral variations of roundness *(A)* and sphericity *(B)* of beach pebbles along Nile Delta coast.

Nile Delta beach pebbles show high size-to-size roundness variation. But eastwards, the rest of the coast shows a small variation and the difference reduced to a minimum value. By tracing the roundness for each pebble size class as shown in *Fig. 8A*, it is clear that pebbles are arranged according to their size. Larger pebbles are less rounded than the smaller ones because they are not always in motion.

East of Burullus outlet, roundness changes most rapidly at first and more slowly later between Kitchener and Gamasa drains. Table 4 illustrates the main differences in rate of roundness between up-and-down drift localities. It is clearly observed from this table, with the exception of pebbles larger than 256 mm, that the rate of variation

TABLE 4

Rate of roundness improvement for pebbles at up-and-down drift localities along Nile Delta coast

size class	up-drift between 0—12 km	down-drift between 30—63 km
>256 mm	0.130	0.023
256—128 mm	0.011	0.011
128— 64 mm	0.032	0.026
64—32 mm	0.120	0.022
32—16 mm	0.150	0.027
average rate	0.089	0.021

increases with decreasing size at both up-and-down drift localities. Smaller beach pebbles introduced in up-drift localities round more rapidly than the larger ones, but progressively more slowly thereafter. These results agree with all previous work that pebble rounding proceeds rapidly at first and then slows down to approach some assymptotic limit (WENTWORTH, C. K. 1919, 1922a; KRUMBEIN, W. C., 1941, 1942; GROGAN, R. M., 1945; PLUMLEY, W. J., 1948; VAN ANDEL, TJ. H. *et al.*, 1954; KUENEN, PH. H., 1956; SNEED, E. D., and FOLK, R. L. 1958].

Beach pebbles that were collected astride Burullus outlet and just east of both Kitchener and Gamasa drains show the worst roundness comparing with the other areas. These three drops in roundness *(Fig. 8A)* could be seen for all pebble sizes. The corners of pebbles are somewhat sharp and show more than four corners. Some concluding remarks are given below concerning the movement of beach pebbles:

1. The three drops in roundness indicate pebbles coming from source areas owing to their worst roundness.
2. Eastward of each drop, there is a significant improvement in roundness due to the general west-east longshore drift.
3. It may be noted that there is a certain similarity between the pebbles of the three secondary sources from the point of pebble size, roundness, and shape parameters (see later).

The preliminary conclusion is that the movement of beach pebbles just west of Kitchener and east of Gamasa drains is not simple as it can be from Kitchener to Gamasa drains. In fact, it influenced by the supplying of pebbles from the secondary sources. Therefore, the roundness is so marked at these areas. The rapid rate of pebble supplying has not allow roundness development to occur yet at these drops. But during movement of pebbles along the coast from west to east, they show better roundness. As far as it can be derived from tracing of roundness, pebbles are actively moving eastwards from Kitchener to Gamasa drains. Such active motion, which follows the eastward drift, is certainly responsible for the regular and excellent improvement in roundness.

Sphericity and movement

Simply stated, there is a general decrease in sphericity with the direction of movement along the coast. *Fig. 8B* shows lateral variation of sphericity of beach pebbles with distance of transport. West of Burullus outlet, the initial sphericity is very low. For size classes, it ranges between 0.191 and 0.236 with an average of 0.210. For a short distance of transport (9 km), beach pebbles become more spherical. Itt is clearly observed that small pebbles attain the maximum sphericity value (0.453) more rapidly than larger ones (0.281). Eastwards of locality 9 km, size classes of pebbles show a decreasing trend in both mean and individual sphericity with definite fluctuations. *Fig. 8B* clearly shows that smallest size always have the higher sphericity.

Tracing of sphericity along the coast reveals the same situations as in roundness. Some pebble beaches show a definite high sphericity differences between size classes, while the others show a significant small differences. These variations could be related to the secondary sources of beach pebbles. At the three secondary sources, there are small differences in sphericity of size classes. Eastward of each locality, these differences become higher owing to sphericity variation during movement on the basis of size classes. Therefore, the up-drift localities (west of Burullus outlet, just east of Kitchener and Gamasa drains) show small size-to-size sphericity variation.

On the other hand, the down-drift localities (i.e. the localities 6, 33, 45 and 69 km, *Fig. 8B)* show the reverse.

Flatness index for beach pebbles shows the same behaviour of sphericity along the coast *(Fig. 9A)*, but the two parameters stood in inverse relations as mentioned before. East of Burullus outlet, flatness index decreases sharply at first and then tends to increase gradually to Kitchener drain. Eastwards, it decreases with some fluctuations and thereafter increases gradually to attain its maximum value at Gamasa coast. The last figure indicates that the small pebbles always have the small flatness index values. Studies carried out by WENTWORTH, C. K. [1922b] and CAILLEUX, A. [1947,

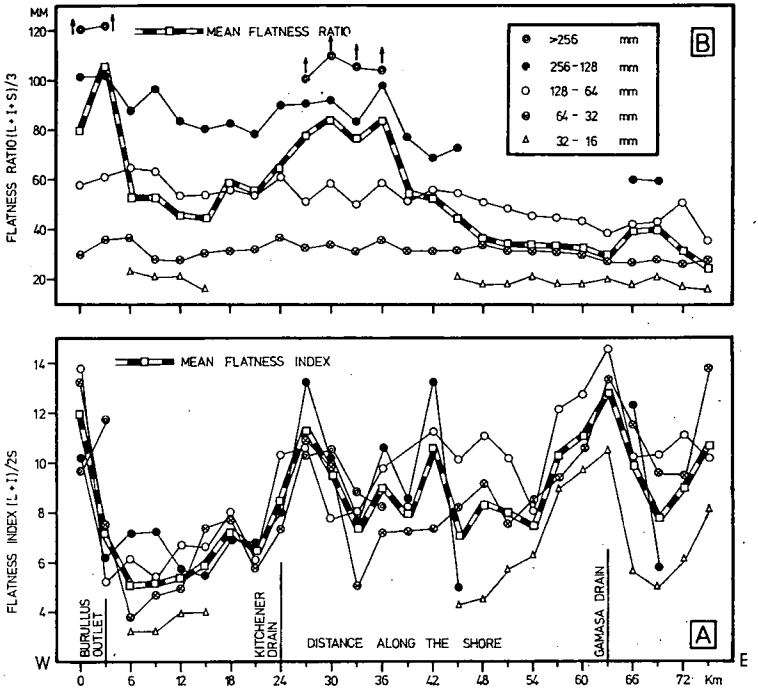

Fig. 9. Lateral variations of flatness index *(A)* and flatness ratio *(B)* of beach pebbles along Nile Delta coast.

1952] mentioned that, however, the flatness of pebbles is strongly influenced by the source material, beach pebbles become less flat, hence acquire a higher sphericity with prolonged wear. But this phenomenon can be observed only on the first 6 km of transport path.

As mentioned before, the flatness ratio (L+I+S)/3 decreases steadly with decreasing pebble size. This phenomenon can be observed also in *Fig. 9B* where flatness ratio for each size is drawn versus the distance along the coast. Mean flatness ratio shows a rapid decreasing trend east of Burullus outlet. Just east of Kitchener drain a peak is observed due to feeding the coast by newly pebbles from source area. Eastward of this peak, there is a gradual decreasing in flatness ratio. It is clearly observed from *Fig. 9B* that the rate of decreasing is higher between Kitchener and Gamasa drains.

To sum up, Nile Delta beach pebbles show a general decreasing in sphericitgy accompanied with increasing in flatness index and decreasing in flatness ratio durind movement along the coast. This could be caused either by actual abrasion towar a disc-like form, or by shape-sorting.

Whether or not beach pebbles show a progressive increase in sphericity with transport is an unsettled problem. In fact, the final shape that any pebble acquires, by abrasion during transport, is essentially depend upon the initial shape librated from bedrock, composition, hardness, inherited partings, size, mode, agent and rigor of transport. A well-bedded sediment with well-developed fissility and cleavage possesses the tendency to produce tabular and elongated pebbles, whereas massive rocks tend to produce spherical pebbles. Regarding to Nile Delta beach pebbles, it is believed that they are derived from well-bedded submarine banks located NW and NE off Burullus headlands. Therefore, they attain low sphericities and are flattened in shape. Data from SNEED, E. D., and FOLK, R. L. [1958] show that rock type controls sphericity of Colorado River pebbles. The sphericity of quartz increases slowly downstream, but the sphericity of chert decreases markedly because chert pebbles split preferentially parallel with bedding.

The mode and medium of transport and transporting agents can affect the form of pebbles. Generally, it is said that beach pebbles tend to be flatter than those of rivers [CAILLEUX, A., 1945; KUENEN, PH. H., 1964]. Therefore, there is a difference in the process of abrasion that leads to increase in sphericity with prolonged fluvial transport (SNEED, E. D., and FOLK, R. L., 1958] and decrease in sphericity with prolonged beach abrasion. According to the evidences of increasing flatness and decreasing sphericity of Nile Delta beach pebbles during movement, it can be mentioned that these pebbles could be transported only with the smooth moving of their maximum projection face over the sandy bottom of nearshore zone. Such mode of moving reduces the short axis of pebbles to a higher degree rather than the other axes. Beach pebble shape is affected strongly by substrate character; whether sandy or gravelly beach. DOBKINS, J. E., and FOLK, R. L. [1970] mentioned that beaches that are dominantly gravel, where pebbles seldom move, have higher sphericities than the other sandy beaches. This may explain the low sphericity of Nile Delta beach pebbles.

Elongation and movement

The elongation index (I/L) and (L—I)/(L—S) value were used for tracing pebbles movement along the coast. *Fig. 10* shows the variation of these two parameters with the distance of transport. Although (I/L) and (L—I)/(L—S) stood in inverse relations to each other, it is clearly observed from the last figure that the two parameters gave the same result and behaviour. Near Burullus outlet, there is a rapid change in the elongation of pebbles. Generally, beach pebbles tend to change from bladed or slightly elongate to platy or equant. Just west of Kitchener and east of Gamasa drains, the beach pebbles seems to be elongated in shape owing to the feeding from source areas. From Kitchener to Gamasa drains, there is a gradual tendency for the pebbles to be more platy and this is probably due to the active motion of pebbles without confusion from the source area. The change of pebbles from bladed to platy can be caused only by wearing the long axis more than the intermediate one. It is also observed from *Fig. 10* that the larger pebbles (>256 mm and 256—128 mm) show somewhat a weak trend to be more elongated with prolonged transport. This is the type of wear that should occur if the pebbles were rolled like a rolling pin with wear mainly on the intermediate axis. Beach pebbles with size 128—64 mm follow

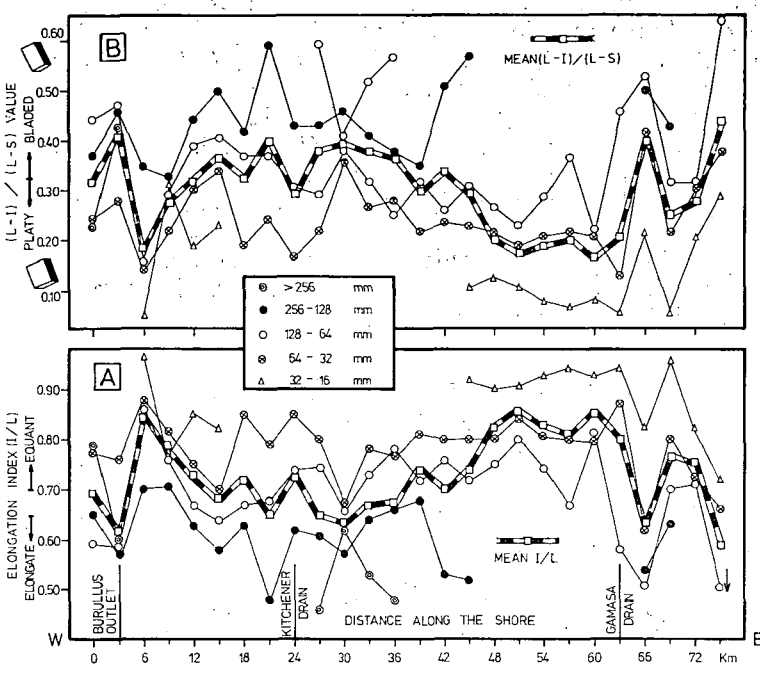

Fig. 10. Lateral variation of elongation parameters of beach pebbles along Nile Delta coast. *A* — Elongation index (I/L). *B* — The value (L—I)/(L—S).

quite closely the mean values of (I/L) and (L—I)/(L—S) along the shore and show a higher rate of variation to be platy in form.

Generally, larger pebbles show lower elongation index than the smaller ones. There is a strong selective tendency for the intermediate axis of larger pebbles to lie halfway between long and short axes to produce bladed forms. On the other hand, the intermediate axis is closer to the long axis for smaller pebbles to produce platy forms. Large and small pebbles show difference in their behaviour during the course of transport. Beach pebbles larger than 128 mm *(Fig. 10)* tend to be more elongate while the smaller ones tend to be more platy. Such difference in shape may be related to the effect of selective wearing on different size classes.

Results of abrasion and movement

Various parameters of beach pebbles are not equally affected during their movement. It was found that rounding and flatness ratio proceed more rapidly and serve better than the other parameters. As a result of movement, roundness increases, sphericity decreases and pebbles become more flat and platy in shape due to the change in the three main axes. Such change related to the effect of abrasion and not to the shape-sorting. The abundance of Nile Delta beach discs is due to the ease of sliding by surf action on a smooth sandy surface which makes abrasional flattening occurs more effectively.

It was found that several combinations of last parameters are effective in differentiation between pebbles from up-and-down drift localities. By plotting round-

ness versus sphericity, flatness ratio and elongation index *(Fig. 11)*, it is possible to determine exactly the behaviour of pebbles during the path that beach pebbles follow. The combination of roundness versus sphericity *(Fig 11A)* shows that down-drift pebbles become more rounded than the up-drift ones. On the same time sphericity is not effective and shows very weak correlation with roundness. Roundness versus elongation index shows a positive correlation *(Fig. 11B)*. Down-drift pebbles tend to be much rounded and less elongate in shape (equant) while the up-drift ones tend be less rounder and range from slightly equant to elongate in shape. Roundness versus flatness ratio *(Fig. 11C)* is most effective and shows a negative correlation between them. Up-drift pebbles are less rounder and have higher flatness ratio than the down-drift pebbles. Generally pebble population markedly increases in roundness and decreases in flatness ratio as it passes from large to small sizes.

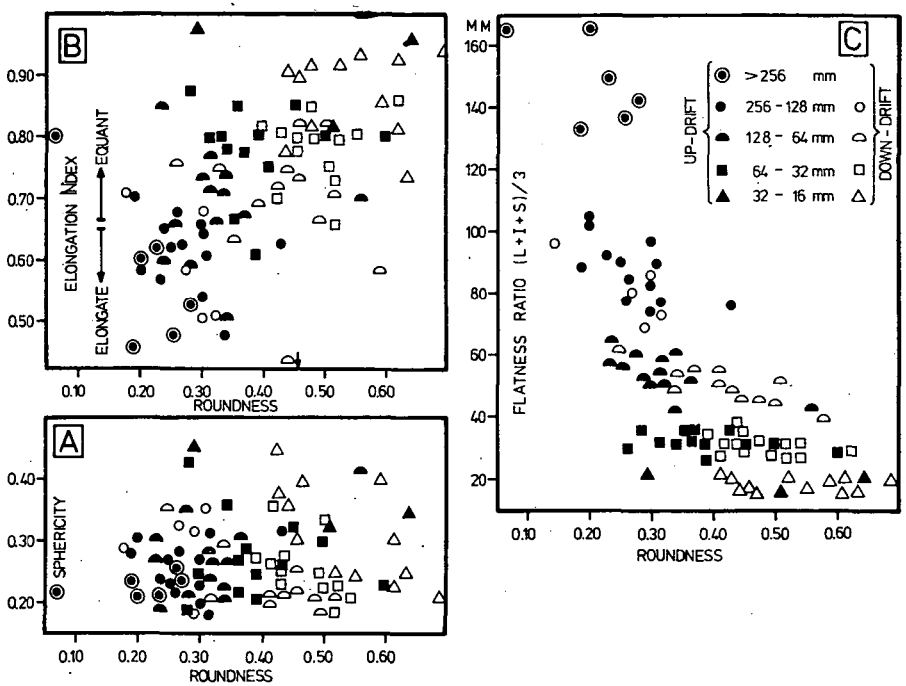

Fig. 11. Relation between up-and-down drift beach pebbles.
A — Roundness *vs* sphericity.
B — Roundness *vs* elongation index.
C — Roundness *vs* flatness ratio.

By examining the relative changes of the three axes that take place during the movement, it could be concluded that pebbles as they move down-drift must suffer most wear on short axes as fast as long axes. This modification causing them to become less bladed and more platy. As a result, their sphericity shows a slight decrease during movement. It is possible also to assume that littoral current carrying beach pebbles will drop the large with elongate-shaped pebbles near up-drift before it drops the smaller and platy-shaped ones near down-drift.

SUMMARY AND CONCLUSION

The study of Nile Delta beach pebbles along 75 km leads to the following results:
1. Roundness measures of WADELL, H. [1934], CAILLEUX, A. [1947] and DOBKINS, J. E. and FOLK, R. L. [1970] follow quite closely each other along pebble beaches with considerable differences. A new method for evaluating roundness have to take into consideration to avoid the complexity of various measurements and to compare easily between pebbles from different environments.
2. The maximum projection sphericity of SNEED, E. D. and FOLK, R. L. (1958) shows lower values comparing to KRUMBEIN, W. C. [1941] measure although the two lines parallell each other along the coast. This difference related to the flaty features of Nile Delta beach pebbles.
3. Flatness index, which reflects the actual settling velocities of irregular particles in water, and sphericity measures stood in inverse relations to each other. Maximum projection sphericity is closely related to flatness index because it takes into consideration the hydraulic behaviour of particles more than KRUMBEIN measure.
4. Roundness and shape parameters are significantly functions of size. Beach pebbles markedly increase in roundness, slightly in sphericity and decrease in flatness index and flatness ratio with decreasing size. Pebbles tend to change from slightly elongate or bladed to platy form with decreasing size. Small pebbles are easily washed by gentle waves and currents which can apparently slide them more easily than larger pebbles.
5. Beach pebbles are derived mainly from west. The difference in roundness and shape parameters are so marked at three areas along the coast. The rapid rate of supply of pebbles has not allow shaping development to occur yet in these areas which can be considered as secondary source areas.
6. The processes of beach pebbles movement from the source area give rise to a progressive improve of roundness, decrease of sphericity and modification of shape parameters. These changes proceed rapidly at first and then slow down and agree with all previous work. Smaller beach pebbles introduced in up-drift localities round more rapidly than the larger ones but progressively more slowly thereafter.
7. Beach pebbles are actively moving from Kitchener to Gamasa drains. This active motion, which follows the eastward drift is certainly responsible for the regular and excellent modification in roundness and shape. Rounding proceeds more rapidly than sphericity, therefore it serves better as an indicator to the movement of beach pebbles.
8. Nile Delta beach pebbles show a significant form change with movement. The pebbles tend to be less spherical with high flatness index which paints to abrasion of the short axes. The pebbles change from elongate-bladed to platy form which geometrically should take by abrasion chiefly of the long axes. Therefore, such change related to the effect of abrasion and not to the shape-sorting.
9. The abundance of discs along Nile Delta coast may be related to the original structure of source area and dynamics factors. The ease of up-and-down slow motion of pebbles on their maximum projection area makes abrasional flattening occurs more effectively.

REFERENCES

BLUCK, B. J. [1967]: Sedimentation of beach gravels: examples from South Wales. Jour. Sed. Pet., **37**, No. 1, pp. 128—156.

CAILLEUX, A. [1945]: Distinction des Galets Marins et Fluviatiles. Soc. Geol. France Bull., 5th Serie, **15**, pp. 375—404.

CAILLEUX, A. [1947]: L'indice d'émoussé. Definition et Premiere Application. C. R. S., Soc. Geol. de France, pp. 250—252.

CAILLEUX, A. [1952]: Morphoskopische Analyse der Geschiebe und Sandkörner und ihre Bedeutung für die Paläoklimatologie. Geol. Rundschau **40**, pp. 11—19.

CARR, A. P. [1971]: Experiments on longshore transport and sorting of pebbles: Chesil Beach, England. Jour. Sed. Pet., **41**, No. 4, pp. 1084—1104.

CARROLL, D. [1951]: Pebbles from a Pothole: a study in shape and roundness. Jour. Sed. Pet., **21**, pp. 205—212.

DOBKINS, J. E., and FOLK, R. L. [1970]: Shape development on Tahiti-Nui. Jour. Sed. Pet., **40**, pp. 1167—1203

DUNN, E. J. [1911]: Pebbles. George Robertson & Co., Melbourne, 122 p.

FOLK, R. L. [1968]: Petrology of sedimentary rocks. Hemphill's, Texas, 170 p.

FÜCHTBAUER, H., and MÜLLER, G. [1970]: Sediment-Petrologie. Teil II Sedimente und Sedimentgesteine. Stuttgart, 726 p.

GOEDE, A. [1975]: Downstream changes in shape in the pebble morphometry of the Tambo River, Eastern Victoria. Jour. Sed. Pet., **45**, No. 3, pp. 704—718.

GROGAN, R. M. [1945]: Shape variation of some Lake Superior beach pebbles. Jour. Sed. Pet., **15**, pp. 3—10.

HUMBERT, F. L. [1968]: Selection and wear of pebbles on gravel beaches. Univ. Groningen, Geol. Inst. Publ., **190**, 144. p.

KING C. A. M. and BUCKLEY, J. T. [1968]: The analysis of stone size and shape in Arctic environments. Jour. Sed. Pet., **38**, No. 1, pp. 200—214.

KRUMBEIN, W. C. [1941]: Measurement and geological significance of shape and roundness of sedimentary particles. Jour. Sed. Pet., **11**, pp. 64—72.

KRUMBEIN, W. C. [1942]: Settling velocity and flume behavior of non-spherical particles. Am. Geophys. Union Trans. **43**, pp. 621—633.

KUENEN, PH. H. [1956]: Experimental abrasion of pebbles: 2-Rolling by current. Jour. Geology **64**, pp. 336—368.

KUENEN, PH. H. [1964]: Experimental abrasion: 6-Surf action. Sedimentology **3**, pp. 29—43.

LANDON, R. E. [1930]: An analysis of beach pebble abrasion and transportation. Jour. Geology **38**, pp. 437—446.

MANOHAR, M. [1976]: Dynamic factors affecting the Nile Delta coast. In: UNESCO /ASRT/ UNDP-Proceedings of Seminar on Nile Delta Sedimentology. Alexandria, Oct. 1975, pp. 104—129.

MARSHALL, P. [1928]: The wearing of beach gravels. Trans. & Proc. New Zealand Inst., **58**, pp. 507—532.

MARSHALL, P. [1930]: Beach gravels and sands. Trans. & Proc. New Zealand Inst., **60**, pp. 324—365.

ORFORD, J. D. [1975]: Discrimination of particle zonation on a pebble beach. Sedimentology **22**, pp. 441—463.

PETTIJOHN, F. J. [1957]: Sedimentary rocks. 2nd ed., Harper & Brothers, New York, 718 p.

PLUMLEY, W. J. [1948]: Black Hills terrace gravels: a study in sediment transport. Jour. Geology **56**, pp. 626—577.

SCHNEIDERHÖHN, P. [1954]: Eine vergleichende Studie über Methoden zur quantitativen Bestimmung von Abrundung und Form an Sandkörnern. Heidelberg Beiträge zur Min. u. Petr. **4**, pp. 172—191.

SNEED, E. D., and FOLK, R. L. [1958]: Pebbles in the lower Colorado River, Texas, a study in particle morphogenesis. Jour. Geology **66**, pp. 114—150.

SPALLETTI, L. A. [1976]: The axial ratio C/B as an indicator of shape selective transportation. Jour. Sed. Petr. **46**, No. 1, pp. 243—248.

VAN ANDEL, TJ. H., WIGGERS, A. J., and MAARLEVELD, G. [1954]: Roundness and shape of marine gravels from Urk (Netherlands), a comparison of several methods of investigation. Jour. Sed. Petr., **24**, No. 2. pp. 100—116.

WADELL, H. [1933]: Sphericity and roundness of rock particles. Jour. Geology **41**, pp. 310—331.

WADELL, H. [1934]: Shape determinations of large sedimental rock fragments. Pan-Amer. Geol., **61**, pp. 187—220.

WENTWORTH, C. K. [1919]: A laboratory and field study of cobble abrasion. Jour. Geology **27**, pp. 507—521.
WENTWORTH, C. K. [1922b]: A method of measuring and plotting the shapes of pebbles. U. S. Geol. Sur. Bull., **730** C, pp. 91—102.
WENTWORTH, C. K. [1922c]: The shapes of beach pebbles. U. S. Geol. Surv. Prof. Paper **131** C, pp. 75—83.
ZINGG, Th. [1935]: Beitrag zur Schotteranalyse. Schweizerische Min. U. Petrog. Mitt., **15**, pp. 39—140.

Manuscript received, May 15, 1981

NABIL M. EL-FISHAWI
Institute of Coastal Research
Alexandria, Egypt.

Present adress:
József Attila University
Department of Geology and
Paleontology
6722 Szeged, Egyetem u. 2.
Hungary

B. MOLNÁR
József Attila University
Department of Geology and
Paleontology
6722 Szeged, Egyetem u. 2.
Hungary

Acta Mineralogica-Petrographica, Szeged, XXV/1, 63—76, 1981

CHARACTERISTIC FEATURES OF COASTAL SAND DUNES ALONG BURULLUS—GAMASA STRETCH, EGYPT

N. M. EL-FISHAWI and M. A. EL-ASKARY

ABSTRACT

Coastal sand dunes play an important protective role due to recent severe erosion along Nile Delta coast, especially in areas where the backshore is low-lying. The study performed in this research illustrates the results of the work carried out on the coastal sand dunes to put a body of basic data to be used in coast protection.

Between Burullus outlet and Gamasa drain, the main geomorphological features of coastal sand dunes are discussed on the basis of dune type, origin, modification, wind velocities, wind ripples, internal structure and dune vegetation.

Along Burullus outlet-Kitchener drain stretch, grain size relationship between coastal sand dunes and beach sands have been studied on light of sand transport by onshore wind action. It is found that there is a fining grain size cycle from the beach, throughout the bottom and up to the top of dune sands. There is a sympathetic relationship between grain size peaks of beach and dune sands. The field can be described as being under dominantly unidirectional wind control from WNW and NW.

An attempt was made to differentiate between the two populations of sorting occurred in coastal dune sands. The differentiation depends upon grain size distribution curves, statistical parameters and scatter diagrams. Top of dune sands are finer, more sorted, slightly positive skewed and has lower kurtosis values than the bottom sands.

Internal structure of barchan dune studied by making three cuts in the windward side, leeward side and in the barchan horn. The three types of stratification can be differentiated depending upon angle of dip and thickness of lamina.

INTRODUCTION

The majority of coastal sand dunes along Nile Delta coast lies between longitudes 30° 59′ — 31° 33′ E, and latitudes 31° 36′ — 31° 23′ S *(Fig. 1)*. The area extends for about 59 km between Burullus outlet and Gamasa drain. The southern extension of the area is from the shoreline landwards for about 10 km. Burullus outlet connects the Mediterranean sea with Burullus lake at Burg El Burullus village.

The study of the geomorphological features of the area was based on the examination of its air photographs of the scale 1:25 000 comparison with older topographic maps and on the field examination. The ERTS satellite photographs have served as a good basis for recognising the important aspects of the geomorphology of the coast.

The main changes that have occurred on the Nile Delta coast during historical times are the reduction of the Nile mouths from seven to two *(Fig. 2)* [TOUSSON O., 1934], and the deterioration of the coastal regions due to the formation of marshes and lakes, following subsidence or other causes.

Estimated volumes along Burullus-Gamasa coast are at least 50×103 tons of sand [SESTINI, G., 1976]. The area is characterized by two belts of different extension

(Fig. 1), type and age. The first dune belt is coastal, recent and runs parallel to the coast between Burullus and Gamasa drain for about 59 km. Most of these dunes are of barchan and longitudinal types with elevations up to 40 m above their base-level, their width ranges between 1—8 km. The other dune belt is older, smaller and extends parallel to the northern shore of Burullus lake for about 8 km east El Burg village. Such lower belts (5—10 m high) consist of dome-shaped dunes, made of yellowish brown sands.

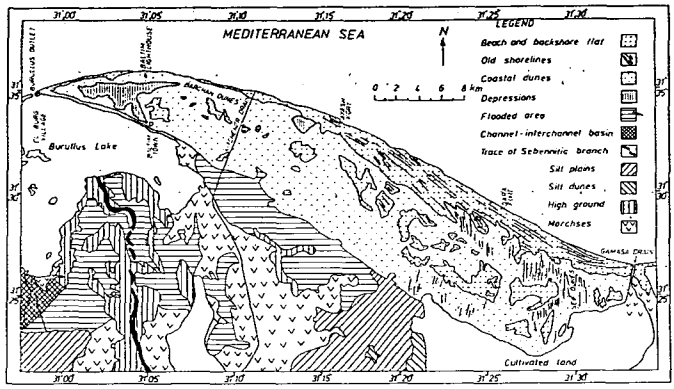

Fig. 1. Geomorphological map of the coastal area between Burullus outlet and Gamasa drain

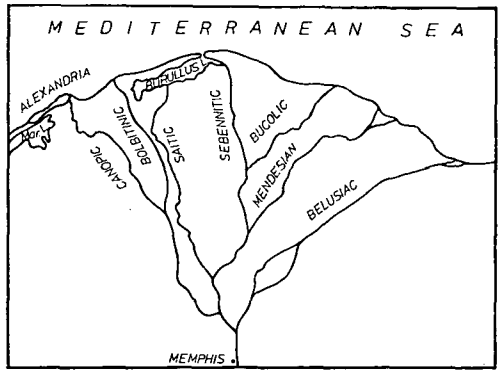

Fig. 2. Nile branches in classical times

The two dune belts represent two distinct periods of dune formations. Between the high coastal dunes, there are hollows with flat or rolling floors made of sand and fixed by grass and clay. This grassy surface is continuons from hollow to hollow under the high dunes. It is moreover marked by pottery fragments, bons and shells. This surface is at elevations of 1.5 to 5.0 m above sea level and was once occupied by settlements (Islamic and not very ancient). East of Burullus outlet, a very clear section is observed in contact with the older, lower surface and the younger, higher dunes *(Fig. 3)*. A similar situation of older, lower dunes fixed by vegetation and (or indurated, and overlain by younger higher dunes occurs south of Rosetta where the Nile cuts the dunes (Coastal Erosion Project, 1973), and at Gamasa [BARAKAT, M. G.

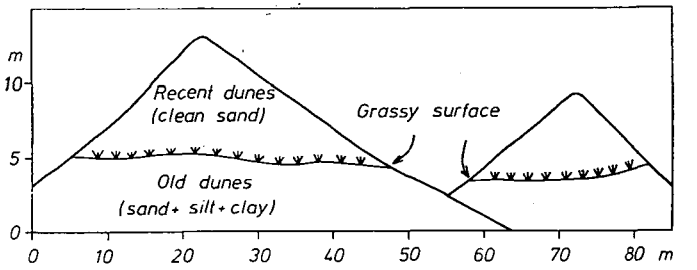

Fig. 3. Vertical section in coastal sand dunes — 1 km west of Burullus outlet

and IMAM, M. 1976]. So, the grassy surface separates two different facies of dune The lower dunes may be derived from the old deposits of Sebennitic branch, whereas the upper ones derived from the beach.

The area between the two dune belts is occupied by numerous depressions, some even below sea level. Between the depressions, there are some mounds and sheets of wind blown sand and low dunes, occupied by small lakes. Others are flooded during the winter and used as salt pans, but none are lagoons or old marshes. A series of elongated flat areas are also present in the depressions, they are oriented parallel to the present beach which may indicate the old shorelines.

The depressions between Burullus outlet and Baltim, and those flat areas west of Gamasa may indicate two periods of different times. The first period include the old shoreline which is followed by the formation of older and lower coastal dunes. The second period represent a past advancing of this part of the coast forming a wide coastal plain, along its newly shoreline the younger coastal dunes have been formed. Consequently, there was a gradual increase in their high due to sand transport from the near beach. On the other hand, due to lack of sedimentation, the older dunes still lower and modified to dome-shaped. Some of the flat areas between the two belts of dunes subjected to subsidence owing to the load of its sediments and the progressive flooding during winter seasons.

SAMPLES AND PROCEDURE

For studying the grain size relationship between beach and coastal dune sands, the stretch of Burullus outlet-Kitchener drain is chosen because the coastal dunes are somewhat near to the beach and it is easy to illustrate the effect of wind action on coastal sediments.

Three series of samples were collected along the coast; one from the beach (12 samples), and the other two series from the bottom and top of coastal dunes facing the sea (11 samples for each). These three series of samples were collected in the same date (18*th* November, 1974). It was intended to collect sample every 2 km.

Mechanical analysis was carried out by the conventional sieving method using a Ro-Tap shaker. About 100 gm split of each sample was sieved for 20 minutes. It is planned to use the half phi interval in between 3—4 phi set of sieves to give more accurate curves and statistical parameters [ISPHORDING, W. C., 1972].

The cumulative percentages were plotted on probability paper and graphical method was used. The grain size statistical parameters were calculated by computer using the formulae of FOLK, R. L. and WARD, W. C. [1957].

WIND DIRECTION AND VELOCITY

Daily measurements made over 4 years from 1972 to 1975, at Baltim city by the Egyptian Meteorological Authority, indicate that the prevailing wind comes from WNW, NW and N (*Fig.* 4), although winds from all directions are represented. Hence, the presence of a prevailing wind, effective in sand transport has been clearly established for the sand dune of Burullus area. The majority of daily readings (74%) range between 1—9 knots/hour, while 26% of these readings range between 9—23 knots/hour.

Through use of data from the original daily wind readings, a total wind rose diagram and monthly rose diagrams result *(Fig. 4)*. The total wind rose diagram *(Fig. 4A)* indicates that both 1—9 and 9—23 knots winds are mainly from the WNW. The strong winds occur most frequently during winter season, especially during December and January. It is observed from *(Fig. 4B)* that during winter season (from December to March) an additional minor trend (from E and NE) was observed which was absent during summer season (June, July and August). However, the dune field may be described as being under a dominantly unidirectional wind control from WNW an NW.

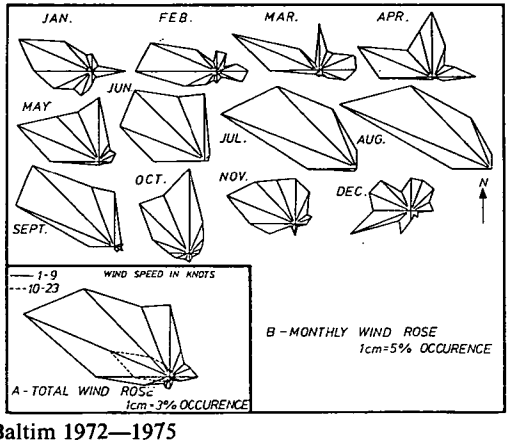

Fig. 4. Wind rose — Baltim 1972—1975

It is observed that the orientation of barchan and longitudinal dunes in relation with wind regime is to NW, but west of Gamasa drain, some of the dune orientations are slightly deviated to the north from that of the prevailing wind while others follow the proper directions.

TYPES OF BURULLUS-GAMASA COASTAL DUNES

Wind blown dunes are commonly found to surmount beach ridge plains on the coast. The beach is narrow and sandy, providing sand to blow onto the dune. The following coastal dune types, based on morphological features as established in the literature, are recognized:

Barchan dunes: They are crescent-shaped sand mounds. Between Burullus outlet and Kitchener drain most of the dunes are of the barchan type. They occur both as isolated and in complex forms tend to concentrate inland, while the isolated barchans are located near and parallel to the coast. On the other hand, between Kitchener and

Gamasa drains, most of barchan dunes occur as isolated bodies, but at 20 km WSW of Gamasa another area of complex barchan forms is present.

The orientation of barchan dunes in relation to wind regime is to WNW and NW, where the gently-shaped windward side of dunes is toward the sea, and the steep leeward side is to SE. The height of the dunes ranges between 10—30 m above their base-level, in length parallel to wind between 20—250 m, and the width across the horns between 15—200 m.

Longitudinal dunes: This type of dunes is common west of Gamasa and extends for 20 km parallel to the shoreline. These dunes are elongated in shape, more or less straight. Their long axis lie parallel to the prevailing wind direction with continuous crest without breaks but serrated. The height of the dunes ranges between 15—40 m and in length between 1200—1400 m.

There are various views regarding the origin of barchan and longitudinal dunes. BAGNOLD, R. A. [1971] believes that the barchan dune-type can only occur when the wind is nearly unidirectional, and the longitudinal dunes are produced when strong winds blow from a quarter other than that of the general drift of sand. MCKEE, E. D. and TIBBITTS, JR. G. C. [1964] and MCKEE, E. D. [1966] suggest that longitudinal dunes are produced in the vector of two converging wind directions blowing from two quarters, about 90° apart. GLENNIE, K. W. [1970] believes that a more important factor for generation of that dunes is the existence of a strong wind of uniform direction, and adds that barchan dunes develop at lower wind velocities and longitudinal dunes are formed when wind velocities are higher. He also believes that during Pleistocene glaciation, because of stronger winds, longitudinal dunes were produced in abundance. Today some of them are undergoing modification to barchan dunes, because wind velocities are not strong enough to maintain them. On the other hand, BAGNOLD, R. A. [1971] mentioned that barchans can be formed in the longitudinal troughs between multiple seif chains where the effect of cross-winds is excluded.

West of Gamasa, it is observed that the southern parts of longitudinal dunes tend to modify a series of isolated barchan dunes *(Fig. 5)*, such modification occur with the direction of prevailing wind. Consequently, the barchan dunes occur together with longitudinal ones in the same series. Moreover, the interdune areas between

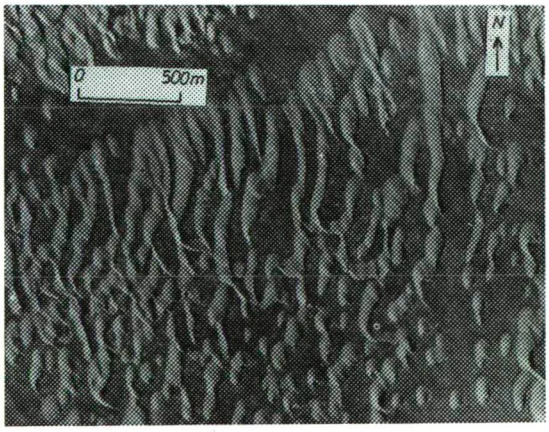

Fig. 5. Aerial photograph of longitudinal dunes — west of Gamasa.

longitudinal dunes contain some well-formed barchans in small scale. Such phenomena may support the last opinions of GLENNIE, K. W. [1970] and BAGNOLD, R. A. [1971] about the occurrence of barchans with longitudinal dunes.

GRAIN SIZE RELATIONSHIP BETWEEN COASTAL DUNE AND BEACH SANDS

Between Burullus outlet and Kitchener drain (22 km), three series of samples have been collected, one from the beach, and the other two from bottom and top of dunes. This system of sampling easily permits comparison and shows a sort of relationship between beach and dune sands on light of sand transport.

Fig. 6 shows the cumulative percentage of coarse plus medium sand and standard deviation against distance between Burullus outlet and Kitchener drain for the three types of sands.

The variation of percentage of coarse plus medium sands in the coastal dune (for both bottom and top), from west to east, follows quite closely those that are found on the beach *(Fig. 6)*. From the beach, passing through the bottom, and up to the top of the dunes, the percentage of coarse plus medium sands decreases, whereas the standard deviation improves. Thus, there is a fining cycle from the beach passing through the bottom and up to the top of dunes.

Generally, the lateral variation of the percentage of coarse plus medium sands for the dunes shows an eastward increase *(Fig. 6)*. But the most observed feature is the presence of a pattern of peaks ("highs" and "lows"). Four major highs could be recognized for the dune sands at 4, 10, 18 and 21 km, and three lows at 6, 12 and 20 km

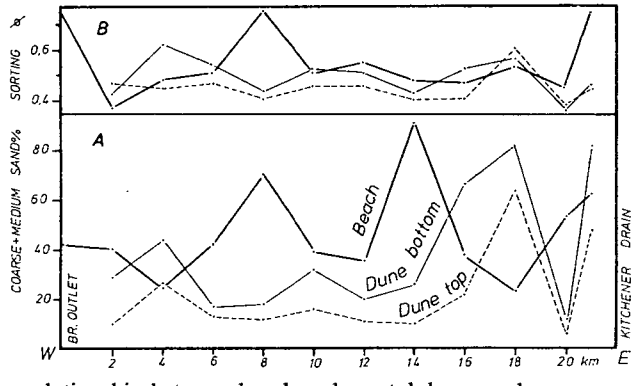

Fig. 6. Grain size relationship between beach and coastal dune sands

east of Burullus outlet. Similarly, the series of beach sands also shows 4 major highs at 0, 8, 14 and 21 km, and 3 lows at 4, 12 and 18 km east of Burulluss outlet.

To discuss the grain size relationship between beach and coastal dune sands, it is of importance to take into consideration the following factors:

1. The dune sands are finer grained than beach sands.
2. The field can be described as being under dominantly unidirectional wind control (WNW and NW).
3. The sand forming the dunes is derived from the beach.
4. The sympathetic relationship between peaks of beach and dune sands.

On light of last factors, it is found that the highs and lows of dune sands are related to those of beach with eastward shifting *(Fig. 6)*. This lateral eastward shifting of sand dune peaks from those of beach sand ones ranges between 2—4 km, due to the prevailing WNW and NW winds.

The following are four major examples for sand transport from beach to dune with their eastward shifting *(Fig. 6)*:

Shifting of highs:

a) Dune sand at 10 km is related to beach sands at 8 km due to decreasing in percentage of coarse plus medium sands from beach (70.34%), through the bottom (31.80%), and up to the top of dunes (16.40%).

b) Similarly, dune sands at 18 km is related to beach sands at 14 km (the percentage of coarse+medium sands for beach, bottom and top of dune being 91.07, 81.44 and 63.36%, respectively).

Shifting of lows:

a) Dune sand at 14 km is related to the beach sand at 12 km due to the decreasing of percentage of coarse+medium sands from the beach (35.61%), through the bottom (26.03 %), and up to the top of dune (9.90%).

b) Similarly, dune sand at 20 km is related to beach sand at 18 km (the percentage of coarse+medium sand for beach, bottom and top of dune being 23.69, 11.62 and 6.03% respectively).

It is now clear that there is a fining grain size cycle from the beach, through the bottom and up to the top of dune sands. The present work maintain that the beach sands are the source of wind blown sands and sand dunes along Burullus coast. Owing to prevailing WNW and NW winds, the sand transport is accompanied with an eastward shifting from the beach to the dune. So, it is reasonable that the dune sands are more sorted than that of the beach ones.

DIFFERENTIATION BETWEEN BOTTOM AND TOP OF COASTAL DUNE SANDS

The results of mechanical analysis and the calculated grain size statistical parameters of both bottom and top of dune sands are used in the differentiation between them. The averages of these data are given in Table 1 and shown in *Fig. 7*.

TABLE 1

Average grain size parameters of bottom and top of dune sands

Sand dune	Weight % of fractions					Statistical parameters			
	C. S	M. S.	F. S.	V. F. S.	C. silt				
	0—1 Ø	1—2 Ø	2—3 Ø	3—4 Ø	4—5 Ø	D_{50}	σ_I	SK_I	K_G
Bottom	2.88	34.87	55.32	6.83	0.07	2.20	0.59	—0.03	1,07
Top	0.52	21.19	68.25	9.91	0.11	2.40	0.52	0.01	1.02

Table 1 and *Fig. 7* show that the top of dune sands are finer, more sorted, slightly positive skewed, and has lower kurtosis value than that of the bottom ones. This is in agreement with ANAN, P. S. [1969] who found that the lower samples of dune sands

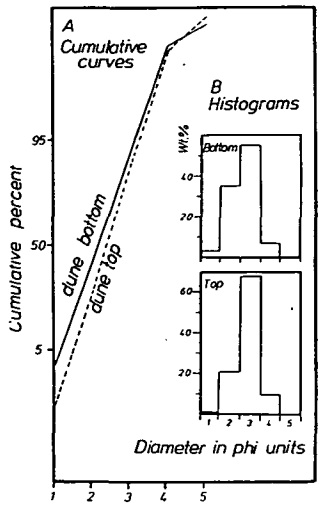

Fig. 7. Average cumulative curves and histograms of bottom and top of sand dunes

were slightly coarser and show some negative skewness values than the upper samples. In a single sand dune, GLENNIE, K. W. [1970] also found that there is a fining of sediment upward to the top of sand dune, at the same time standard deviation also improves.

To differentiate between bottom and top of dune sands, it is useful to plot the grain size parameters against each other in the form of scatter diagrams *(Fig. 8)*. In this way, their relationship can be determined. Such diagrams are very effective in differentiating and correlating the two types of sands. Boundary lines have been drawn so that many samples as possible from the same type of sand are on the same side of the line. A mixed area may be developed in some diagrams owing to overlap of such fields due to somewhat similarity of some sands of both type.

Median versus standard deviation *(Fig. 8A)* indicates that top of dune sands tend to be finer and more sorted than those of bottom ones. Kurtosis versus standard deviation shows that the bottom sands are less sorted and the samples have relatively higher kurtosis values than those of top ones *(Fig. 8B)*. Median versus skewness and skewness versus standard deviation indicate that some bottom sands tend to be negatively skewed *(Fig. 8C* and *D)*. Coarse percentile (D_5) versus fine percentile (D_{95}) shows that bottom sands are more scattered parallel to the D_5 axis *(Fig. 8F)* indicating their wider range of coarse fractions [PASSEGA, R., 1957]. The last combinations are effective and succeeded to differentiate between sands of bottom and top of dunes. On the other hand, kurtosis versus skewness seems to be ineffective in such differentatiation *(Fig. 8E)*.

It is observed from *Fig. 8* that the top sands tend to concentrate in a narrow field, while bottom ones, on the other hand, tend to spread in a wider range. Few samples of top are located in the field of bottom sands, this is due to the fact that these dunes which are located at 4, 18 and 21 km east of Burullus outlet *(Fig. 6)* are characterized by their higher median (for both top and bottom) than the neighbouring dunes.

The sand forming the dune is derived from the foreshore zone at low tide, from the beach sediments, and also from the backshore plain. So, the relatively coarser character of bottom sands than the finer top ones of dunes is probably due to processes associated with wind action. The onshore wind, when strong enough, is able to

carry inland the coastal sediments lying on beach surface. The fine sediments can be easily transported by means of suspension, and are blown far up into the air, and deposited on the top of dunes due to presence of grassy surface or fences in exposed situations which act as a continuons deposition area. On the other hand, the coarse grains are difficult to be carried by wind action to the top of dunes. Thus, they are

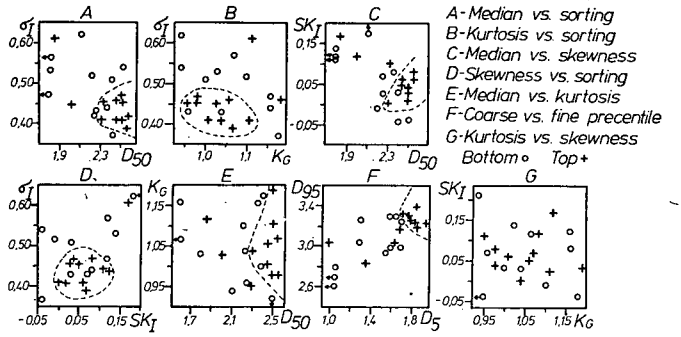

Fig. 8. Relationship between statistical parameters of bottom and top of sand dunes

transported close to the backshore surface by means of creeping and saltation. As a result, the coarse grains concentrate near the foot of dunes. According to ANAN, P. S. [1969], the lower samples were coaser than the upper ones because the larger particles can be easily rolling down and give negative skewness to the lower samples, while their loss gives the high positive values to the upper samples.

INTERNAL STRUCTURE OF BARCHAN DUNE

BAGNOLD, R. A. [1971] recognized that sand dunes are composed of accretion and avalanche deposits. These two types of deposits can easily be observed and have been described by various authors [MCKEE, E. D. and TIBBITTS JR., G. C., 1964; and MCKEE, E. D., 1966].

Internal structure of dunes may be known from the natural exposures of the interiors of the dune or by excavating it. Three cuts were made in a barchan dune *(Fig. 9)*, one in the windward side near the foot, the second in the leeward side near the crest, and the later in the barchan horn. The height of the barchan was about 10 m, and in length parallel to wind was 22 m, and the width across the horns was 8 m.

The stratification of wind blown sand is clearly observed and involves three types of laminae and bounding surfaces between sets of laminae. It was found that most of bounding surfaces are straight and showed apparent dips almost entirly towards leeward side.

Windward side lamina and those near the foot of dune are composed of low-angled lamina of sand. The angle of dip ranges between 5°—20°, although dips as high as 20° are not common. The individual laminae is rather thin and ranges between 0.7—1.2 cm thick. It is observed that heavy mineral-rich laminae alternate with heavy mineral-poor ones. The planer-tabular type of laminae is the most common. The sand of the horizontal bedding is rather firmly packed grains, deposited directly from the creep and saltation loads of the wind [ALLEN, J. R. L., 1970].

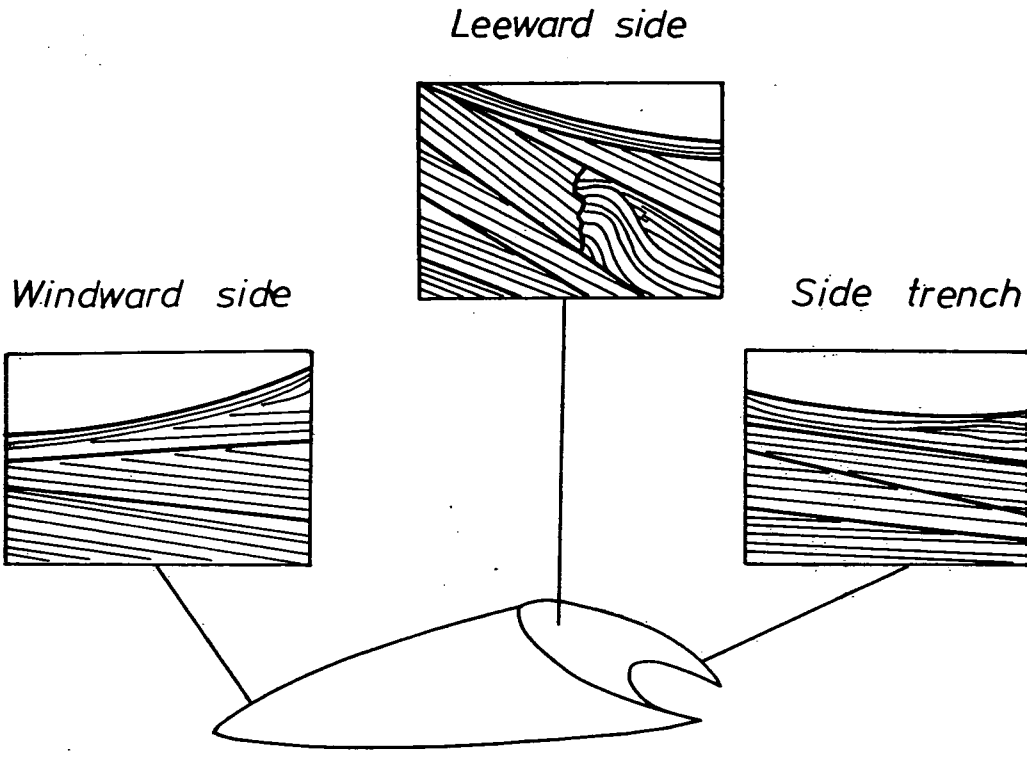

Fig. 9. Internal structure of barchan dune

Leeward side lamina near crest consists of cross-bedded units which are formed chiefly on the leeward slopes and are more steeper than those of the windward side due to avalanche deposits. Most surfaces bounding sets of cross-strata dipped from 18°—33° to leeside, and most lamina within them are dipping somewhat more and varies between 22°—35° (dips as low as 22° are not common). The individual laminae are rather thick, about 2—6 cm. A series of deformational structures such as irregularity of bedding, slump folds and fractures are observed and are probably formed as a result of local slumps on the avalanche side.

A cut in the curving barchan horn (side trench) shows a stratification pattern which consists of nearly flat surfaces bounding cross-strata sets with dip varying between 5°—13°. Laminae within each set dipped outward from the dune center and ranging between 3°—15°.

WIND SAND RIPPLES

On the dunes under investigation, wind ripples abound on surfaces of blown sand. These ripples are laterally extensive, straight, and parallel crested to slightly sinous crested. Their gentler slope side lying at the windward direction (WNW and NW). The wavelength is seldom less than 10 cm and rarely greater than 14 cm, the amplitude ranges between 0.4—0.5 cm. Accordingly, the ripple index ranges between 25—28. It is well known that wind ripples have greater ripple index (20—90) than the asymmetric water ripples (4—10).

The coarsest grains are commonly seen to collect on and near the crest of sand ripples where the average median size is 1.90 phi. On the other hand, the finest ones tend to concentrate in the trough of the ripples where the average median size is 2.15 phi. This fact is in agreement with TWENHOFEL, W. H., [1932] and BAGNOLD, R. A., [1971].

DUNE VEGETATION

Vegetation is very important in establishing the character of many coastal sand dunes. It plays an important role in the stabilization of the dune and also promotes its growth by porividng a trap for wind-blown sand.

The most important dune plants are the grasses which flourish in loose sand, beside grasses, it is observed that *Euphorbia terracina, Alhagi maurorum* and *Salicornia sp.** covered the coastal dunes between Burullus outlet and Kitchener drain. BARAKAT, M. G. and IMAM, M. [1976] observed that the characteristic plants which cover the longitudinal dunes west of Gamasa are: *Zygophyllum albam, Halocnemon strobiloceum* and *Salicornia fruticosa.*

Such plants play an important role in binding together the sand by their complex root system and thus help to protect the dunes from the erosive action of wind. If the vegetation is weakened for any reason, for example by trampling of people walking over the dunes, as a result, sands are exposed to wind action and the loose grains will blown away. Thus, the form of dunes will altered and appears as dome-shaped. Such phenomenon has been observed in the old dune belts which extend parallel to the northern coast of Burullus lake where that area is largely inhabited.

IMPORTANCE OF COASTAL DUNES FOR COAST PROTECTION

EL-FISHAWI, N. M., [1977] discussed the causes of beach erosion along Burullus coast and differentiated between accretional and erosional areas depending upon grain size parameters. He also studies the relationship between beach, coastal dune and nearshore zone sands. Eroded areas of the sandy coast are abundant where the beach and former coastal dunes are subjected to severe erosion. The ridges are cut in the coastal dunes due to the attack of waves on their foot *(Fig. 10)*. A single powerful storm may cut away a beach strip about 20 m wide and the sea washed away the coastal dunes up to 8 m high. More powerful erosion has been recorded near Burg El-Burullus village where numerous palm trees are observed today to be submerged by the sea. Nowadays also, many summer houses of Baltim resort located on the beach have been destroyed *(Fig. 11)* due to great advancing of sea water.

For the last reasons, coastal dunes are important forms of protective nature for the coast, especially in some locations where the backshore is low-lying. Coastal dunes along Burullus coast act as barriers against severe action of onshore winds. Other dune ridges slightly further inland are also protective but to a lesser degree than the front ones and help as second line of defence.

To prevent destruction, blow-outs of sand and instability in coastal dunes, suitable stabilization methods should be undertaken. American scientists have carried out successful methods [KING, C. A. M., 1972] for stabilization the coastal dunes. These methods are: *1* — providing of suitable plants which make much contribution

* Identification based on personal communication with PROF. DR. SHUKRI IBRAHIM, Botany Dept., Fac. Sci., Alex. Univ.

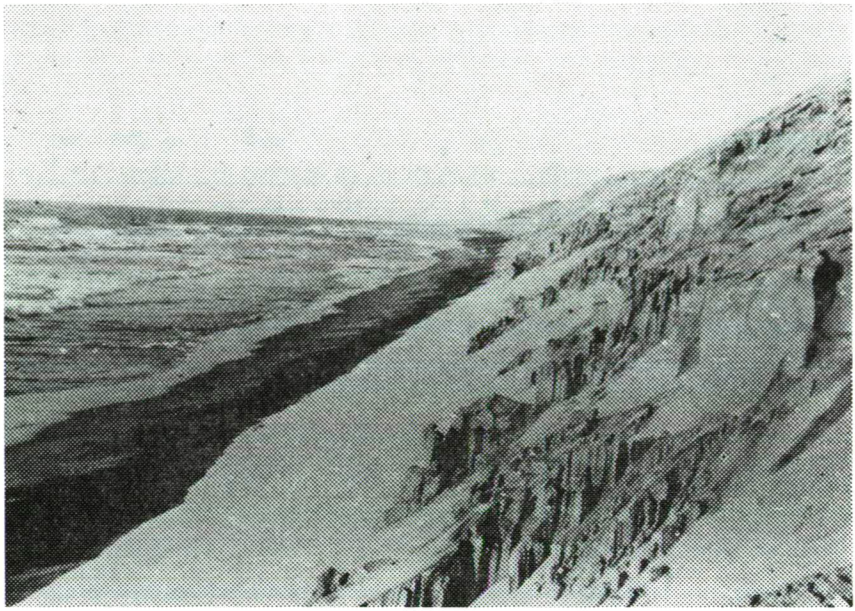

Fig. 10. Waves attack on the coastal dunes — 2 km west of Burullus outlet

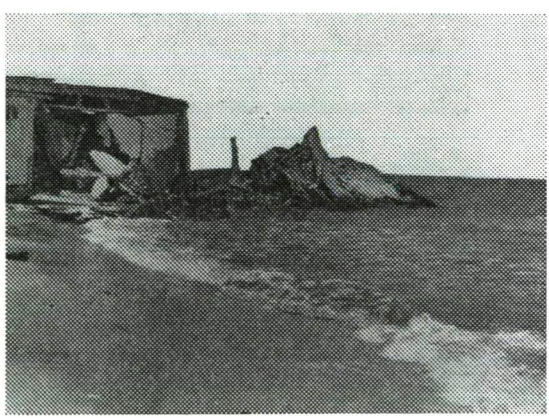

Fig. 11. Sea advancing and destruction of summer houses-Baltim resort.

to the trapping of sand. *2* — sand accumulation can be encouraged by placing brushwood fences in exposed situations. *3* — stabilization of the bare sand by spraying it with a suitable solution that holds the sand in place.

In fact, the vegetation and fences, which are successful methods for dune protection, have been carried out by inhabitants themselves on some restricted areas east of Burullus outlet and west of Gamasa to prevent the covering of their cultivated land by sands.

SUMMARY AND CONCLUSION

Along Burullus-Gamasa coastal dunes, two belts of different extension, type and age can be observed. The first dune belt is coastal, recent, high and run parallel to the coast. The other dune belt is older, smaller, lower and extends parallel to the northern shore of Burullus lake. The two dune belts represent two distinct periods of dune formation due to past advancing of the coast, forming a wide coastal plain and along its newly formed shoreline the younger coastal dunes have been formed. In some locations, a grassy rolling or flat floor separates the two types of dunes.

West of Gamasa, southern parts of longitudinal dunes tend to modify to series of isolated barchan dunes. Such modification occurs with the direction of prevailing wind. This may be an indication to the unstability of longitudinal dunes because recently wind velocities are not strong enough to maintain them.

On light of sand transport from beach to coastal dunes, by wind action, it is found that the variation of percentage of coarse plus medium sands in coastal dunes, follows quite closely those ones that are found on the beach. There is a fining grain size cycle from the beach, throughout the bottom of sand dune, and up to the top whereas the sorting also improves. It is observed that the grain size peaks of coastal dunes are related to those of beach sands with an eastward shifting due to WNW and NW winds. Such sympathetic relationship maintains that beach sands are the source of wind-blown sands.

Grain size parameters are sensitive and used to differentiate between bottom and top of coastal dune sands. The combinations of median and kurtosis *vs.* standard deviation, median *vs.* skewness, skewness *vs.* standard deviation, and coarse percentile *vs.* fine percentile are effective in such differentiation. On the other hand, combination of kurtosis *vs.* skewness is ineffective and failed to differentiate between the two types of sand. The present work indicates that top of dune sands are finer, more sorted, slightly positive skewed and has lower kurtosis values than the bottom sands. Owing to onshore wind affecting the coast, fine sediments can be easily transported from the beach by means of suspension and deposited on the top of dunes due to presence of grassy surface or fences placed in exposed situations. On the other hand, coarse grains are transported close to the backshore surface by means of creeping and saltation. At last, the coarse sediments concentrate on and near the foot of dunes.

Internal structure of barchan dune is clearly observed by excavating it. The stratification of wind blown sand involves three types of laminae of different thickness and dips, and bounding surfaces between sets of laminae. Most of bounding surfaces are straight and show apparent dips almost entirely towards leeward side. Leeward side laminae are more steeper and thicker than both windward and side trench laminae. A series of deformational structures are observed and probably formed as a result of local slumps on the avalanche side.

REFERENCES

ALLEN, J. R. L. [1970]: Physical processes of sedimentation — London: G. Allen and Unwin, p. 248.

ANAN, P. S. [1969]: Grain size parameters of the beach and dune sands, northeast Mass. and New Hampshire coasts — In: Coastal environments. Univ. Mass., p. 266—280.

BAG NOLD, R. A. [1971]: The physics of blown sand and desert dunes — *5th* impression, Chapman and Hall, London. p. 265.

BARAKAT, M. G. and IMAM, M. [1976]: Preliminary note on the occurrence of old indurated sand dunes in the district of Gamasa, northern Nile Delta — In: UNESO /ASRT/ UNDP — Proceedings of seminar on Nile Delta sedimentology. Alex., Oct. 1975. p. 33—39.

COASTAL EROSION PROJECT [1973]: Detailed technical report — Coastal erosion studies, UNESCO /ASRT/ UNDP, Alex., Oct. 1973.
EL-FISHAWI, N. M. [1977]: Sedimentological studies of the present Nile Delta sediments on some accretional and erosional areas between Burullus and Gamasa — M. Sc. Thesis, Fac. Sci., Alexandria Univ. p. 143.
FOLK, R. L. and WARD, W. C. [1957]: Brazos river bar: A study in the significance of grain size parameters — Jour. Sed. Petr. **27**, pp. 3—27.
GLENNIE, K. W. (1970): Desert sedimentary environments — Developments in Sedimentology. Elsevier 14, p. 222.
ISPHORDING W. C. [1972]: Analysis of variance applied to measures of central tendency and dispersion of sediments — Jour. Sed. Petr. **42**, pp. 107—121.
KING, C. A. M. [1972]: Beaches and coasts — London: Edward Arnold Ltd. p. 570.
MCKEE, E. D. [1966]: Structures of the dunes at White Sands National Monument, New Mexico (and comparison with structures of dunes from other selected areas) — Sedimentology **7**, p. 69.
MCKEE, E. D. and TIBBITTS JR. G. C. [1964]: Primary structures of a seif dune and associated deposits in Lybia — Jour. Sed. Petr. **34**, pp. 5—17.
PASSEGA, R. [1957]: Texture as characteristic of clastic deposition — Am. Ass. Pet. Geol. Bull., **41**, pp. 1952—1984.
SESTINI, G. [1976]: Geomorphology of the Nile Delta — In: UNESCO /ASRT/ UNDP — Proceedings of seminar on Nile Delta sedimentology. Alex. Oct. 1975. pp. 12—24.
TOUSSON, O. [1934]: Les ruines sous-marines de la baie d'Abuquir — Bull. Soc. Roy. Arch. Alex., **29**, pp. 342—354.
TWENHOFEL, W. H. [1932]: Treatise on sedimentation — Baltimore, The Williams and Wilkins Co. p. 926.

Manuscript received, June 18, 1981

M. A. EL-ASKARY
Alexandria University
Egypt

N. M. EL-FISHAWI
Institute of Coastal Research
Alexandria
Egypt

Present andress:
József Attila University
Department of Geology and Paleontology
H—6721 Szeged Pf. 428.
Hungary

Acta Mineralogica-Petrographica, Szeged, XXV/1, 77—84, 1981

GEOLOGY OF GACHERI DHORO BARITE DEPOSIT, LASBELA, PAKISTAN

S. J. MOHSIN, M. A. FAROOQI and GHULAM SARWAR

ABSTRACT

Barite alongwith sulphide minerals occurs at several places in the southern part of axial fold belt of Pakistan. The deposits are confined within a lower-middle Jurassic rock sequence consisting of medium thick bedded limestones alternating with shales. In Lasbela area, allochthonous mineralized Jurassic blocks are embedded in a melange belt consisting of serpentinized ultramafics, doleritic sills and spilitic lava flows. Gacheri Dhoro deposit comprises of about 20 meters thick mineralized zone of interbedded limestone, shale and baritic rock. The precipitation of barite has taken place in the Jurassic sediments at structural highs by circulating connate brines or by mixing of meteoric water with ore fluids during late diagenetic-epigenetic stage of the host rock.

INTRODUCTION

Barite deposits in Pakistan are located at several places within the well defined tectonic unit known as Axial Belt. Most important deposits occur around Khuzdar where reserves are estimated as 1.5 million tons and a grinding plant for barite has recently been set up. Several deposits are known in Lasbela District but only two have briefly described by KLINGER and ABBAS [1963]. The barite occurrence at Gacheri Dhoro, known for quite sometimes and quarried on a small scale in the past, has not been described before.

Gacheri Dhoro, a perennial stream originating from Mor Range and flowing to the plains of Lasbela, is on Survey of Pakistan Topo-sheet No. 35.J/12. The deposit can be reached from Uthal which is 125 km north of Karachi on R.C.D. Highway. From Uthal a jeepable track follows the stream bed for 40 km and ends up at a ridge whose peak is locally known as Bhuji (838 m). The deposit is located about 200 m below the peak. The terrain is rather rugged and rock types of widely varying nature impart a high relief to the area.

REGIONAL GEOLOGICAL SETTING

Major tectonic activity during late Cretaceous-Tertiary has shaped the fundamental geologic structures of Pakistan. The most dominant among them is an axial fold belt which runs sinuously throughout the country from north to south. This fold belt is the result of northward movement of the Indian plate and its subsequent collision with the Afghan and Central Iran blocks of the Eurasian plate [POWELL, 1979]. The northern part of the fold belt shows southward thrusting, varied grades of metamorphism and anatectic granitic intrusions. The Central and southern part of the fold belt appear to be generally devoid of these features since the northward move-

ment of the Indian plate after collision appears to have been absorbed by the Chaman transform system of faults. However, a number of ophiolitic occurrences with varying thicknesses of melange are conspicously present all along the belt near the western boundary of the Indian plate.

The Lasbela region constitutes the southern part of the fold belt and consists of well defined north-south running Pab and Mor ranges, and less defined Jaisar and Kulri ranges *(Fig. 1)*. Mor Range forms the structural high and is the most prominant geomorphic feature of the area. The range is composed of Jurassic limestones succeeded by the Cretaceous formations on the flanks. A stack of thrust sheets consisting of ophiolitic rock lies over Cretaceous argillaceous strata west of Mor Range. The ophiolitic sheet is composed of more or less thoroughly serpentinized ultramafic rocks, thick gabbroic-doleritic sills and spilitic pillow lava. The ultramafics are mainly harzburgite with minor dunites, periodites and chromitites. The sills and flows are intercalated with a varied assemblage of sediments such as radiolarian cherts, siliceous argillites, shales, marls and limestones. Manganiferous and cupriferous sediments are also present locally. In between the Cretaceous argillaceous sequence and the allochthonous ophiolites is a narrow belt of sedimentary melange. The melange belt named as Kanar melange (DEJONG and SUBHANI, 1979] is made up of blocks which vary in size from a few tens of metres to over a kilometre and are set in a variegated pelitic matrix. The blocks consist of ophiolitic and Mesozoic, mainly Jurassic, shelf rocks of the area.

The oldest rocks exposed in the Lasbela area represent the lower-middle division of Jurassic as in other parts of the fold belt (Table 1). The unit is named Windar

TABLE 1

Mesozoic succession of the southern part of axial belt

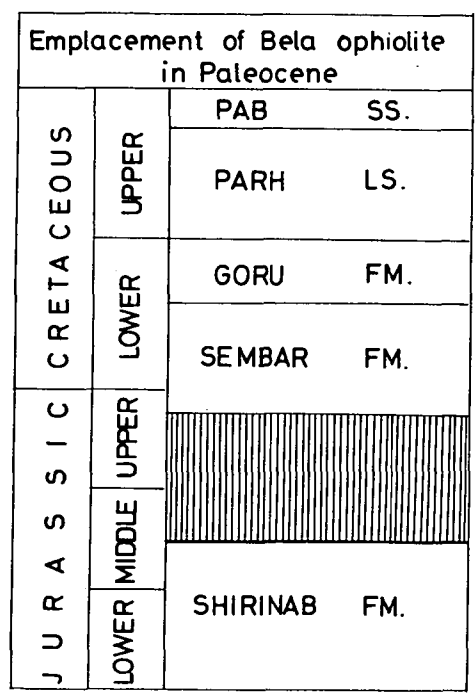

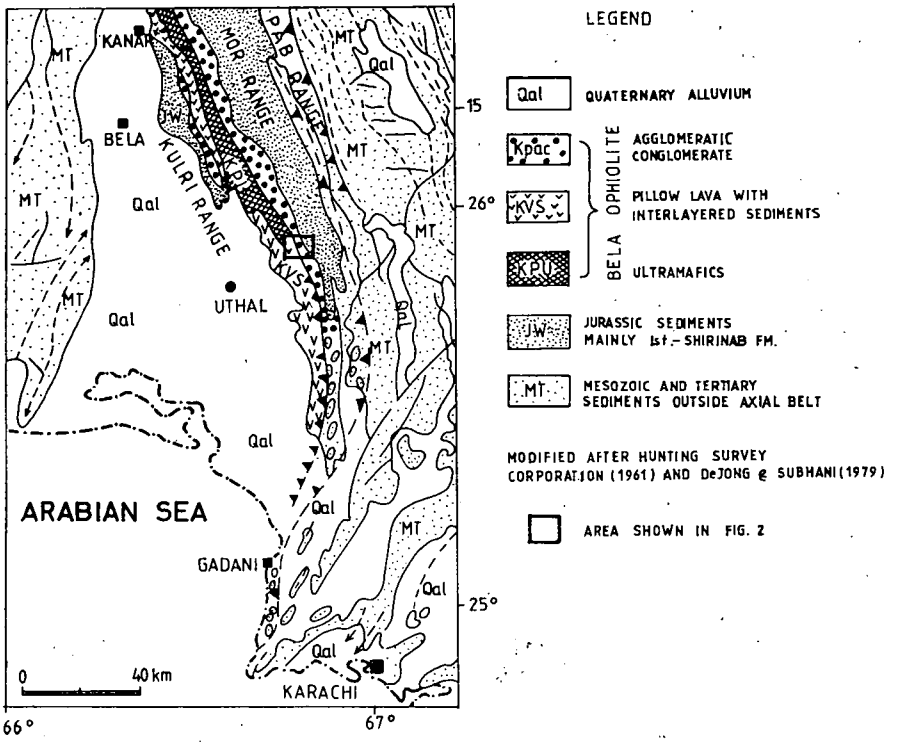

Fig. 1. Geological map of southern part of axial belt (Lasbela region)

group by Hunting Survey Corporation [1961] and Shirinab formation by FATMI [1977]. The formation dominantly consists of medium to thick bedded limestone with subordinate dark calcareous shales. The thickness of the formation is measured more than 1500 meters in the Mor Range.

A monotonous sequence of regularly bedded brownish gray, finely laminated mudstones with thin intercalations of shale and marl overlies the Jurassic rocks. The strata are deformed by open flexural folding. The sequence has the stratigraphic position and lithology of Sembar formation though it does not display the characteristic greenish hue and abundance of belemnite. The maroon shales and limestones of Goru formation are not seen in the area.

The argillites are overlain by volcanic rocks with interflow shales and ultramafics. The volcanic rocks consisting of a heterogenous assemblage of pillow basalts, radiolarian cherts, argillites and manganese bearing sediments are named as Bela Volcanic group by Hunting Survey Corporation [1961]. The ultramafics and doleritic sills were considered to be intrusive in nature and were named as "Porali Intrusions". The volcanics and ultramafic bodies are now interpreted as obducted oceanic crust. The ultramafic slivers are taken as a part of layer 4, pillow basalts with dolerite sills as layer 2 and radiolarian cherts with manganese bearing sediments as layer 1. Layer 3 of gabbro sheeted dykes is not known in the area but has been reported in the adjacent area (SUBHANI, pers. comm). A typically intact sequence has not been observed

either in the area under study or in the adjoining Kanar Area [DEJONG and SUBHANI, 1979]. The partial sequences met in the area meay even be reversed. According to ALLEMAN [1979] the obduction has taken place in Paleocene.

GEOLOGY OF THE DEPOSIT

A barite quarry is situated at an elevation of about 600 m where work has been done on two levels along the strike of the beds. In the upper working level 4 m thick beds have been opened for 25 m along the strike while the lower working level exposes 14 m thick beds for 56 m in the strike direction. The section shows half to one meter thick limestone beds, alternating with shale beds having intercalation of thin limestone bands. Barite-sulphide mineralization is confined to limestone beds. The thicker beds of limestone are more intensively mineralized as compared to thinner beds which contain a number of stringers and lenticles. These layers and stringers lie parallel to the bedding. The details of the section exposed in the lower level of the quarry and the extent of mineralization is shown in *Fig. 3*. Some late fractures 2—5 cm thick and oblique to the bedding are filled wiht slightly greenish coloured and granular barite. However, such fractures are confined to a single thick bed and do not cross the underlying or overlying beds.

Barite is transluscent, clear to milky white with well developed elongated basal cleavage. Crystalline aggregates of barite often display a radiating structure; the rosettes of barite are well developed where thick mineralization has taken place, though it can be descerned even in the stringers. Cubes of galena about one inch size are frequently observed in the limestone in association with barite.

Assuming the ore body to be tabular, a highly conservative estimate of the reserves is calculated on the basis of exposed quarry sections. The estimate is 1500 tons for the upper level and 12 000 tons for the lower level. The reserves are expected to be more since the mineralized beds have not been opened fully in their strike direction as the overburden increases appreciably for an open cut. Similarly one may expect more mineralized beds below the lower most unmineralized shale bed. Nevertheless, the quarrying has been abandoned as it proved to be unprofitable. Most of the barite, apart from two continuous layers, is in the form of stringers and can only be recovered from the limestone by crushing and hand sorting.

Two samples of barite (BG—1 and BG—2) from the richly mineralized 2.1 metres thick bed of limestone and one (BG—3) from less mineralized limestone bed below, have been analysed. The analyses of Khuzdar main barite [KLINGER and AHMED, 1967] are also given for comparison (Table 2).

The Jurassic rocks containing the mineralized beds and forming Bhuji peak is an allochthonous block resting over the Cretaceous strata *(Fig. 2)*. The Lasbela region displays a compressional tectonics and the presence of ultramafics are explained by thrusting. An obvious explanation for the presence of Jurassic block over the younger strata would be overthrusting of older rocks towards east. Moreover, role of gravity tectonics as an active process during initial emplacement of the rocks appears significant.

The reversal of the ophiolitic sequence may be due to isoclinal and recumbent folding [ABBAS, 1979]. A complete intact sequence, however, has not been observed in the area and the reversal of partial ophiolitic sequence in Kanar area, Lasbela District has been compared with "diverticulation" in Alps [DEJONG and SUBHANI, 1979] and are shown to be indications of emplacement by gravity. The mechanism

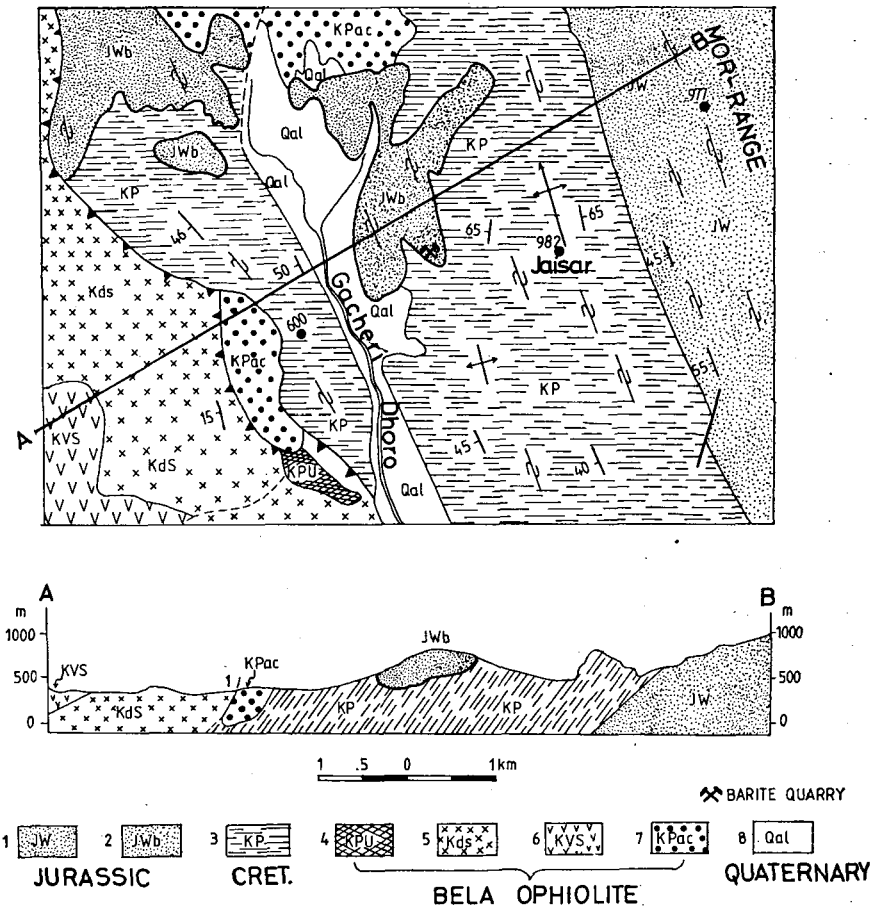

Fig. 2. Geological map of Gacheri Dhoro area, Lasbela. Legend: see *Fig. 1*

is envisaged as beginning with the uplifting of the source area and sliding of the upper layer followed successively by lower layers resulting in a reversal of the sequence. For gravitational emplacements it is sufficient that the upper surface of the cover material slopes in the direction of the displacement [HUDLESTON, 1977]. The Mor uplift provides the necessary slope where gliding under gravity would cause a reversal of the ophiolitic sequence as well as the emplacement of the Jurassic blocks on Cretaceous volcano-sedimentary sequence between Kulri Range and Mor Range. The Jurassic blocks are much more defor medthen the surrounding mudstone and conglomerate. The discrepancy between the structural style clearly indicates a prior deformational history of the blocks before their final emplacement.

ORIGIN OF THE DEPOSIT

In Khuzdar area, barite deposits are known from Gunga, 16 km south of Khuzdar. The deposits extend for 1200 metres in length in Jurassic limestones and consist of barite lenses varying in thickness from 3 to 6 metres in the south to 15 metres in

TABLE 2

Analysis of barite samples

CONSITUENTS %	SAMPLE NOS. BG—1	BG—2	BG—3	Ba—1	Ba—2
$BaSO_4$	97.86	95.34	63.76	91.86	95.92
SiO_2	0.07	0.32	3.71	2.48	1.84
Fe_2O_3	0.05	0.13	0.14	0.02	0.03
Al_2O_3	0.37	0.38	2.11	2.73	0.26
CaO	0.70	1.75	12.10	0.98	0.49
MgO	0.00	0.13	3.65	1.91	0.76
Ignition loss	0.96	1.88	14.23	1.63	0.67
TOTAL:	99.99	99.93	99.70	99.62	99.97

NOTE

BG — 1 Barite samples from Gacheri Dhoro
BG — 2
BG — 3 Barite with limestone, Gacheri Dhoro
Ba — 1 Barite from Khuzdar main barite deposits
Ba — 2 [KLINGER and AHMED, 1967]

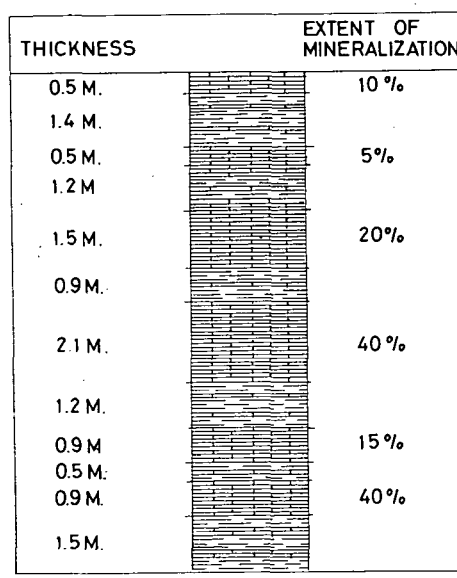

Fig. 3. Barite quarry section (lower level)

the north. Small amounts of calcite and quartz, minor amounts of goethite, haematite, and traces of galena, cerussite, cinnabar and rhodochrosite are associated with barite. Three kilometres further south, a porous gossan containing galena associated with pyrite and traces of copper is an extension of the barite horizon. At Shekran, 25 kilometres northwest of Khuzdar, galena associated with siderite and limonite is known to occur in the same horizon. Minor occurrences of barite and fluorite are also reported from Shekran.

In Lasbela area, barite deposits are reported from Kundi, Bankhri and Siro Dhoro. At Kundi, 65 kilometres north of Bela, barite occurs in a 8 metres thick zone in Jurassic limestone. The barite zone consists of alternating layers of barite and dark gray fissile shales. Thickness of barite layers vary from 0.3 to 1.5 metres. Association of galena and traces of copper minerals are often observed. The Gacheri Dhoro and few smaller barite deposits in Kulri Range occur in allochthonous Jurassic blocks emplaced in volcano-sedimentary sequence of lower Cretaceous.

The origin of the stratiform barite bodies in carbonate rocks can be explained by preferential replacement of certain favoured beds along bedding planes. The deposits have generally been considered to belong to an epithermal suite precipitated from low-temperature hydrothermal solutions [KLINGER and AHMED, 1967; SCHEGLOV, 1969: ZAIDI, 1972]. In the absence of a nearby igneous source, the term telethermal has been used to indicate a distant source and a cooler nature of the solutions. SILLITOE [1975] relates the deposits to the precipitation by connate brines in Jurassic host rocks on the continental shelf of the Indian Plate prior to its seperation from Gondwanaland. The mixing of a barium rich circulating connate water with ascending telethermal solutions may account for deposition of barite [SAWKINS, 1966]. Ground water-ore fluid interface may also cause the deposition of barite as the solubility of barium in the ore fluid is considerably decreased on coming in contact with meteoric water [PLUMMER, 1971]. The laterally upward movement of pore fluids in the depositional basin due to compaction under the weight of overlying sediments has been suggested by JACKSON and BEALS [1967] for Mississippi Valley type ores.

A mechanism for the origin of stratiform barite bodies under discussion is suggested here. The telethermal solutions reach the northwestern shelf of Indian shield where the sediments are being laid down during Lower-Middle Jurassic period. The floor of the basin is marked by an uplift forming an elongated ridge which trends north-south. The subsequent movements lead to the emergence of ridge at many places to form intermittent island like areas along the whole length. The ore fluids move laterally upwards as a result of compaction under the weight of overlying sediments. The ascending ore fluids finally reach the structural highs in the basin where emergent Lower-Middle Jurassic limestones form island like areas. The mixing of ore fluids with meteoric water causes a marked decrease in the solubility of barium ions in the ore solutions and leads to the precipitation of barite. The role of barium-rich connate water trapped during early sedimentation stages can not be ruled out. The compaction of sediments during the late Jurassic period may expel the ore fluids to suitable sites such as bedding planes where barite is precipitated.

The stratiform nature of the deposits, their occurrence within a confined stratigraphic interval and insignificant wall rock alteration of the host rocks, suggest that the barite mineralization has taken place during the late diagenesis of Lower-Middle Jurassic sediments. The occurrence of barite nodules in the overlying Sembar formation at Naka Pabni also indicates that the mineralization has taken place before Late Jurassic — Early Cretaceous shales were laid down.

ACKNOWLEDGEMENTS

We are thankful to M. HUSSAIN and S. I. SALEEM of Resource Development Corporation Laboratories for the chemical analysis of barite samples. We also thank M. U. QUADRI for the help in the preparation of maps and figures.

REFERENCES

ABBAS, S. G. [1979]: A plate tectonic model for emplacement of manganese ore in Axil Belt, Abs., 26th/27th Annual All Pakistan Science Conference, Lahore.

ALLEMAN, F. [1977]: Time of emplacement of the Zhob Valley Ophiolites and Bela Ophiolites, *in:* Farah and DeJong, (eds.) Geodynamics of Pakistan, Pak. Geol. Surv., pp. 215—242.

DEJONG, K. A. and SUBHANI, M. A.: [1979] Note on the Bela Ophiolites with special reference to the Kanar area, *in*: FARAH and DEJONG (eds.), Geodynamics of Pakistan, Pak. Geol. Surv., pp. 263—270.

FATMI, A. N. [1977]: Mesozoic, *in:* SHAH, S. M. I, (ed). Stratigraphy of Pakistan; Pak. Geol. Surv., Memoir, **12** pp. 29—55.

HUDLESTON, P. J. [1977]: Similar folds, recumbent folds and gravity Tectonics in ice and rocks, Journal of Geology. **85** pp. 113—122.

HUNTING SURVEY CORPORATION (H. S. C.) [1961]: Reconnaissance geology of part of West Pakistan, Colombo Plan Cooperative Project Canada Government, Toronto, pp. 550.

JACKSON, S. A. and BEALES, F. W. [1967]: An aspect of sedimentary basin evolution the concentration of Mississippi Valley-type ores during the late stages of diagenesis, Bull. Can. Petrol. Geol, **15**. pp. 383—433.

KLINGER F. L. and ABBAS, S. H. [1962]: Barite deposite of Paksitan, *in:* CENTO Symposium, Industrial Rocks and Minerals, Lahore, pp. 418—428.

KLINGER F. L. and AHMED, M. I [1967]: Barite deposits near Khuzdar-Kalat Division, West Pakistan: Pak. Geol. Surv. report (Unpub.).

PLUMMER, L. N. [1971]: Barite deposition in Central Kentucky, Econ, Geol., **66**, pp. 252—258.

POWELL, M. A. [1979]: A speculative tectonic history of Pakistan and surroundings: some constraints from the Indian Ocean, *in:* Geodynamics of Pakistan, Pak. Geol. Surv., pp. 5—24.

RAZA, H. A. and IQBAL, M. W. A. [1977]: Mineral deposits, *in:* SHAH, S. M. I., (ed. Stratigraphy of Pakistan, Pak. Geol. Surv., Memoir **12**, pp. 98—120.

SAWKINS, F. J. [1966]: Ore genesis in the North Pennine Ore field in the light of fluid inclusion studies, Econ. Geol. **61**, pp. 385—401.

SHCHEGLOV, A. D. [1969]: Main features of endogenous metallogeny of the Southern part of West Pakistan: Pak. Geol. Surv., Memoir **7**, pp. 12.

SILLITOE, R. H. [1975]: Metallogenic evolution of a collisional mountain belt in Pakistan, Pak. Geol. Surv., Rec. **34**, pp. 16.

ZAIDI, M. M. [1972]: Note on barite-galena occurrence of Lasbela; Geonervs, Pak. Geol. Surv. **11**, No. 2, pp. 32—34.

Manuscript received, January 27, 1980

S. I. MOHSIN & M. A. FARAOOQI
Department of Geology,
University of Karachi
Karachi, Pakistan.

GHULAM SARWAR
Department of Geology
University of Cincinnati
Cincinnati, Ohio. 55221, U.S.A.

Acta Mineralogica-Petrographica, Szeged, XXV/1, 85—96, 1981

SOME PETROCHEMICAL CHARACTERS OF SAMADAI GRANITIC COMPLEX, SOUTH EASTERN DESERT, EGYPT

MAHMOUD LOTFY KABESH, ABDEL-KARIM AHMED SALEM, MOHAMED E. HILMY and EL-SAID RAMADAN EL-NASHAR

ABSTRACT

The Samadai granitic complex in the Central Eastern Desert of Egypt is petrochemically evaluated. Major oxides data of 13 new chemical analysis are advanced and processed following several chemical parameters. The serial characters, NIGGLI values and normative minerals are discussed. The rocks of the complex belong to the calc-alkaline series and are dominantly potassic with some sodic tendencies. Chemical classification of the granitic complex is presented.

INTRODUCTION

The granitic complex of Samadai is considered by EL-RAMLY and AKAAD [1960], SABET [1961] and EL-RAMLY [1972] as belonging to the younger group of granitoids. SABET *et al.*, [1976] grouped the granitic complex of Samadai with several granitic plutons in the Eastern Desert of Egypt as belonging to the Late-Proterozoic-Early Paleozoic intrusions. The same authors also [*op-cit.*, 1976] assigned these granitic plutons to the "Gattarian group" and to the phase of the coarse-grained biotite granite and the leucocratic granite.

The examined rocks of Samadai granitic complex occur along the Eastern border of the basement rocks in the Red Sea Coast, *(Fig. 1)*. The northern part of the complex has been previously examined by ESSAWY, [1967]. He mentioned some details of the field characters and petrography of the complex. According to ESSAWY *(op. cit.)* the complex consists essentially of medium-grained adamellites and granodiorites associated with tonalites and minor granites. However, ESSAWY *(op. cit.)* gave no details of the petrochemical characters or the chemical classification of Samadai granitic complex. Later, ESSAWY [1972] in an attempt to reveal the genetic relationships between members of the complex advanced the results of partial analysis for certain elements (Na, K, Rb, Sr) of the rock units of the complex. He concluded that the calc-alkaline granites bear no parental relation to the adamellite and granodiorites.

The present study forms part of a continuing investigation of the petrochemistry and petrogenesis of the younger granitoids of Precambrian age in the Eastern Desert of Egypt.

GEOLOGIC SETTING OF SAMADAI AREA

Samadai area is dominantly formed of Precambrian basement rocks. According to ESSAWY [1967] the basement rocks of the examined area comprise metasediments, serpentinites, metagabbro-diorite complex, granites, adamellites and granodiorites.

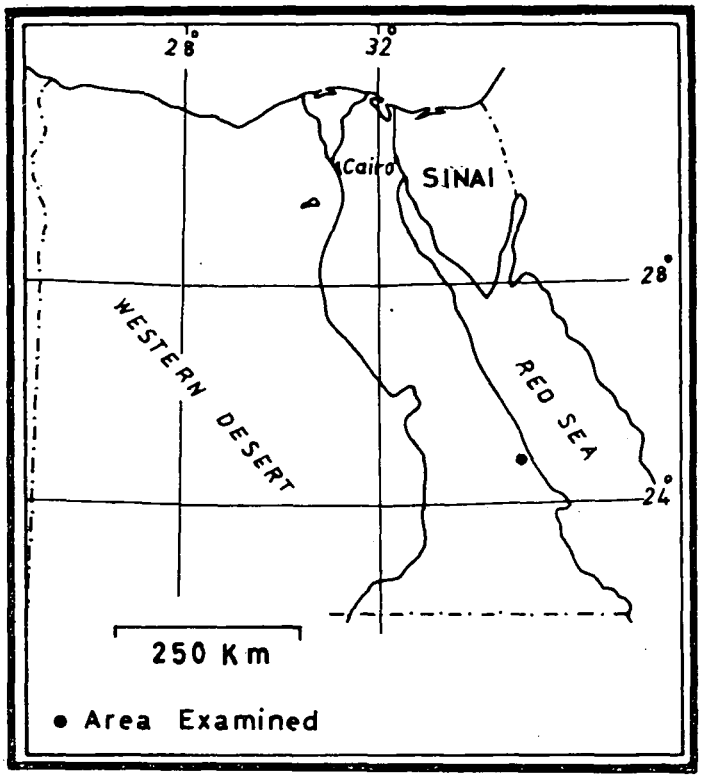

Fig. 1. Location map

The present work deals mainly with the granitic complex of Samadai which comprise two field types: pink — red granitic rocks and greyish-white granodiorites. The granitic rocks of Samadai form a rather circular body showing sharp intrusive contacts with older country rocks to the north, west and south and which comprise metasediments, Serpentinites and metagabbro-diorite rocks. The various basement rocks are traversed by few post-granite dykes *(Fig. 2)*. Based on field observations and crosscutting relations as well as the presence of xenoliths of the country rocks within the host granitic rocks, it is believed that the granitic complex is of younger age. Contacts between the various members of the granitic complex may be sharp but more commonly they are gradational. The granitic complex appears to have reached the present position probably as a result of forcible intrusion pushing aside and shouldering apart of the country rocks. According to ESSAWY [1967] the emplacement was reasonably accompanied by some kind of the granite tectonics resulting in thrusting, phyllonitisation of metasediments and brecciation of serpentines.

PETROGRAPHY

The detailed petrography of Samadai granitic complex has already been mentioned by ESSAWY *(op. cit.)*. Generally rocks of the complex are medium-to rather coarse-grained with holocrystalline hypidiomorphic granular texture. They are usually

non-porphyritic and even-grained. Few types are porphyritic with quartz and plagioclase megacrysts. Intergrowths such as micrographic and myrmekitic are sometimes striking. Both biotite and hornblende represent the mafic minerals. Rarely biotite is the sole mafic. Secondary chlorite is not uncommon while apatite, zircon, epidote, sphene, magnetite and ilmenite are notable accessories.

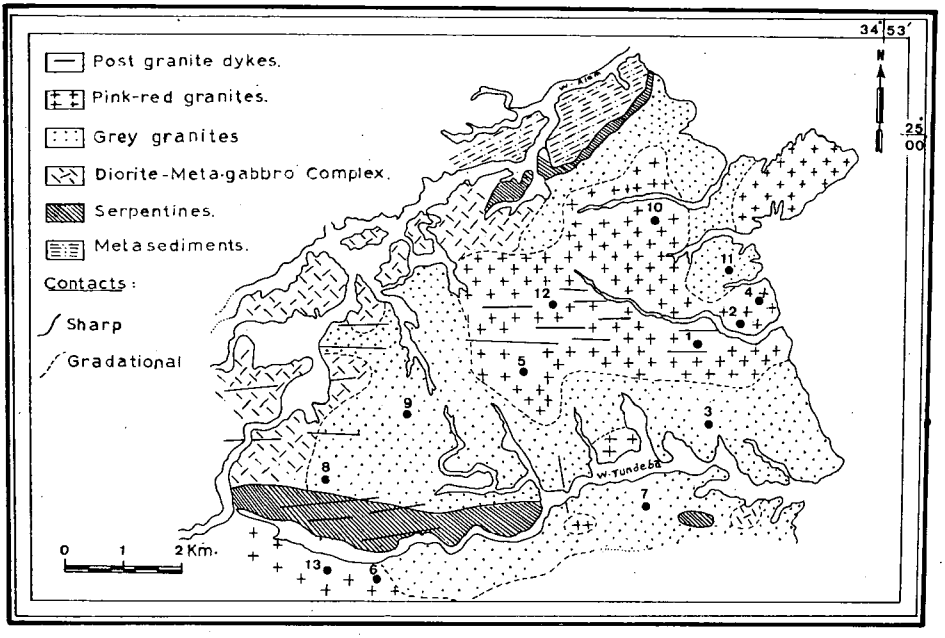

Fig. 2. Generalized geological map of Samadai area showing granitic types with samples location

PETROCHEMICAL INVESTIGATION

The petrochemical characters of the granitic rocks were clarified from RITTMAN's Suite Index, normative minerals, NIGGLI values and variation diagrams as calculated from the chemical data obtained.

Complete chemical analysis of 13 samples representing the different types of Samadai granitic complex were carried out and the results are given in Table 1 while the location of the analysed samples is shown in *Fig. 2.*

RITTMAN'S INDEX

RITTMAN's Suite indices, [1957] for Samadai granitic rocks are given in Table 1 and plotted graphically in *Fig. 3* against SiO_2. It is clear from the diagram and according to the quantitative subdivisions of RITTMAN that these granitic rocks range between weak pacific and strong pacific (2.24—4.53) which correspond on the average to calc-alkaline character.

The chemical composition of rocks in Table 1 has been recalculated in terms of $K_2O + Na_2O$, $FeO + Fe_2O_3$ and MgO and the results are plotted on an AFM diagram

TABLE 1

Chemical analyses of Samadai granitic rocks

	1	2	3	4	5	6	7	8	9	10	11	12	13
SiO_2	70.93	71.53	72.14	65.08	70.55	69.75	68.11	70.97	70.16	72.55	71.70	64.30	67.81
Al_2O_3	14.10	13.13	13.25	15.68	15.29	14.78	13.55	14.53	15.29	13.32	13.74	17.84	14.50
Fe_2O_3	2.27	1.85	0.24	4.33	0.52	1.18	3.56	0.74	1.52	0.67	0.82	2.88	2.20
FeO	1.19	1.45	2.35	1.06	1.24	1.29	2.30	0.76	1.63	1.27	1.31	3.42	1.79
MnO	—	—	0.01	—	—	—	0.03	—	—	—	—	0.02	—
MgO	0.43	0.54	0.42	0.50	1.74	1.71	0.27	0.58	0.29	0.50	0.50	0.95	0.89
CaO	0.66	0.60	0.91	2.73	0.42	0.49	0.88	0.49	0.49	1.02	0.49	1.20	0.66
Na_2O	4.25	3.88	4.81	4.50	4.00	4.13	4.00	5.00	4.38	4.75	3.94	4.25	4.63
K_2O	5.00	4.78	4.88	5.50	4.88	5.25	4.88	5.06	4.50	3.38	5.38	3.13	5.00
TiO_2	0.38	0.38	0.03	0.55	0.03	0.03	0.49	0.03	0.64	0.15	0.30	0.66	0.40
P_2O_5	0.31	0.31	—	—	—	—	—	0.24	—	—	—	0.24	0.24
H_2O	0.98	0.72	0.68	0.46	1.58	0.80	1.00	0.72	1.08	1.50	1.12	1.12	1.07
TOTAL	100.50	99.17	99.72	100.39	100.25	99.41	99.07	99.12	99.98	99.11	99.30	100.01	99.19
RITTMAN'S Index	3.06	2.63	3.22	4.53	2.86	3.31	3.14	3.61	2.89	2.24	3.02	2.56	3.73
Agp. Coef.	0.88	0.88	0.96	0.85	0.78	0.84	0.88	0.94	0.79	0.86	0.90	0.58	0.90

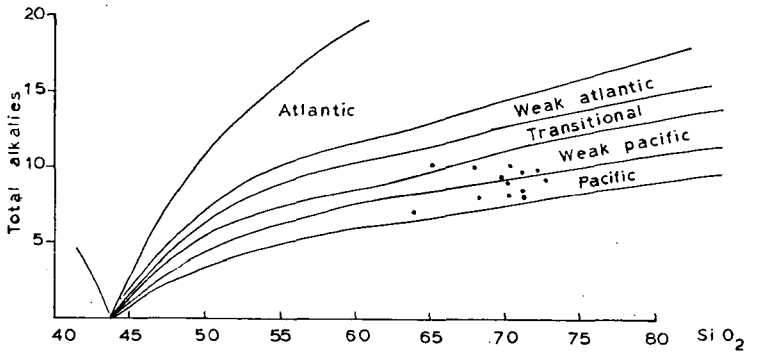

Fig. 3. SiO_2—$(Na_2O + K_2O)$ diagram [after RITTMANN, 1957]

(Fig. 4). The diagram shows that the Samadai granitic rocks are enriched in alkalies and impoverished in magnesium and iron.

The analyses have been plotted on the ternary diagram K_2O — CaO — Na_2O (Fig. 5.) and follow a calc-alkaline trend [*cf.* NOCKOLDS and ALLEN, 1953].

Fig. 6 shows the relation between agpaitic coefficient and SiO_2 percent. The agpaitic coefficient from Zavaritski parameter [*cf.* BAILEY and MACDONALD, 1970] is plotted against SiO_2 to show the nature of Samadai granitic rocks. The diagram shows that all the examined rocks are of miaskitic nature i.e. mol. ratio of $Na_2O + K_2O$ Al_2O_3 is less than unity.

The examined granitic rocks have K_2O/Na_2O ratio >0.6 *(Fig. 7)*. According to RAGUIN [1965] these granitic rocks have potassic character with very few showing sodic tendency.

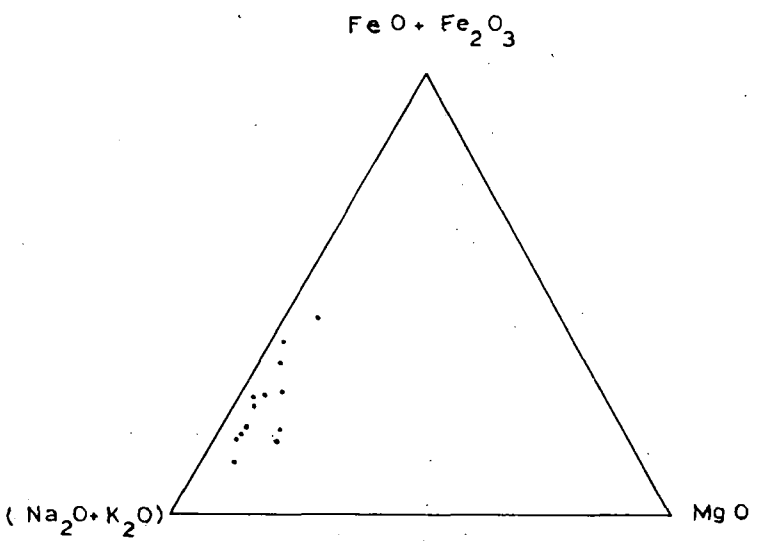

Fig. 4. Variation diagram showing the relationship between MgO—$(Fe_2O_3 + FeO)$—$(Na_2O + K_2O)$

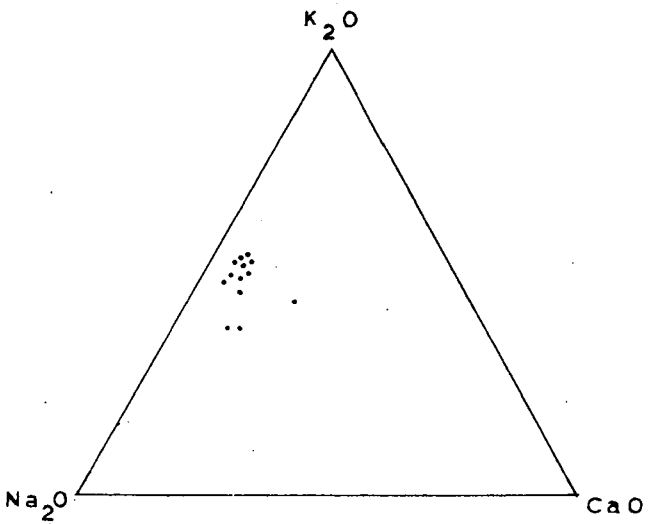

Fig. 5. K_2O—Na_2O—CaO diagram of the investigated granitic rocks

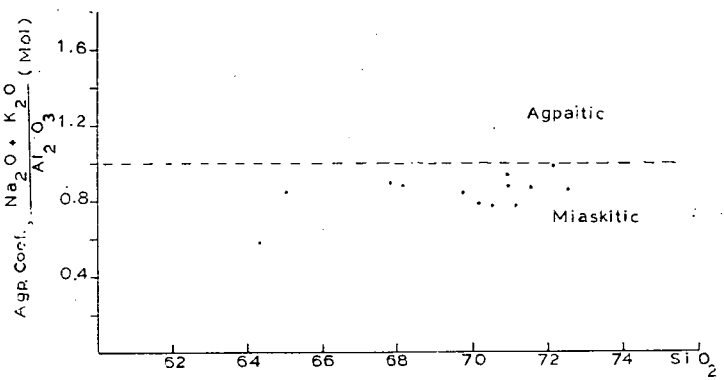

Fig. 6. Agpaitic index — silica diagram

The calculated NIGGLI values of the investigated granitic rocks are given in Table 2. The values of *al* are plotted against *fm* values of NIGGLI *(Fig. 8)* showing that the nature of the magma is salic according to NIGGLI's classification.

The values of *al* are plotted against *alk* of NIGGLI *(Fig 9.)*. It is clear that almost all the granitic rocks of Samadai fall within the relatively alkali-rich, with one sample representing granodiorites falling in the intermediate alkaline rocks [BURRI, 1964].

The NIGGLI values are plotted on the appropriate D-diagram of NIGGLI's series of *(al-alk)—fm—e* triangular diagram [1954] which includes the rock categories I and II (alkali-aluminous), III (alkali-calc-aluminous) VI (alkali-calc-femic) and VII (aluminous). It is evident from the diagram on *Fig. 10* that all the samples plot in the categories I and II.

The calculated norm values of the examined granitic rocks are given in Table 3. *Fig. 11* shows normative quartz plotted against normative anorthite. It is evident

TABLE 2

NIGGLI *values of the investigated granites*

	1	2	3	4	5	6	7	8	9	10	11	12	13
al	42.24	41.60	40.37	37.07	44.01	41.27	38.17	44.55	45.99	43.57	44.17	43.13	39.71
fm	17.00	18.33	14.38	19.62	19.64	21.40	23.90	10.70	15.00	12.83	13.41	26.50	20.92
c	3.60	3.46	5.04	11.73	2.20	2.49	4.51	2.73	2.68	2.07	2.86	5.27	3.30
alk	37.16	36.61	40.21	31.58	34.15	34.84	33.42	42.01	36.32	37.53	39.56	25.09	35.86
si	360.60	384.58	373.02	261.10	344.61	330.52	325.60	369.26	358.12	402.73	391.15	263.79	316.75
k	0.44	0.45	0.40	0.45	0.45	0.46	0.45	0.40	0.40	0.32	0.47	0.33	0.42
mg	0.19	0.24	0.23	0.15	0.64	0.56	0.07	0.42	0.15	0.32	0.30	0.22	0.30
qz	+111.96	+138.14	+112.20	+34.79	+108.02	+91.15	+91.92	+101.22	+112.84	+152.61	+132.91	+63.43	+73.31

TABLE 3

Norm-values for the examined granites

	1	2	3	4	5	6	7	8	9	10	11	12	13
gz	24.28	27.78	20.54	11.94	22.67	20.04	22.59	19.56	24.15	26.97	24.42	21.69	18.25
or	29.85	28.95	29.05	32.60	29.10	31.30	29.91	30.15	27.00	20.45	32.50	18.85	30.10
ab	38.60	35.75	43.55	40.55	36.25	37.47	37.15	45.30	39.90	43.70	36.15	38.85	42.35
an	1.20	1.00	0.15	6.40	2.10	2.45	4.50	0.85	2.45	5.20	2.50	4.45	1.75
c	1.40	1.37	—	—	2.92	1.56	0.11	0.57	2.58	—	0.60	6.51	0.94
w	—	—	1.76	2.88	—	—	—	—	—	—	—	—	—
en	1.20	1.52	1.18	1.38	4.84	4.76	0.72	1.62	0.82	1.42	1.42	2.68	2.50
fs	—	0.44	3.48	—	1.54	1.16	0.46	0.62	0.58	1.32	1.08	2.46	0.70
mt	1.86	1.98	0.25	1.32	0.54	1.24	3,85	0.78	1.62	0.72	0.87	3.06	2.34
il	0.54	0.54	0.04	0.76	0.04	0.04	0.70	0.04	0.90	0.22	0.42	0.94	0.56
ap	0.67	0.66	—	—	—	—	—	0.51	—	—	—	0.51	0.51
ht	0.40	—	—	2.15	—	—	—	—	—	—	—	—	—
Total	100	99.99	100	99.98	100	100	99.99	100	100	100	100	100	100

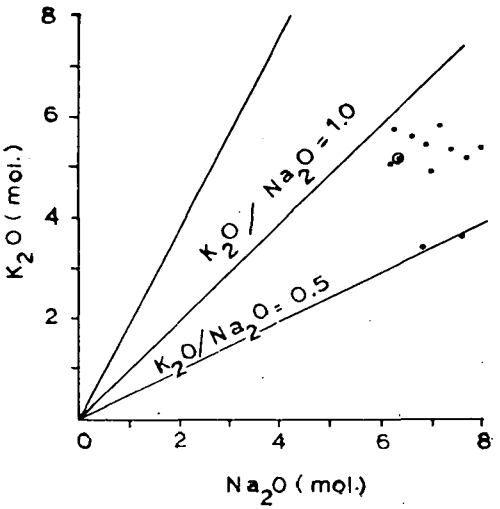

Fig. 7. Variations in alkalies of the granitic rocks ⊙ superimposed point

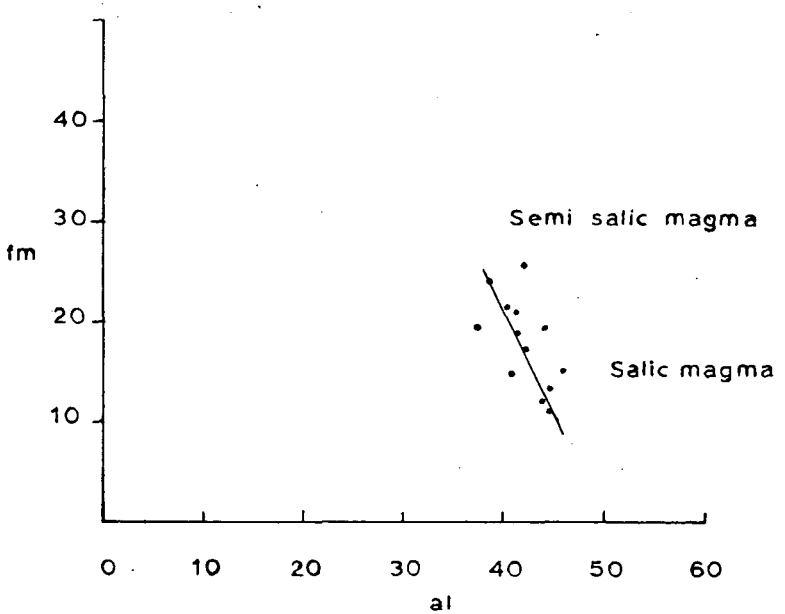

Fig. 8. al — fm diagram

from the diagram that nearly all the granitic rocks fall within the calc-alkalic series with only one sample plotting in the alkalic-calc series.

The normative Ab, Or and Qz are recalculated to 100% for Samadai granitic rocks and plotted on the ternary diagram (Ab—Or—Qz) the residua of TUTTLE and BOWEN [1958]. The plots *Fig. 12* show that the granitic rocks are rather enriched in albite. It is clear that all the analysed samples fall within the area of maximum con-

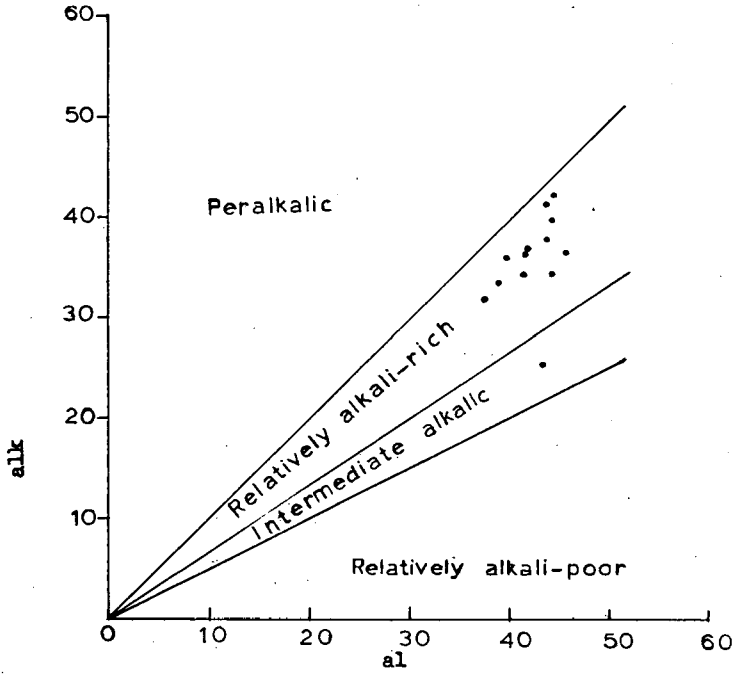

Fig. 9. Relationships of al and alk in the granitic rocks [after BURRI and NIGGLI, 1945]

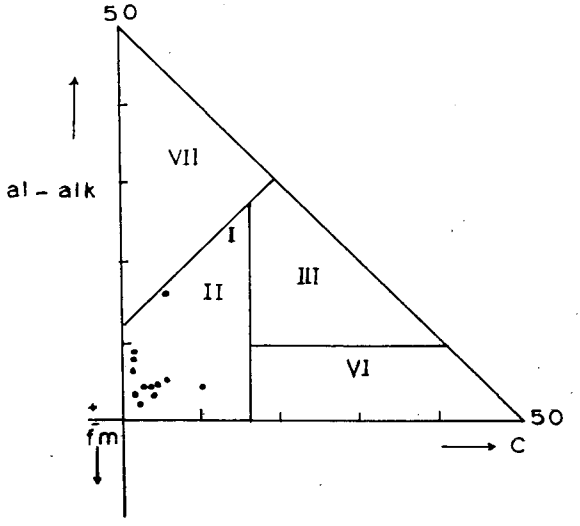

Fig. 10. Relationships of *al-alk* and *c* in the granitic rocks. NIGGLI's D-diagram
I—II: Alk-al silicate rocks
III: Alk-calc-al silicate rocks:
VI: Alk-calc-femic rocks
VII: Al-silicate rocks

centration of analyses of the granites of the world according to TUTTLE and BOWEN (*op. cit.* 79) "the concentration of the analyses near the centre of the diagram is readily explained if the magmatic history is involved in the origin of most granites". The granitic rocks of Samadai are thus considered to possess a magmatic history.

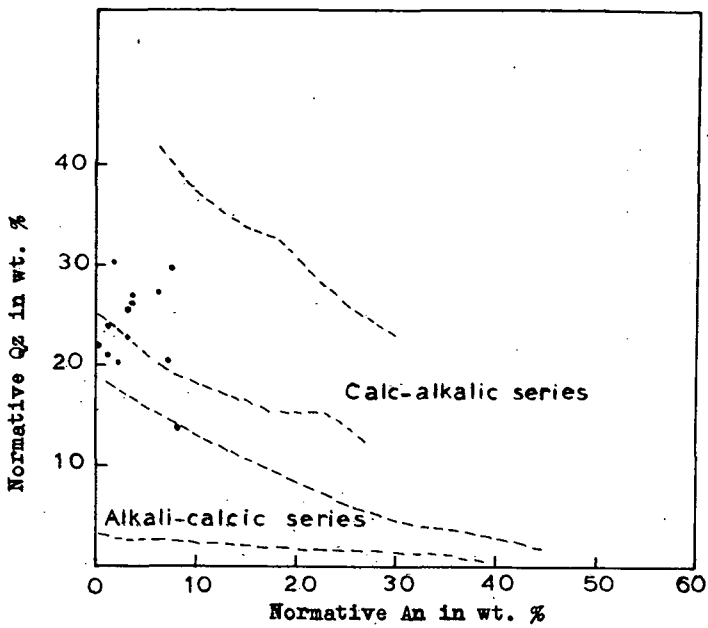

Fig. 11. Normative Qz — An relation for the investigated granites

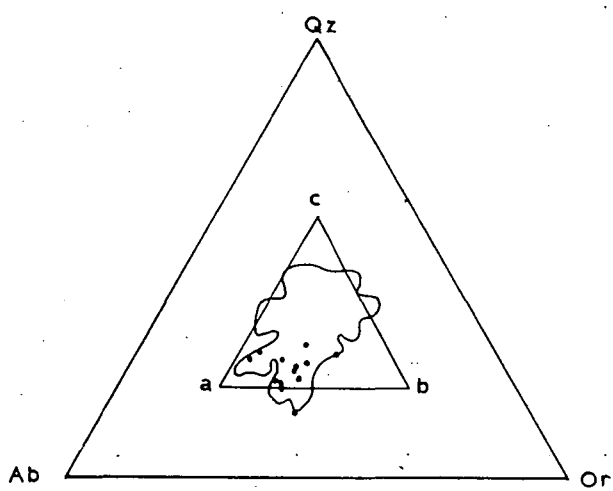

Fig. 12. Contoured triangular diagram showing the distribution of normative Ab — Or — Qz in all analysed rocks (1269) in WASHINGTON's Tables, containing 80% or more Ab+Or+ +Qz [after TUTTLE and BOWEN, 1958 and MARMO, 1971]

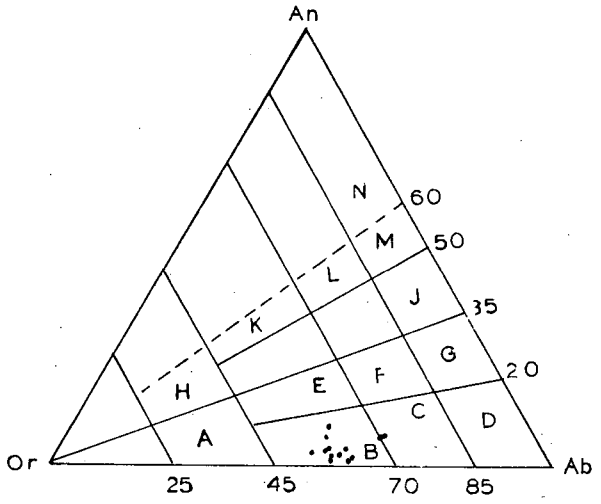

Fig. 13. Triangular diagram for An, Ab, Or normative ratio in granitic rocks [after HIETANEN 1963]

A Kali-granite
B Granite
C Granite trondhjemite
D Trondhjemite
E Quartz-monzonite
F Monzonite
G Tonalite
H Calci-granite
I Granodiorite
J Quartz-diorite
K Calci-monzonite
L Granogabbro
M Gabbro
N Mafic gabbro

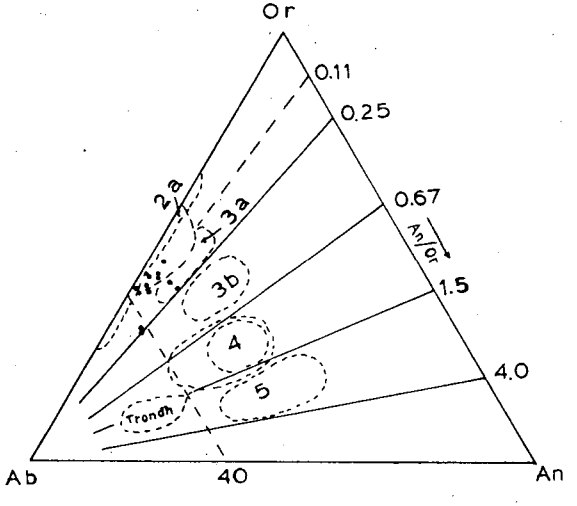

ig. **14.** Quartz — feldspar rocks [after STRECKEISEN, 1976]

2a [Alkali-granite / Alkali-rhyolite
2b [Alkali-feldspar granite / Rhyolite
3a [(Syeno-) granite / Rhyolite
3b [(Monzo-) granite / Rhyodacite
4 [Granodiorite / Dacite
5 [Tonalite / Plagidacite / Trondhjemite

Acta Mineralogica-Petrographica, Szeged, XXV/1, 97—107, 1981

RELATION BETWEEN THE MINERALOGICAL COMPOSITION AND FACIES OF THE SEDIMENTARY FORMATION OF THE NORTHERN AND NORTH-EASTERN CSERHÁT MTS (HUNGARY)

J. ANDÓ

GEOLOGICAL SETTING

The following review is only a short outline of geology of the northern and north-eastern Cserhát Mountains, introducing only details sufficient for understanding of the methods and sediment-petrographic and faciological conclusions.

The Börzsöny, Cserhát and Mátra areas are built-up of Paleogene and Neogene sedimentary sequences, which are parts of a Tertiary basin bordered by the Veporid and Gemerid crystalline masses. These regions form separate mountains due to young tectonic movements and volcanism producing different materials. Consequently heir geomorphological developments are different, too. The tectonic movements resulted the orographic separation of the Cserhát from the Mátra Mountains, while he volcanic activity caused the separation of the Cserhát from the Börzsöny Mountains. The surficial Upper Oligocene psammitic rocks occurring in western and north-estern Cserhát Mts. extend, with similar bedding, under eastern margin of the volcanic mass of the Börzsöny Mts. The sedimentary and magmatic sequences of the eastern Cserhát Mts. and the western Mátra are the same even in details.

The elevated, strongly eroded western, northern and central parts of the Cserhát Mts. are characterized mainly by Upper Oligocene and Lower Miocene sediments and subvolcanic andesite dykes, while the tectonically deeper eastern and south-eastern parts are prevailed by younger, Middle and Upper Miocene and Pliocene ediments and subvolcanic andesite sequence.

Subsidence of the metamorphic basement and the majority of marine sedimen-ation took place in Middle Oligocene concluded from the data of borehole samples. he Paleogene sedimentary basin deepened eastward. It was proved by the Middle ligocene sequences of clay, clay-marl and silty clay-marl ("Kiscell Clay"). These ocks do not outcrop in the studied region.

After the deposition of the so-called "Kiscell Clay" a littoral — shallow-bathyal asin — with tendency for heteropic facies has been formed in the Cserhát region during Oligocene and Miocene. The inherited depth of the sedimentary basin resulted in different depositional conditions in the western and eastern parts of the Cserhát ts. Complete Oligocene-Lower Miocene sequence has been formed in the eastern nd north-eastern Cserhát containing open-sea, clastic sediments, while the western parts became a land after the Upper Oligocene delta-marginal sedimentation. This ontinuous sedimentation caused several problems in delimitation of the Upper Oligo-ene (Egerian) from Lower Miocene (Eggenburgian), as well as the Middle Oligocene strata from Upper one [BÁLDI, 1973]. According to the results of detailed studies he western Cserhát is characterized by a regression shifted from West to East during

the end of Upper-Oligocene and beginning of Lower Miocene, while in the eastern Cserhát a marine sedimentation prevailed lasting to the end of the Lower Miocene.

The terrestrial sediments (variegated clay, fluviatile sand, gravel, rhyolitic tuffs,) which indicate end of the regression, are thin and can be traced only in patches.

Eastward from the studied area, in the Nógrád basin the terrestrial formations are overlain by parallic *coal-bearing sequence* with considerable thickness (Ottnangian) In the studied area the coal with sandy intercalations occurs only as an incomplete series, which pinching out westward. The coal-bearing or the continental sequences are overlain by silty clay (Schlier) indicating open-sea conditions due to the transgression of *Carpathian* times. This formation has been completely eroded later in the northern Cserhát area, but in the eastern Cserhát Mts. this forms the underlying of the *Carpathian — Lower Badenian volcanic sequence.* After the volcanic activity archipelago formed with shallow-water limestone ("Leitha-limestone"), and in the deeper parts with clay and marl, respectively. The formation of these rock-types endured into the *Sarmatian* stage. The marine sequences were changed to lacustrine-lagoonal-deltaic clastic and argillaceous sediments caused by the emergence and gradual enclosure of intervening basins during the Upper Sarmatian.

The last partial transgression of *Early Pannonian*, caused rapidly enclosing and freshening sounds, up to the line of the Pásztó and Alsótold basins. These sounds were infilled by fine-grained, argillaceous and marly clastic sediments.

This brief description shows that the area of the northern north-eastern Cserhát Mts. is formed overwhelmingly by Upper Oligocene — Lower Miocene, and subordinately by Middle Miocene clastic sediments. The lack of subsurface, borehole data, the studies concern only the surficial formations of these ages.

THE EVOLUTION OF THE DEPOSITIONAL ENVIRONMENTS, ON THE BASIS OF THE FACIES STUDIES

The Oligocene and Lower Miocene rocks form a continuous sequence in the studied area. During the mapping work sedimentological units have been distinguished characterizing an extended area becaused of the large variety of lithofacies which intersect the chronostratigraphic boundaries. The transport and deposition terrain has been reconstructed [ANDÓ, 1973] for the given sequences with evaluation of log-probability distribution, using the data of VISHER [1969]. In some sequences the evaluation of litho- and biofacies was possible [ANDÓ, 1975], based on the simultaneous biostratigraphical and biofaciological studies of BÁLDI and HORVÁTH [1970].

The discussion of the results of the mineralogical and sedimentological studies, which were done for each beds and sequences, are outside the aims of the sequences, the facies reconstructions and ages are summarized in Table 1. The reconstruction of depositional terrain from log-probability grain distribution diagrams is a suitable approach for calculating the former water-movement velocity. This gives the most important quantitative depositional character [ANDÓ, 1973] which serves the basis for comparing numerically the given beds and sequences. With this method it can be determined the critical velocity, *i.e.* the limit of transport and resting states, and the mean and bottom velocities (on the basis of the mean size of the saltated and rolled grain populations, respectively). From these two data it can be calculated the velocity, and averaging the values of the individual bed, average water-movement velocity was calculated which is characteristic for to the whole sequence.

The quantitative and qualitative data of the facies of Upper Oligocene and Lower Miocene formations are shown in *Fig. 2.* This map shows clearly the evolutionary

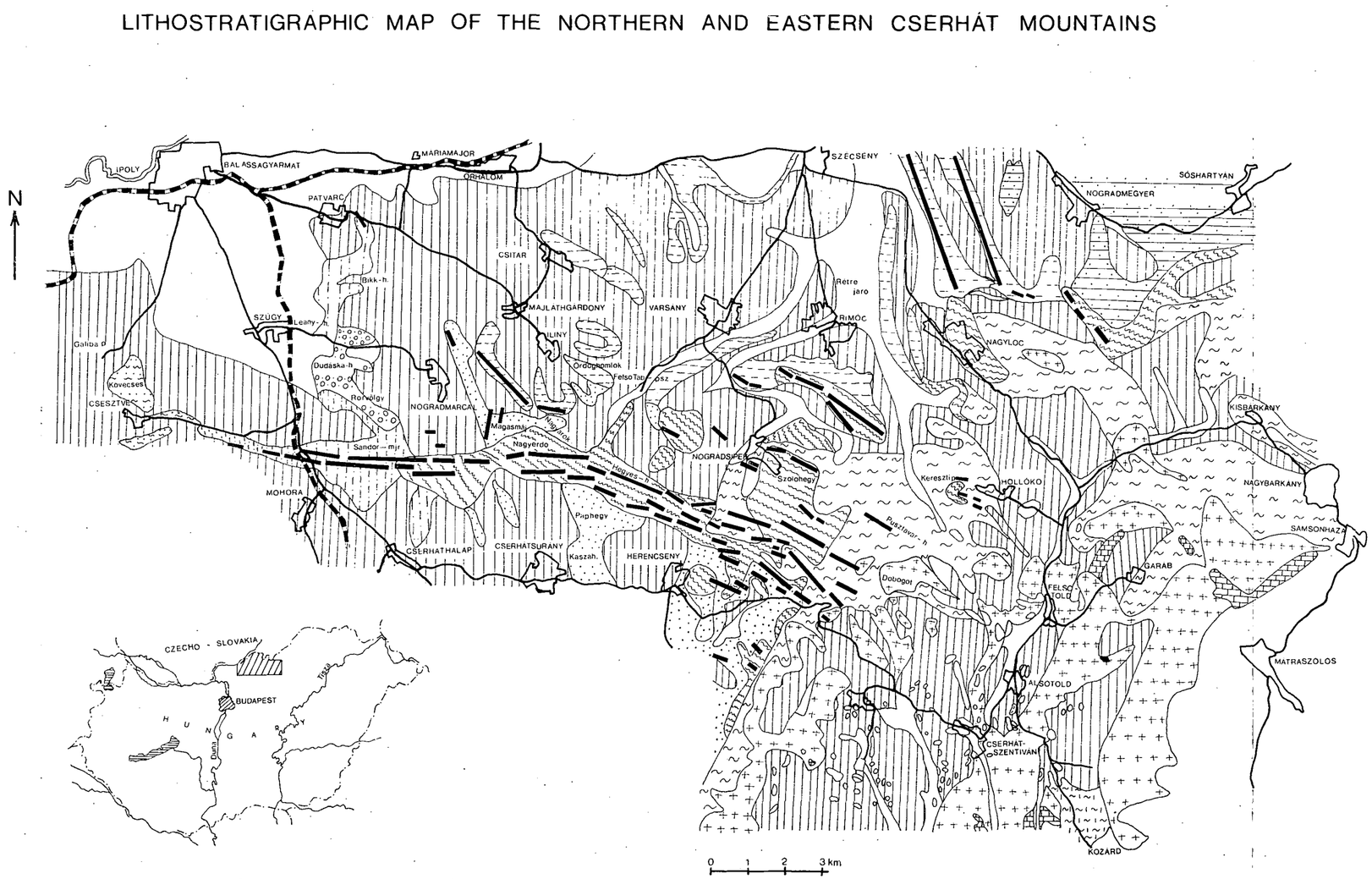

Fig. 1. Lithostratigraphic map of the northern and eastern Cserhát Mountains

Lithostratigraphic map of the northern and eastern Cserhát Mountains

L E G E N D

Holocene	flood-plain sediments, stream deposits etc.
Pleistocene	loess, talus
Pliocene	loose sandstone, clay
"Meotian"	terrestrial sediments
Sarmatian	coarse limestone, marl, clay, loose sandstone
Badenian	Lithakalk, marl, sandstone
	andesite dikes
	bedded volcanites
Carpathian	"Schlier" of eastern Cserhát
Ottnangian	Terrestrial variegated clay - loose sandstone of Nagylóc
	cross-bedded loose sandstone - variegated clay - coal of Herencsény
Eggenburgian	glauconitic sandstone of northeastern Cserhát
	sandstone with clay intercalations of Csesztve
	loose sandstone of Iliny
	loose sandstone - silt of Csitár
	Anomia-bearing sandstone of Szügy
	Szécsény "Schlier"
Egerian	Mohora silt and sandstone with plant remains
	concretionary sandstone of Borsosberény

TABLE 1

Main characters of surfacial sedimentary sequences of the northern and northeastern Cserhát Mts.

Sequence	General petrological characters	Age	Facies
Concretionary sandstone of Borsosberény	Coarse- and medium-grained, loose sandstone with fine pebbles; with concretions and coquina beds	Upper Oligocene (Egerian)	Marginal deltaic, littoral
Mohara silt with plant remains	Siltstone with plant remains (underlying the Anomia-bearing sandstone of Szügy)	Egerian	Prodeltaic, deltaic lagoon
Szécsény „Schlier"	Calcareous silt; clayey silt, arenaceous silt	Egerian to Eggenburgian	Deep sublittoral to shallow sublittoral
Anomia-bearing sandstone of Szügy	Medium- to coarse-grained sandstone; fine-grained arenaceous silt; pebbly sandstone with traces of cross-bedding	Eggenburgian	Shallow sublittoral to littoral
Loose sandstone — silt of Csitár	Pebbly, coarse- to medium-grained sandstone with Ostrea banks and silty and pebbly intercalations (Overlying the Szécsény „Schlier")	Eggenburgian	Littoral to shallow sublittoral
Loose sandstone of Iliny	Alternation of loose, fine-grained sandstone and silt (Overlying the Szécsény „Schlier")	Eggenburgian	Shallow sublittoral to middle sublittoral
Sandstone with clay intercalations of Csesztve	Fine-to coarse-grained sandstone with clay intercalations and with cross-bedding in some places	Eggenburgian	Shallow sublittoral
Glauconitic sandstone of northeastern Cserhát	Loose sandstone with variable, fine to coarse grain-size	Eggenburgian	Shallow sublittoral,
Cross-bedded loose sandstone — variegated clay of Herencsény	Coarse-grained, cross-bedded and gray, fine-grained, loose or cemented sandstone; silty sandstone	Eggenburgian — Ottnangian	Deltaic-littoral and continental
Garáb „Schlier"	Clayey to fine-grained sandy calcareous silt	Carpathian (Middle Miocene)	Middle- and deep-sublittoral

tendencies and spatial connections of the facies observed on the surface. Within the Upper Oligocene the water-movement intensity decreased from west to east — northeast direction. A similar direction can be observed regarding of the sedimentary environments from deltaic-littoral to deep sublitoral. The Lower Miocene sequences how a similar tendency, too. These formations, however, deposited far easterly, and their accumulation terrain changed from west to east form deltaic-littoral only to iddle sublittoral depth, and the glauconitic sandstone in the eastern Cserhát Mts. suggests the renewed shallowing of the sedimentary basin.

Fig. 2 shows the schematized cross-sections of the studied sequences. These made possible to study the features of the Upper Oligocene — Lower Miocene regression

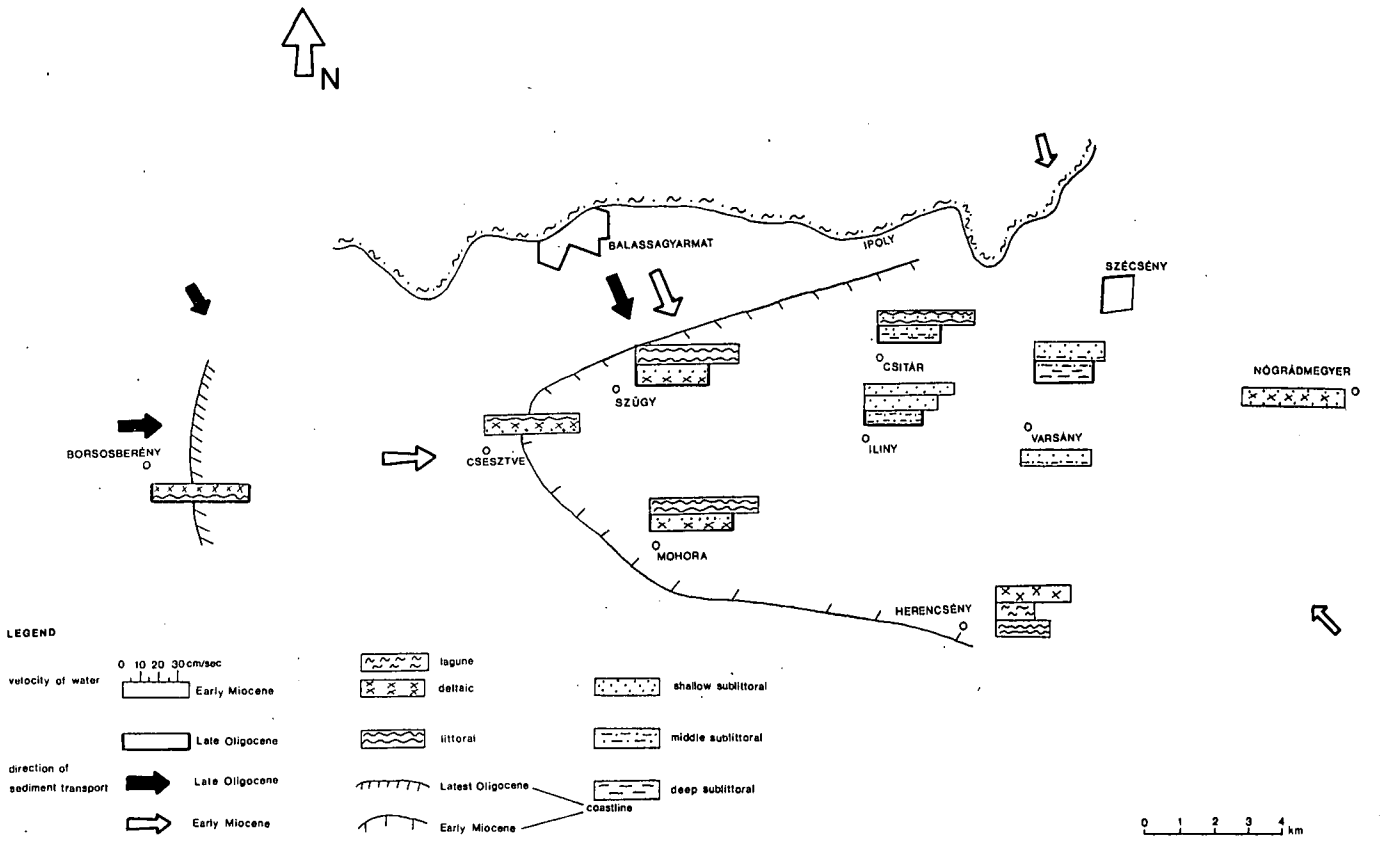

Fig. 2. Relation of the Upper Oligocene and Lower Miocene lithofacies types in the northern Cserhát Mts.

nd the paleogeographic consequences of the event as well. The shoreline of the Uppermost Oligocene sedimentary basin, with the recorded deltaic-littoral formations, ran in the western part of the mountains, near Borsosberény, along the present margin of the Börzsöny and Cserhát Mountains. Thus the fluvial material, which is characterized by the deltaic formations, may have transported from north-west — west direction. The deltaic zone can be traced to the Szügy — Mohora line, with a shallow sea easterly, and with deep subblittoral sea from Szécsény, respectively. During the Early Miocene, the sea-shore shifted to the Szügy — Csesztve — Mohora line, which corresponds with the above-mentioned basin-ward boundary of the deltaic zone of Uppermost Oligocene. The depth of the inner parts of the basin decreased simultaneously. On the basis of the upper Lower Miocene deltaic-terrestrial formations around Herencsény, occurring in the south-eastern part of the area, a south-eastern transportation and shoreline advancement can also be suggested. A large quantity of material transport and gradual infilling from this latter direction is a possible explanation of the Egerian-Eggenburgian shoreline shift from west to east direction, then causing simultaneous south to north land-formation — advanced by elevation too —, concluded from the deltaic zones *(Fig. 2)*.

EVALUATION OF THE MICROMINERALOGICAL STUDIES IN THE LIGHT OF THE SEDIMENT-ACCUMULATION ENVIRONMENT

The quality and the size-distribution of the detrital grains of the sediments are controlled mainly by the erosion terrain, the transportation-accumulation circumstances and the diagenesis. The different sedimentary environments may result spatially and temporally rather varied mineral composition of detrital material, transported simultaneously from the source area. Consequently simple evaluation of micromineralogical data may lead to an erroneous conclusions regarding the source area and the direction of transportation. In the interpretation the role of the relation between the energy of the transportation-deposition medium, the average grain-size of the sediment, as well as the density and size of the minerals enriched together [MOLNÁR, 1969] is significant. To solve this problem, the regional evaluation of the heavy minerals was carried out according to deposition environments of similar hydrodinamics. (The presentation of the basic data of the ca. 70 micromineralogical samples seems unnecessary, only the applied evaluation methods and the results are outlined here.) The following considerations were the basis for the evaluation.

It was possible to count of the average grain-sizes of rolling clastics moving together with heavy minerals by determination of densities, grain-sizes of heavy minerals and using the equation referring to rolling transportation: $\frac{r_1}{r_2} = \frac{d_2 - 1}{d_1 - 1}$. The rolling clastics are mostly quartz feldspar and rock-fagments. Those layers deposited from these transported grain-size domain can easily be determined from the log-probability grain distribution diagrams.

The calculations have been done for heavy minerals having 0,15 mm average grain-size, and following densities.

Group 1: chlorite (2.8 g/cm^3)
Group 2: tourmaline (3.2 g/cm^3)
epidote-zoisite (3,3g/cm^3)
titanite (3.5 g/cm^3)
apatite (3.1 g/cm^3)

andalusite (3.1 g/cm³)
disthene (3.6 g/cm³)
staurolite (3.7 g/cm³)
amphiboles (3.3 g/cm³)
pyroxenes (3.3 g/cm³)

Group 3: magnetite-ilmenite (5.2 g/cm³)
zircon (4.7 g/cm³)
rutile (4.1 g/cm³)
garnet (4.0 g/cm³)

The above mentioned heavy minerals can be compared with the following grain-sizes (in order of increasing specific gravity): smaller than 0.20 mm; 0.20 to 0.27 mm; above 0.27 mm average size transported by rolling. The average frequencies of heavy minerals having different density were calculated in the different grain-size of the clastic sediments group (Table 2). The heavy minerals of smallest density enrich in rocks containing small to medium, those of medium specific gravity enrich in rocks of medium to big, and the heaviest minerals enrich in rocks containing biggest rolling-transported grains, respectively.

On the basis of this method, the heavy mineral frequencies were compared regionally, within groups having been distincted by the size of the rolling-transported grain populations *(Figs 3* and *4)*. This procedure enables to eliminate the factors originated from the different transportation-sedimentation circumstances which distort the mineral frequency percentages, and gives a good result which characteristic for the original source area. Taking these considerations into account, studies were made — from surficial formations — on the regional distribution of some heavy minerals. These were selected from those of evaluable frequency and of reference to the erosional area. Evaluating the distribution, of the mainly metamorphic garnet and chlorite data on the transport directions and the build-up of the erosional area were expected *(Fig. 3)*. The comparison of these data to those in Table 2 shows that the changes of frequencies of garnet and chlorite are controlled mainly by the hydrodynamic properties of the sedimentary basin but according to the above-mentioned considerations, the effect of this factor can be eliminated. Namely, these two minerals area represented with nearly identical percentages within the hydrodynamically uniform Upper Oligocene — Lower Miocene, as well as Middle Miocene sediments of the studied region. This suggests a source area of rather uniformly-distributed epi- and mesometamorphic rocks. The percentage distribution is slightly shifted toward the garnet in the Upper Oligocene beds of the central North-Cserhát area (*i.e.* around Szügy, Mohora, Iliny), and in the Middle Miocene beds of the south-eastern parts. This corresponds with the position of the sedimentary facies and the shoreline, and the erosional-transportational directions determined from the grain-distribution studies (see *Fig. 2*). The smaller fluctuations in the ratio of these two minerals can be interpreted by the different energy and composition of the western and south-western material supply, and by the somewhat diferent structure of the drainage areas. The somewhat irregular garnet/chlorite ratio of the Ottnangian beds in the south-eastern part of the area may be connected with the Late Miocene changes of the terrain and the supposed south-eastern transportation (see *Fig. 2*).

The presence of andalusite, disthene, staurolite, pyroxene, and tourmaline in the heavy mineral fractions suggests smaller magmatic and metamorphic masses beside the main garnet and chlorite containing source area. The former metamorphic minerals originated from metamorphic rocks having diferent facies. The above-

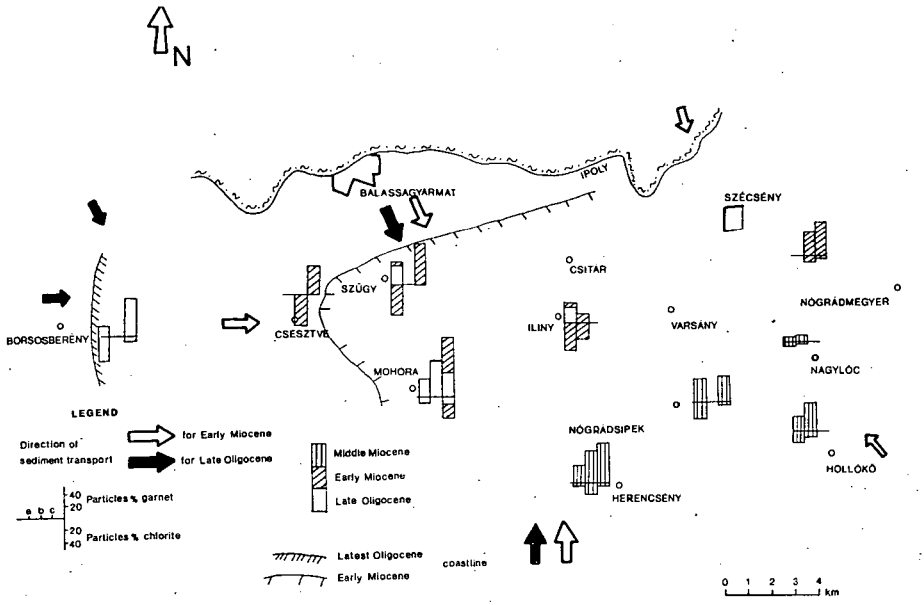

Fig. 3. Spatial distribution of garnet and chlorite in the Upper Oligocene, Lower and Middle Miocene surfacial rocks of the northern Cserhát Mts. *a*: <0.20 mm; *b*: 0.20 to 0.27 mm; *c*: >0.27 mm dominant sizes for grains shifted on the bottom. Direction of sediment origin supposed by micromineralogical studies: → for Late Oligocene; ⇒ for Early and Middle Miocene.

TABLE 2

Average frequency of heavy minerals in the 0.1 to 0.2 mm grain-size portion, calculated for the size-selected, rolled-saltated grain population (//// = greatest average frequency)

	Mineral	Average size of particles rolled-saltated on the bottom		
		<0.20 mm	0.20—0.27 mm	>0.27 mm
		Frequency of minerals in particles %		
	Chlorite	/23.0///	//24.0////	7.5
Specific gravity ↓	Apatite	0.2	///1.0///	0.4
	Andalusite	0.1	—	///0.9///
	Actinolite	0.1	—	///0.3///
	Tourmaline	2.2	4.5	///6.0///
	Epidote-zoisite	1.1	///2.0///	1.4
	Biotite	1.7	///3.3////	0.3
	Oxi-and green amphibole + glaucophane	0.6	///1.6////	1.1
	Pyroxenes	1.0	2.7////	0.4
	Titanite	0.4	///1.0////	0.1
	Disthene	0.2	0.7	///0.8///
	Staurolite	0.1	0.6	///1.0///
	Garnet	15.0	36.0	//54.0///
	Rutile-anatase	1.0	///1.5////	0.9
	Zircon	0.2	///0.3////	0.2
	Magnetite-ilmenite	3.4	6.8	///8.5///
	Dia-and epigenetic ingredients	50.3	22.7	15.9

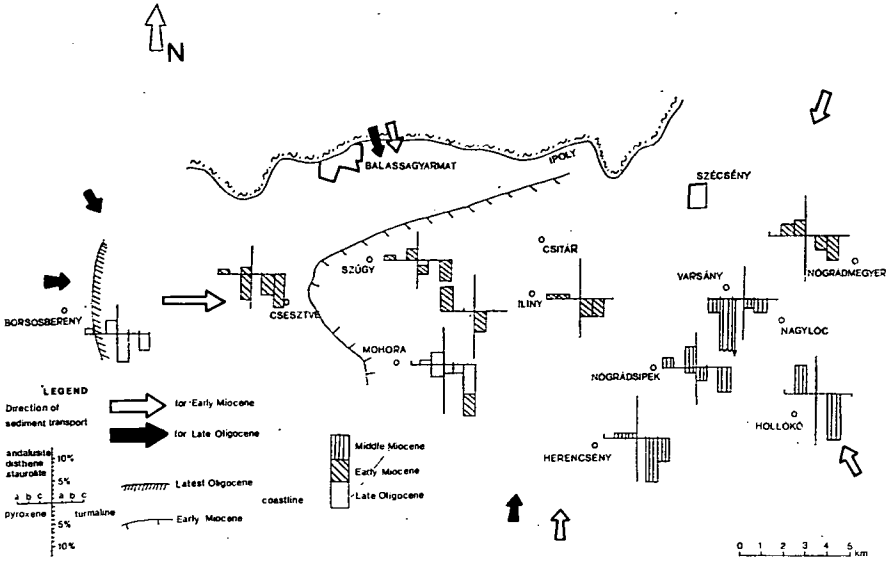

Fig. 4. Spatial distribution of andalusite, disthene, staurolite; and pyroxene and tourmaline in the Upper Oligocene, Lower and Middle Miocene surfacial rocks of the northern Cserhát Mts. *a*: <0.20 mm; *b*: 0.20 to 0.27 mm; *c*: >0.27 mm dominant sizes for grains shitfed ont the bottom. Direction of sediment origin supposed by micromineralogical studies: → Late Oligocene; ⇒ Early and Middle Miocene.

mentioned minerals were studied in areal distribution, too *(Fig. 4)*. The comparison of the corresponding rock-types shows that the temporal and areal distribution of andalusite, disthene and staurolite (mineral association suggesting strong metamorphism have not any significant orientation. On the other hand, the pyroxene appears as an anomaly, occurring merely in some places, with medium to high amount. The significant amount of pyroxene together with the associated hyaline content of the "light-fraction" in the continental sequence around Nagylóc can be attributed to the local effect of the Middle Miocene volcanism. However, in the interpretation of the recorded smaller enrichment westerly (at Mohora and Cseztve), one should bear in mind temporal transport from the basic magmatites in the basement of the southern area. This latter interpretation is made probable by the fact, that the scarce Upper Oligocene — Lower Miocene volcanic detritus is dominantly of rhyolitic and rhyodacitic in composition.

The tourmaline is relatively common in the studied formations. The study on the areal distribution suggested some enrichment in the Middle Miocen sandy beds (i.e. in the south-eastern terrain), in contrast to the rather uniform tourmaline-content of the Upper Oligocene — Lower Miocene beds. On the basis of the appearance of the tourmaline as tiny euhedral brown or greenish-brown, sometimes fragmented violet-blue grains, the origin from granitic or related rock-types is probable. According to the areal distribution, this supports the assumption of a northward transport of erosional material from the basement of the Great Hungarian Plain having been on the surface in Late Oligocene — Middle Miocene times (see *Fig. 2*).

All possibilities of mistakes cannot be cleared even with the above-outlined procedure. In the method the rolled and the saltoted grains are counted together, and there is no information either on the long transportation phase, or on the possible repeated redeposition of the mineral. Other distorting factor may be those quantitative changes of the diagnetic and altered minerals, which are independent of the hydrodynamic circumstances. However, one must take into account these factors in the appraisal of the reliability of the conclusions.

The sedimentary formations of the Cserhát Mts. contain fine-grained (*i.e.* suspended) fraction in different quantity [ANDÓ, 1973; 1975]. Important in this fraction the role of the *clay minerals*. On the basis of the derivatographically studied fine-grained fraction, the following main type of clay minerals were distinguished; illite, montmorillonite, kaolinite, a mineral with mixed illite-montmorillonite structure, montmorillonite plus kaolinite; illite plus kaolinite, illite-montmorillonite plus kaolinite.

The clay minerals of the clasts are mainly detrital in origin [NEMECZ, 1973]. Thus the clay-mineral composition is firstly determined by the weathering in the erosional region, and by the differential deposition. According to observations, this latter is markedly influenced by the chemical properties of the depositional medium. In spite of this fact, a kaolinite — illite — montmorillonite depositional rate succession is established, and this corresponds to a similar clay-mineral succession from the river delta toward the basin. This suggests a facies-index value for the clay-mineral composition. Following these considerations, a study has been carried out on the clay minerals of the sedimentary terrains distinguished by the energy of the depositional media (see *Fig. 2)*. In the evaluation it was considered, that there are possibilites for slight syngenetic changes of the minerals and structural fragments, as well as hydrolysis or clay-mineralization of the magmatic material entering the basin. The relation of the characteristic mineral association and the accumulation terrain is tabulated — on the basis of studies on 60 samples — in Table 3. (N.B. Because of the small amount, the detailed derivatographic determination of the chlorite encountered difficulties, thus its respective analyses are given in the microminer-alogical studies.)

The data of Table 3 (first row) show, that the detrital formations of the studied region are dominated by the minerals with mixed illite-montmorillonite structure, and by associations prevailed by illite. The facies distribution of the certain frequency of the minerals shows, that the proportion of the *illite* decreases in the marine sequence of the delta. On the other hand, this mineral cannot be traced in littoral — shallow subareas without direct connection with river inflows. Illite predominates again in the continental formations. In accordance with the data of the literature on the differential deposition, *montmorillonite* shows an opposed distribution in the formations. However, montmorillonite has a relative frequency in the near-shore accumulation terrain connected to the river delta. Kaolinite, without association to other clay minerals, appeared only in the continental formations.

Most general in occurrence, *i.e.* most independent of the characters of the accumulation terrain is the mineral with mixed *montmorillonite-illite* structure. The *montmorillonite-kaolinite* mineral association appeared in the low-energy marine, and in the continental sediments. The *illite-kaolinite* mineral association characterizes mainly the sublittoral areas.

Examination of the proportions of mineral associations within single facies contributes the detailed evaluation of the outlined relationships. According to data in Table 3, the deltaic formations are characterized mainly by illite and partly by

TABLE 3

Interrelation of the clay-mineral composition and the site of deposition of the surfacial detrital rocks of the northern and eastern Cserhát Mts.

	Illite	Montmorillonite	Kaolinite	Illite montmorillonite	Montmorillonite-Kaolinite	Illite + Kaolinite	Illite montmorillonite
1. total frequency found in all sedimentary rocks	25	10	3	32	6	22	2
Deltaic	6.6 57	1.6 15	—	3.4 28	—	—	—
Lagoon, Prodeltaic	3.4 26	1.7 12	—	3.4 26	1.5 12	1.6 12	2 12
Deltaic-sublittoral	3.4 40	1.6 20	—	3.4 40	—	—	—
Littoral	—	—	—	5 50	—	5 50	—
Shallow sublittoral	—	—	—	5 43	—	6,7 57	—
Middle subblittoral	1.6 17	3.4 33	—	1.6 17	—	3.4 33	—
Deep sublittoral	—	—	—	3.5 77	1.5 33	—	—
Terrestrial „variegated" rocks	8.4 33	1.7 6	3 13	6.7 26	1.5 6	3.5 26	—
Fluviatile or eolian deposits	1.6 33	—	—	—	1.5 33	1.6 34	—

Remarks: Numbers in the upper right corners show the facies distribution of the mineral frequencies found in the studied sedimentary rocks (vertical columns), those in the lower left corner show the percentage mineral frequencies within the facies (horizontal lines).

illite-montmorillonite. It is striking, that while the kaolinitic mineral associations are lacking in the deltaic sediments, the montmorillonite of low deposition rate is represented here. This suggests, that the deposition in the deltaic circumstances differ from that under undisturbed, experimental conditions. The rapid sedimentation, the pH and concentration changes, the redeposition, mixture may result in getting of the coagulable montmorillonite also into the sediment. Other possible factor to be considered is the usual hydratational weathering, i.e. the post-depositional clay-mineralization of the poorly-sorted detritus.

The most heterogenous mineral composition characterizes the sediments of the delta-marginal bay, and the continental formations. In the former terrain only the independent appearance of kaolinite is missing. The appearance of this mineral supposes intensive leaching. The diverse mineral composition can be interpreted by the possible enclosure, and thus slighter sorting effect of the delta-marginal bay, and by redepositional-mixtural possibilities and local variations in the depositional conditions on the land, respectively. The illite-montmorillonite, illite and kaolinite content of the littoral — shallow sublittoral zones, as well as the montmorillonite

mineral content of the deep sublittoral zone supports the role of the differential deposition. The middle sublittoral zone is characterized by more varied mineral ssociations and locally formed volcanogenic clay deposits (Szécsény Schlier, Varsány). The fluvial and eolian sediments are distinguished, as a result of the more intensive leaching, by illitic-montmorillonitic mineral associations.

SUMMARY

The lithostratigraphic mapping of the mainly Tertiary, detrital surficial sedimentary formations of the northern and eastern Cserhát Mts. served as basis for the reconstruction of the sediment accumulation environments. The basis for the facies nalyses was the grain-size distribution study by log-probability diagrams. The derived grain-size distribution curves show clearly the distinct fractions of the differently transported (rolled, saltated or suspended) grains. The diagram indicate the size ranges of the grain populations. The literature on sediment transport gives equations for the relationship of grain-size and water movement, velocity and the depositional boundary-velocity can be calculated from the size of the differently transported grain populations. These values give one of the most important quantitative characteristic of the former environment. Analyzing the data regionally, the changes in the accumulation terrain can be traced.

The method enabled also a more reasonable evaluation of the heavy mineral studies. From the specific gravity — grain-size equation for rolled sediment transport made possible to count the size of the light minerals transported and deposited together with the heavy mineral associations of 0.1 to 0.2 mm size and different density. On the basis of the fact, that the light fraction constitutes the main quantity of the rock, this calculation gives what size of rolled grain population serves as basis for the comparison of heavy mineral frequency of the given rock. Those beds, which were deposited from these rolled grains of calculated size range can be easily assigned from the log-probability grain distribution diagrams. The heavy mineral data, which were evaluated regionally by this method, are in good agreement with the results having been derived from facies and environmental reconstruction on the basis of grain-size distributions.

REFERENCES

ANDÓ, J. [1973]: A szállítási-leülepedési térszín vizsgálata a log-normál szemcsepopulációk elemzése alapján. Földtani Közlöny, **103** Budapest

ANDÓ, J. [1975]: Method for a common evaluation of petrographical and paleontological investigation of detrital sedimentary formations. Annales Univ. Sci. Budapestiensis de R. Eötvös, Sectio Geologica **19.**

BÁLDI, T. [1973]: Mollusc Fauna of the Hungarian Upper Oligocene (Egerian). Akadémiai Kiadó, Budapest

BÁLDI, T., HORVÁTH, M. [1970]: Jelentés az 1970. évi Cserháti rétegtani vizsgálatokról. Manuscript. Eötvös Loránd Tudományegyetem, Kőzettan-Geokémiai Tanszék. Budapest, 1970.

MOLNÁR, B. [1969]: A szemcsenagyság- és nehézásványösszetétel összefüggései. Földtani Kutatás **12**, 2, Budapest.

NEMECZ, E. [1973]: Agyagásványok. Akadémiai Kiadó, Budapest

VISCHER, G. S. [1969]: Grain size distributions and depositional procces. Journal of Sed. Petrol., **39.**

Manuscript received, June 9, 1980

J. ANDÓ
Department of Petrology and Geochemistry
Eötvös Loránd University
Budapest, VIII., Múzeum krt. 4/A.

Acta Mineralogica-Petrographica, Szeged, XXV/1, 109—116 1981

EFFECT OF OXYGENATED PORE-WATER ON ANKUR IRON ORE, NE SUDAN

A. M. EL-KAMMAR and H. M. OSMAN

ABSTRACT

The present work deals with the mineral alterations that have taken place in Ankur iron ore and its associated country rocks, by means of oxygenated pore-water. The investigations were carried out by the electron-scanning microscope. The alteration products involve; goethite, hematite, hydromuscovite, chlorite, kaolinite, dolomite, gypsum and amorphous silica. Some of the alteration products exist in small concentrations that can not be detected by the X-ray diffraction or the chemical analyses of the bulk samples.

The alteration mechanisms are believed to be direct response to the stability framework of the primary mineralogical composition and the nature of the pore-water as well.

INTRODUCTION

The Ankur area is located between latitudes 21°15′ and 21°55′ N, and longitudes 36°00′ and 36°25′ E, within the Sofaya (Salala) village, in the northeast of Sudan. The area lies about 320 km northwest of Port Sudan and about 90 km west of Abu Imama harbour, on the Red Sea coast *(Fig. 1)*.

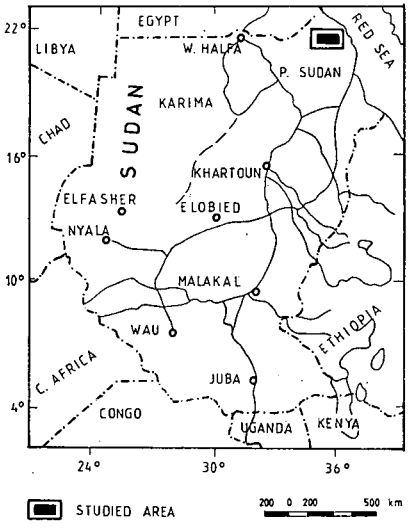

Fig. 1. Location map

The iron ore of Ankur area is characterised by being massive, compact, finely crystalline with steel metallic luster and is intruded into basic schistose rocks. The studied iron ore rank is estimated to be about four million tons of 50—60% Fe.

Two categories of the iron ore can easily be distinguished, namely; massive and disseminated ores. The calculated normative composition is determined to cover a wide variety of minerals, including; quartz, orthoclase, albite, anorthite, corundum, acmite, wollastonite, enstatite, ferrosilite, magnetite, hematite, ilmenite, apatite and pyrite. The V module of the studied magnetites reflects a metamorphic origin of the deposits. V^{3+} occurs in the magnetite lattices substituting for Fe^{3+}, while Cr, Cu, Co, Ni, Zn and Rb are most probably accommodated in the structures of the different aluminosilicates [OSMAN, 1980).

EXPERIMENTAL

Representative samples of the different grades of the ore, as well as the country rocks were examined by the electron-scanning microscope (ESM). The used instrument is of the JSM—35, JEOL type, and it is accommodated with a computerised X-ray fluorescence unit to facilitate a rapid and precise chemical analysis of the examined field.

The samples were prepared for the ESM examination by mounting a fresh piece of rock sample on an aluminium holder. The exposed surface was coated by a thin filament of gold and palladium.

DISCUSSION

The present article is concerned with the mineralogical modifications that have taken place in the studied ores and their country rocks, via interaction with oxygenated pore-waters. The studied area, being tropical, is affected by periodical and aperiodical rainfall, and waters of other sources, which may percolate through dissection and fracture planes in the deposits. Such water may cause slight or extensive break down of minerals, depending upon their stability framework as well as the nature of the

Fig. 2. SEM photomicrograph showing iron-rich flakes on surface of oxidized pyrite

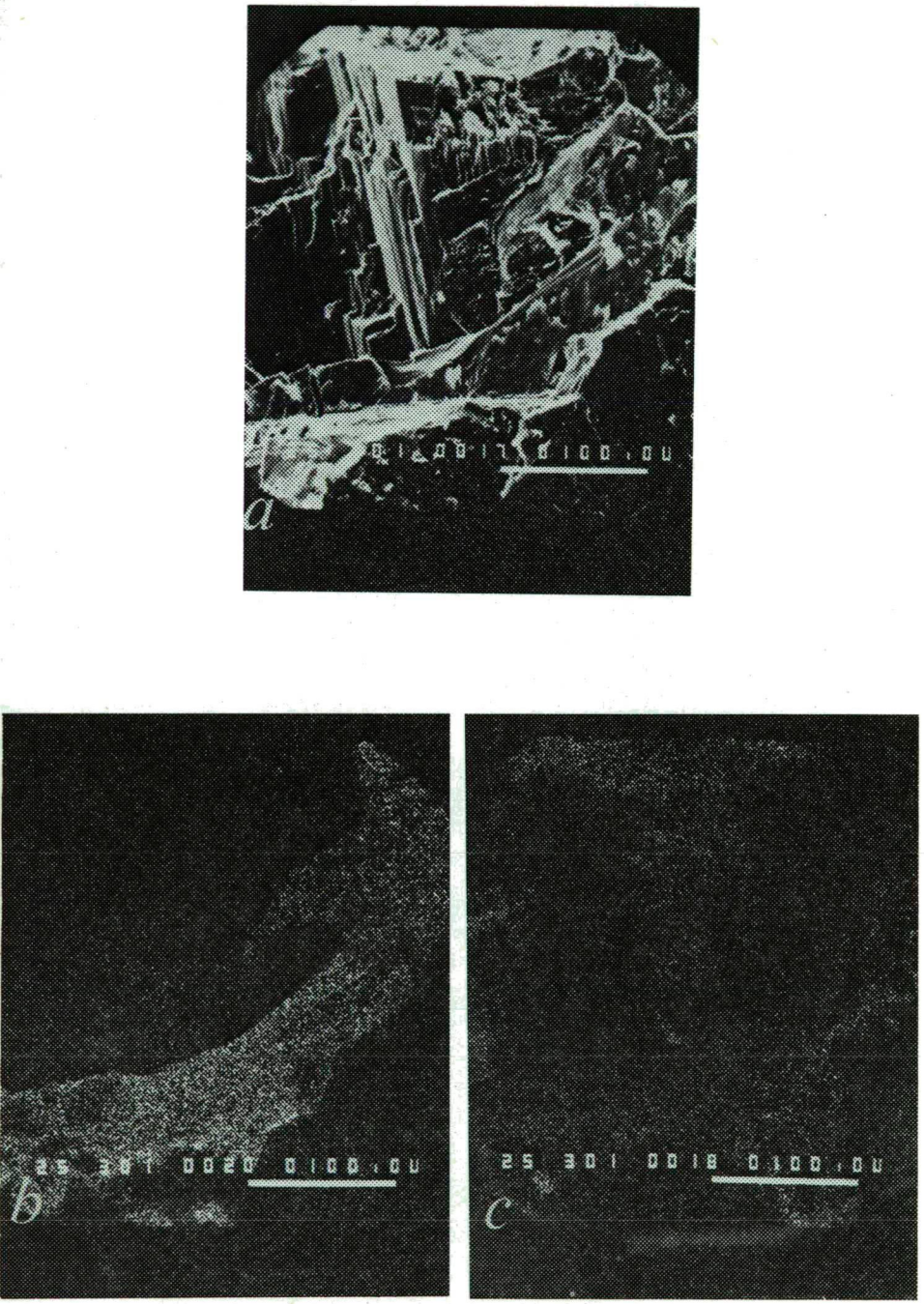

Fig. 3. a) SEM photomicrograph showing aggregates of biotite surrounded by pyrite; notice the development of the iron rich flakes on the oxidized pyrite; b) and c) distribution patterns of Fe and Si, respectively

acting pore-water. The process leads, decisively to certain dispersion of elements which may facilitate possibilities of geochemical prospection.

The electron-scanning microscope (ESM) investigations proved that new minerals have been formed on the expense of others, by the action of the oxygenated pore-water. Some of the alteration products (e.g., dolomite and goethite) do exist in minor amounts that can not be detected by the petrographic microscope, X-ray diffraction or chemical analysis.

Pyrite seems to be the most affected by the oxygenated pore-water. The beginning of its break down appears as etching and pitting on the crystal faces. Predominant flakes, remarkably rich in iron and poor in sulfur, oftenly grow on the surfaces of the oxidized pyrite *(Figs 2* and *3)*. The oxidized chalcopyrite possesses thin coats of almost pure iron *(Fig. 4)*. This is principally because sulfur is readily mobile compar-

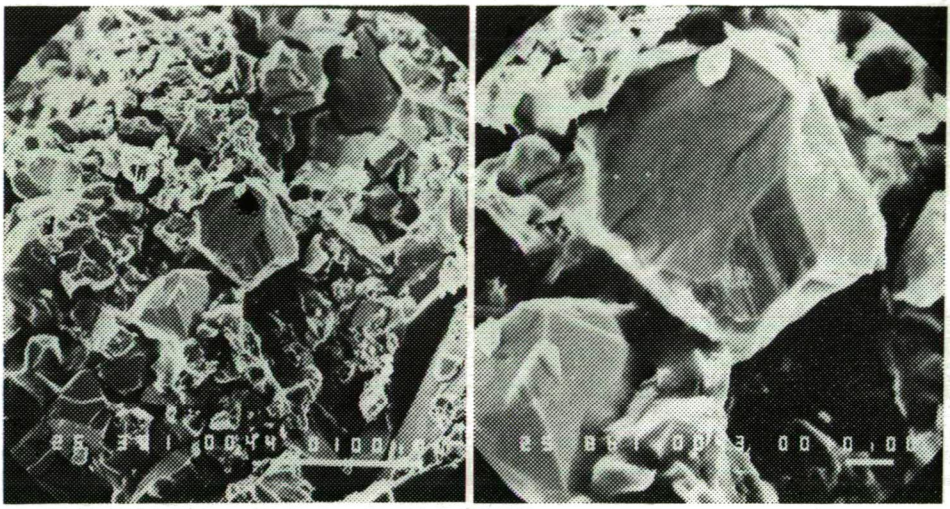

Fig. 4. SEM photomicrographs showing aggregates of chalcopyrite affected by diagenetic solutions; the same field by different magnification

ed to iron. The resultant sulfates may, therefore, move longer to form diagenetic sulfate minerals (e.g., gypsum). The field observations and the petrographic examinations indicated the presence of secondary gypsum as fracture and cavity filling [OSMAN, 1980].

The break down of pyrite by the oxygenated pore-water, has been formalized by KRAUSKOPF [1967], as follows:

$$2FeS_2 + 15/2\ O_2 + 4H_2O \rightarrow Fe_2O_3 + 4SO_4^{2-} + 8H^+$$

$$SO_4^{2-} + 2H_2O + CaCO_3 \rightarrow CaSO_4 \cdot 2H_2O + CO_3^{2-}$$

The reaction between the oxygenated pore-water and magnetite is rather significant. It is partly or entirely oxidized into hematite and/or goethite, which are commonly reprecipitated in situ. The produced hematite is poorly crystalline and keeps, sometimes, a colloidal aspect *(Fig. 5)*. Goethite exhibits a colloform texture, and it fills many pore-spaces and factures *(Fig. 6)*. Sometimes, goethite is reprecipitated on the surfaces of the oxidized magnetite crystals *(Fig. 7)*.

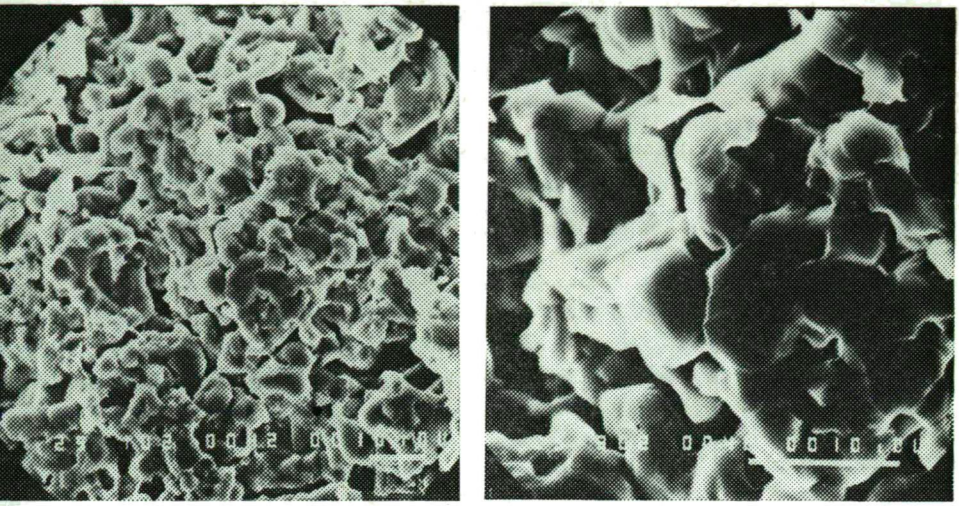

Fig. 5. SEM photomicrographs showing the precipitation of diagenetic hematite. Two different magnifications

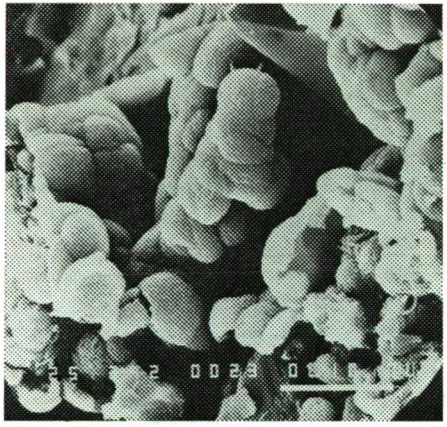

Fig. 6. SEM photomicrographs showing the precipitation of colloidal goethite on euhedral quartz crystals

Limited break down of amphiboles, micas and felspars has frequently been encountered in the studies ores and their country rocks. The alteration products are commonly hydromuscovites, chlorite, kaolinite, amorphous silica and poorly crystalline alumino-silicates. The later is a rare constituent and it occurs as pore-filling *(Fig. 8)*.

The break down of biotite starts oftenly along the flakes with partial removal of iron *(Fig. 9)*. Kaolinite and chlorite are main alteration products of the primary alumino-silicates. The alteration mechanisms have been formalized by SOMMER [1978] and NAGTEGAAL [1980], as follows;

$$2KAlSi_3O_8 + 2H^+ + 9H_2O \rightarrow Al_2Si_2O_5(OH)_4 + 2K^+ + 4H_4SiO_4$$

K-Feldspar Kaolinite

$$2K(Mg, Fe)_3AlSi_3O_{10}(OH)_2 + H_2O + 14H^+ \rightarrow \underset{\text{Kaolinite}}{Al_2Si_2O_5(OH)_4} + 4H_4SiO_4 + 2K^+ + 6(Mg^{2+}, Fe^{2+})$$
Biotite

The formation of kaolinite requires an almost fresh water containing very low K^+/H^+ ratio [READING, 1978]. The released K^+, Mg^{2+} and Fe^{2+}, from the breakdown of biotite and feldspar, can be used for the formation of other diagenetic minerals such as chlorite and dolomite [EL-KAMMAR *et al.*, 1980].

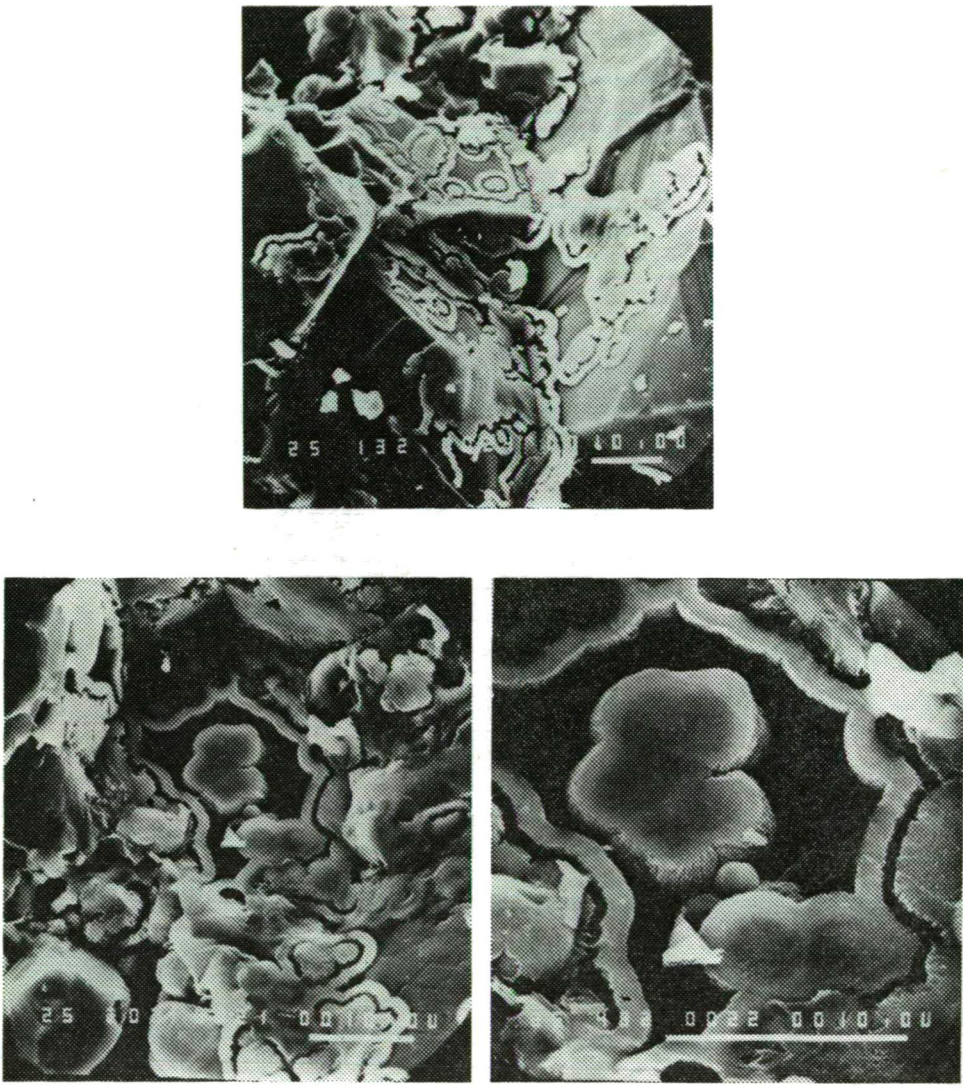

Fig. 7. SEM photomicrographs with different magnifications showing the precipitation of colloidal goethite on the surface of magnetite crystal. The goethite displays clear colloform texture. The crumbled surfaces of the colloidal goethite is due to shrinkage during solidification

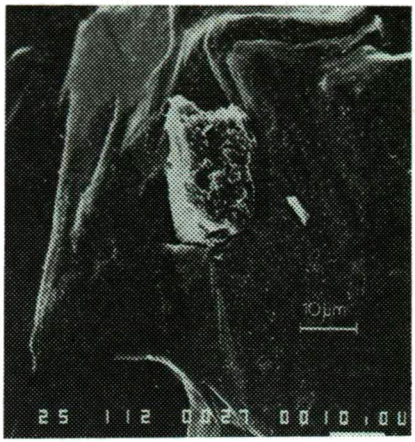

Fig. 8. SEM photomicrograph showing a cavity-filling by poorly crystalline alumino-silicates

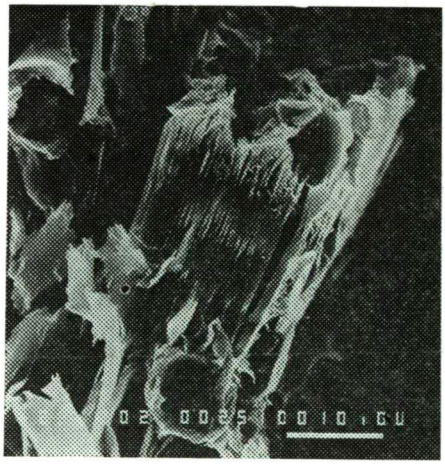

Fig. 9. SEM photomicrograph illustrating the effect of the oxygenated pore-water on biotite crystal

As a result of the late diagenetic activity, xenotipic fine grained dolomite has been observed in some pore spaces *(Fig. 10)*. The precipitation of dolomite requires, according to KINSMAN [1969] and AL-HASHIMY [1976], a slightly acidic medium.

The above study of the electron-scanning microscope proves undoubtedly that a part of the chemical constituents of the studied deposits were redistributed or dispersed due to diagenetic effect of oxygenated pore-water.

ACKNOWLEDGEMENT

The writers appreciate very much the help and the critical reading of the manuscript given by PROF. DR. M. A. EL-SHARKAWI, Geology Department, Faculty of Science, Cairo University, Egypt.

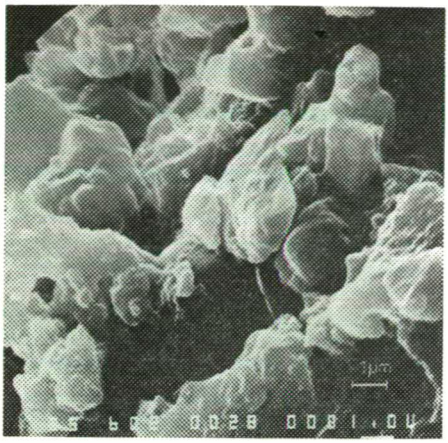

Fig. 10. SEM photomicrograph showing the precipitation of late diagnetic xenotipic dolomites in a pore-space

REFERENCES

AL-HASHIMY, W. S. [1975]: Significance of Sr distribution in some carbonate rocks in the Carboniferous of Northumberland, England. J. Sed. Petrol., **46**, 2, pp. 369—376.

EL-KAMMAR, A. M., EL-AMIN, H. and SADEL DIN, M. [1980]: Diagenetic and weathering activities in the phosphate-bearing sediments of southeast Edfu, Upper Egypt: An electron-scanning microscope study. Bull. Fac. Sc. Aswan Univ., Egypt (in press).

KINSMAN, D. J. J. [1969]: Modes of formation, sedimentary association, and diagnostic features of shallow water and supertidal evaporites. Am. Assoc. Petr. Geol. Bull. **53**, pp. 830—840.

KRAUSKOPF, K. B. [1967]: Introduction to Geochemistry. McGraw-Hill Book Company, New York, London, Sydney.

NAGTEGAAL, P. J. C. [1980]: Clastic reservoir rocks- origin, diagenesis and quality. International Meeting on Petroleum Geology 18—25 March 1980. Beijing, China.

OSMAN, H. M. [1980]: Mineralogical and Geochemical Studies on Ankur Iron Ore Deposits, Sudan. M. Sc. Thesis, Geol. Dept., Fac. Sc., Cairo Univ., Egypt.

READING, H. G. [1978]: Sedimentary Environments and Facies. Blackwell Scientific Publications, 557 p.

SOMMER, F. [1978]: Diagenesis of Jurassic sandstones in the Viking Graben. J. Geol. Soc., **135**, pp. 63—68.

Manuscript received, May 10, 1981

A. M. EL-KAMMAR
Geol. Dept., Cairo Univ.
Cairo, Egypt
M. H. OSMAN
Geol. Surv. Dept.
Khartum, Sudan

Acta Mineralogica-Petrographica, Szeged, XXV/1, 117—126, 1981

GEOCHEMISTRY OF ANKUR IRON ORE DEPOSITS, NE SUDAN

A. M. EL- KAMMAR. M. B. SHAALAN and H. M. OSMAN

ABSTRACT

The iron ore deposits of Ankur area, northeast Sudan, occupy a constant geological position slightly transverse and discordant to the general foliation of the host rocks (biotite schists and andesitic tuffs). The normative composition of the studied ore is calculated to cover the following mineral assemblage; quartz, orthoclase, albite, anorthite, corundum, acmite, wollastonite, enstatite, ferrosilite, magnetite, hematite, ilmenite, apatite and pyrite. Magnetite and hematite showed opposit distribution patterns, which may suggests that hematite is a product of martitization of magnetite.

The iron ore of the area under investigation are remarkably enriched in the trace elements; Y, Cu, Co and Cr, and depleted in the content of Ni, Zn, Rb and Sr, compared to the average of the earth's crust. The V module of magnetites reflects a metamorphic origin of the deposits. V^{3+} is believed to be accommodated in the magnetite lattice, substituting for Fe^{3+}, while Cr, Co, Ni and Zn are most probably accumulated by the alumino-silicates. Rb occurs in the potash alumino-silicates, replacing for K. The absence of the correlation between Sr and Ca may favour the believing that the studied deposits are of metamorphic origin.

INTRODUCTION

The iron ore rank of Ankur area is estimated to be about four million tons (of 50—60% Fe). The area belongs to the most important iron ore occurrence in Sudan, namely; Sofaya (Salala), northwest Port Sudan, Red Sea coast.

The rock mass of Ankur area (Precambrian) may be regarded as minor intrusives associated with abundant effusive rocks. The iron ore occupies a constant geological position slightly transverse and discordant to the general foliation of the host rocks, which are composed of biotite schists and weakly schistosed andesitic tuffs.

The petrographical and mineralogical investigations on the same ore (SHAALAN, *et. al.*, in preparation) indicated that the ore occurs mainly as magnetite lenticular masses, tabular bodies, veins, disseminated stringers and beds. Five types of country rocks were recognized, namely; metarhyolites, andesitic tuffs, biotite schists, granites and andesites.

EXPERIMENTAL

Complete chemical analyses for forty representative bulk samples of the ore were performed. The samples were collected from three bore holes (BH2 BH3 and BH4). The major oxides; SiO_2. Al_2O_3, total Fe, MgO, CaO and MnO were determind by means of the atomic absorption spectrometry. Na_2O and K_2O were analysed by flame-photometer, while TiO_2 and P_2O_5 by the photocolorimetric techniques. The ferrous iron was determined by the oxidation reduction titration against potassium dichromate. The total sulphur and the ignition loss were determined gravimetrically. The analysis

was done in duplicate, for some samples, using a standardized X-ray fluorescence technique, to ensure the accuracy of the obtained data.

The trace elements; V, Cr, Co, Ni, Cu, Zn, Rb, Sr, Y, Zr, Nb, La, Co and Nd were analysed quantitatively by the X-ray fluorescence spectrometry, using Co and Mo Kα radiation. The methods used for the analysis are given in detail by NORRISH and CHAPPELL [1966] and EASTON [1972].

DISCUSSION

The averages of the obtained results are given in Table 1. The iron ores were classified into three main categories, according to their total Fe content, namely; high grade (>50% Fe), medium (50—30% Fe) and low grade (30—20% Fe). The country rock contains less than 20% Fe.

TABLE 1

Averages of the Chemical Analysis Data of Ankur Iron Ores, NE Sudan

	High Grade N=15	Medium Grade N=13	Low Grade N=2	Country rocks			
				Meta-rhyolite N=1	Biotite Schist N=4	Andes-ite N=2	Andes-itic tuffs N=3
SiO_2	11.56	26.00	41.05	62.91	48.00	45.00	43.50
Al_2O_3	2.32	5.86	8.90	13.13	12.10	15.90	11.60
TiO_2	0.65	0.40	0.18	0.05	0.16	0.40	0.14
FeO	13.65	14.36	10.39	1.32	5.40	6.80	8.70
Fe_2O_3	64.73	41.14	22.53	7.31	7.32	13.00	16.50
Total Fe	55.85	39.91	23.82	6.29	9.32	14.40	18.30
MgO	2.47	5.87	6.09	2.00	15.50	5.80	7.50
CaO	2.74	4.36	1.98	2.75	0.80	4.90	2.20
Na_2O	0.34	0.22	2.72	5.25	2.60	4.88	4.76
K_2O	0.30	1.22	2.00	0.50	5.60	0.84	1.92
MnO	0.14	0.14	0.09	0.12	0.09	0.15	0.10
P_2P_5	0.61	0.72	0.21	0.28	0.29	0.37	0.67
S	0.16	0.52	0.83	0.07	0.60	0.34	1.01
L. O. I.	1.87	2.37	3.31	4.51	1.77	2.30	1.84
V	279	224	86	13	47	192	62
Cr	38	59	44	15	149	150	92
Co	43	47	38	32	57	111	36
Ni	15	18	19	15	28	56	18
Cu	65	92	154	323	176	194	164
Zn	12	20	19	19	77	37	65
Rb	9	21	32	24	160	26	48
Sr	10	23	40	56	72	319	76
Y	7	29	85	205	127	95	120
Zr	63	154	107	157	24	24	72
Nb	7	10	10	32	21	9	12
La	61	77	59	53	11	16	27
Ce	162	220	166	184	30	50	78
Nd	240	271	195	191	38	52	106

Trace elements in ppm, major components in weight-percent

A. Geochemistry of the Major Elements

The geochemical distribution of the major elements was determined by the calculation of the normative composition. The calculation method given by BARTH [1962] and modified by HUTCHISON and JEACOKE [1971] was followed. The averages of the obtained normative composition are given in Table 2.

TABLE 2

Averages of the Normative Composition of the Ankur Iron, Ores, NE Sudan

Minerals	High Grade N=15	Medium Grade N=13	Low Grade N=2	Country rocks			
				Meta-rhyolite N=1	Biotite Schist N=4	Andes-ite N=2	Andes-itic Tuffs N=3
Quartz	3.75	2.38	6.16	22.11	1.10	—	—
Orthoclase	2.32	7.84	13.07	3.10	21.56	5.10	11.82
Albite	3.75	11.62	26.55	49.65	20.67	42.85	41.47
Anorthite	3.37	3.88	4.86	11.35	2.29	18.34	3.13
Corundum	0.64	1.56	0.80	—	0.99	0.50	0.81
Acmite	—	—	—	—	—	—	—
Wollastonite	2.71	4.91	1.57	0.46	0.03	1.74	1.57
Enstatite	8.40	17.60	18.63	5.86	31.11	15.37	18.49
Ferrosilite	—	0.24	—	—	2.47	—	1.11
Magnetite	38.58	33.03	24.39	3.72	11.49	13.70	15.61
Hematite	33.43	14.33	1.30	2.88	0.39	0.13	1.56
Ilmenite	0.90	0.68	0.27	0.08	0.21	0.60	0.21
Apatite	1.67	1.57	0.48	0.61	0.57	0.80	1.47
Pyrite	5.50	1.71	2.43	0.20	1.58	0.92	2.83

The normative calculations showed that iron is distributed among wide variety of minerals. The Fe^{2+} is accommodated within pyrite, ilmenite and ferrosilite as accessory or minor constituents. The main bulk of Fe^{2+} occurs in the magnetite form, with an equivalent quotient of the Fe^{3+} oxidation state. The rest of the Fe^{3+} is mainly present as hematite.

The main alumino-silicates are orthoclase, albite and anorthite. The excess of alumina is calculated as corundum. The extra Ca ofter the calculation of the anorthite was calculated in the form of enstatite.

In general, it can be stated that magnetite and enstatite are main theoretical minerals of the Ankur iron ores and their country rocks. Hematite is a main constituent of the high and medium grades, and it diminishes towards the low grade and the country rocks. The iron ores of the Ankur area are commonly diluted by the alumino-silicates (e.g., feldspars), in addition to enstatite. The three minerals; apatite, pyrite and ilmenite are of minor abundance in all ore deposits.

The contents of magnetite and hematite of the high and medium grades have strong antipathetic distribution patterns. This may support the believing that hematite is a product of martitization of magnetite. Consequently, hematite is formed on the expenses of magnetite.

The distribution patterns of the minerals is very irregular, except that enstatite follows magnetite, wollastonite follows hematite, and orthoclase follows albite, only in the case of the medium grade ore.

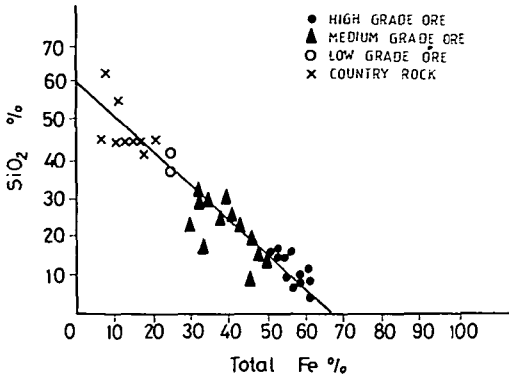

Fig. 1. Relationship between total iron and silica in ores of different grade

The total Fe content of the high grade ore (50 to 64.3% Fe), is almost similar t that of the economic iron ores of Egypt [BASTA *et al.*, 1969], and the Idsas pegmatiti and massive iron ores of Saudi Arabia [ABDELAZIZ, 1977].

The total Fe shows sharp negative relationship with SiO_2 *(Fig. 1)*. Such relation ship may indicate that the iron ores are mainly diluted by silicate minerals. The corre lation between the two oxidation states of iron is not that simple *(Fig. 2)*. The corre lation is antipathetic for the high grade ore, while it is remarkably proportional fo the medium and high grades, as well as the country rocks. This may indicate tha both Fe^{2+} and Fe^{3+} are mostly accommodated in one mineral form (i.e., magnetite in case of the country rocks and the medium and low grades. In case of the high grad ore, the Fe^{3+} state is predominant, and magnetite is not that preferable mineral form as a result of extensive martitization.

Titanium has a relatively low concentration in all the analysed samples (max 0.78% TiO_2). Ti^{4+} (0.68Å) has a close geochemical affinity to, and may proxy fo

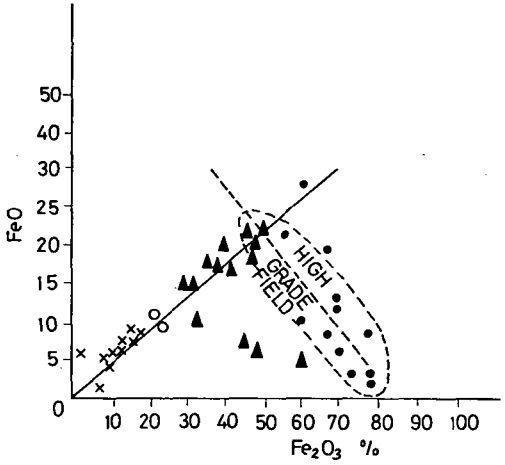

Fig. 2. Relationship between ferrous and ferric iron (denotation of grades is the same as in Fig. 1)

Fe^{3+} (0.67 Å). BASTA [1957] pointed out that a considerable amount of Ti can enter to the magnetite structure. Moreover, LISTER [1966] advocated for the opinion that the amount of Ti in magnetite is a rough estimate of the amount of ilmenite in the ilmenite-magnetite intergrowths. Buddington and LINDSLEY [1964] illustrated that the Ti content of magnetite co-existing with ilmenite can be used as a geological thermometer, the Ti content decreases with progressive crystallization, i.e., with decreasing temperature. Regarding the above opinion, the iron ores of Ankur may probably be formed at relatively low temperature.

8. Geochemistry of the Trace Elements:

The mutual abundance distribution of the average trace elements for the different grades of the studied ore *(Fig. 3)* illustrates that the contents of Ti, V, and Mn increase proportionally with iron. Opposite relationships are found for Co, Ni, Cu, Zn, Rb, Sr and Nb, where these elements are relatively enriched in the country rocks.

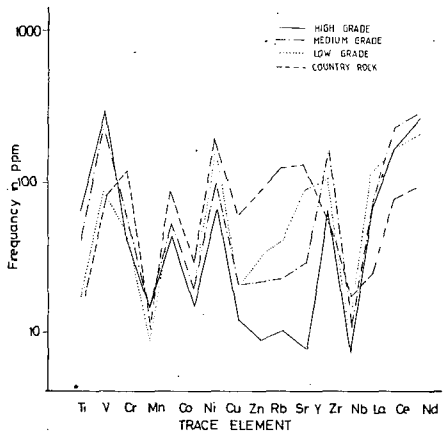

Fig. 3. Distribution of the average of minor elements in the ores of different grades of the Ankur iron ore deposits

The comparison between the obtained average trace elements of Ankur ores and the published averages of other iron ores showed that the heavy metals; V, Cr, Co, Ni, and Cu are much less than their contents in magnetite separated from the pegmatitic ore, magmatic segregation and lavas [ABDELAZIZ, 1977, CHIL-SUP SO, 1978; DUNCAN and TAYLOR, 1968]; But they show some similarities to the metamorphic magnetite deposits of Korea (CHIL-SUP SO, *op. cit*) and the remobilized sediments of Chile (FRUTOS and OYARZUM, 1975].

The following is, however, a brief discussion about some of the analysed trace elements which showed genetic or geochemical significances:

Vanadium: V^{3+} (0.74Å) may substitute for Fe^{3+} (0.67 Å) in magnetite or in the ilmenite-magnetite intergrowth. The titaniferous magnetite is richer in V compared to the pure magnetite [LANDGREEN, 1948]. The relationship between total Fe and V *(Fig. 4)*. favours the above assumption. The segregation of the high grade ore samples in a separate field below the main trend is most probably due to the fact mentioned before that magnetite is not the prevailed mineral form of the high grade ore. GIRGIS [1969]

and SHAALAN [1970] are also of the opinion that the content of V increases proportionally with the magnetite content of the rock. MASON [1966] believes that the early segregated magnetite is richer in V.

A quantitative measure of V in magnetite, called the vanadium module (=100 V/Fe in magnetite) was introduced by CARSTENS [1939], and followed by many authors, has been calculated for the studied ore. The average V module of the high, medium and low grades are found to be; 0.16, 0.10 and 0.05, respectively, and 0.10 for the country rocks. Such low values reflect, according to VASSJOKI and HEIKKINEN [1952] various effect of metamorphism.

Chromium: Cr^{3+} (0.64 Å) is known to substitute for Al^{3+} (0.56 Å) and Fe^{3+} (0.67 Å) of the iron-alumino-silicates (*e.g.*, spinels), or for Fe^{3+} in magnetite. The Cr content

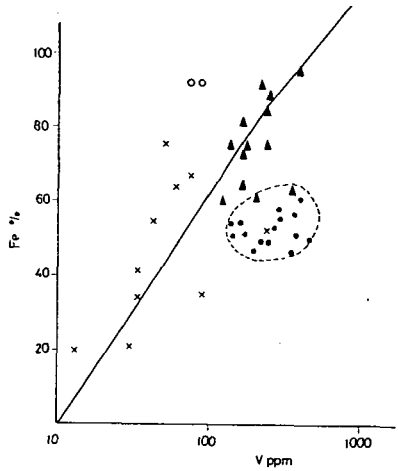

Fig. 4. Relationship between total iron and vanadium (denotation of grades is the same as in Fig. 1).

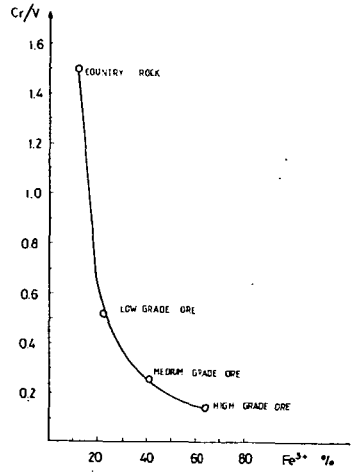

Fig. 5. Relationship between ferric iron and Cr/V ratio

of magnetite had been correlated to the genetic conditions by WAGER and MITCHEL [1951] and VINCENT and PHILIPS [1954]. They suggested that Cr is separated from the magma mainly during the earliest stage of the fractionation, and accordingly the earlier formed magnetites are richer in Cr. Moreover, TAYLOR [1965] gave the Cr/V ratio similar genetic value, where the ratio decreases as the fractionation temperature decreased.

In the present study the Cr content increases with decreasing of the iron content, and accordingly the highest Cr content is found for the country rocks. V behaves in an opposite manner. Therefore, the Cr/V ratio increases gradually as the Fe^{3+} content decreased *(Fig. 5)*.

The Cr/V ratio of the country rocks (mostly andesitic in composition) is more than 10 times higher than that of the high grade ore. The writers believe, however, that the differences in the Cr/V ratio are related to the mineralogical composition of the ore, and not genetic controls. The ratio increases towards the low grade ore and the country rocks due to the increase of the alumino-silicates, where Al^{3+} can be substituted by Cr, and also because of the decrease of Fe^{3+} which can easily be substituted by V^{3+}.

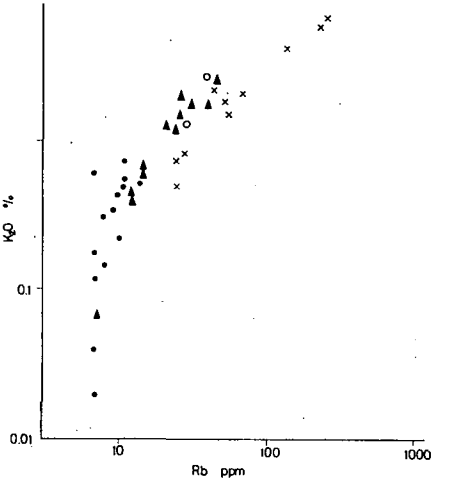

Fig. 6. Relationship between K_2O (in per cent) and Rb (in ppm)

The elements Co, Ni and Zn show tendency to follow Cr in the Ankur ores. Cu shows also some enrichment in the country rocks.

Rubidium: Rb^+ (1.47 Å) is preferentially incorporated in the "12 co-ordination" sites of K^+ (1.33 Å) in the K-bearing minerals. Strong positive correlation is found between Rb and K *(Fig. 6)* in the studied ore. Therefore, the content of Rb increases progressively in the country rocks, where the K-alumino-silicates are predominant.

Strontium: Sr content increases as the total Fe decreases. Y displays similar, but more gradual abundance distribution pattern like Sr *(Fig. 7)*. Sr shows no affinity to follow the Ca content or any Ca-bearing minerals (*e.g.*, anorthite or wollastonite). FAIRBRIDGE [1972] believes that a low level of coherence or the absence of it between Sr and Ca may suggests a degree of metamorphism that is not high enough to allow mass migration and equilibration of the Sr-Ca system. In the studied deposits, Sr (1.12 Å) is most probably entrapped in the alumino-silicate lattice in the K^+ (1.33 Å)

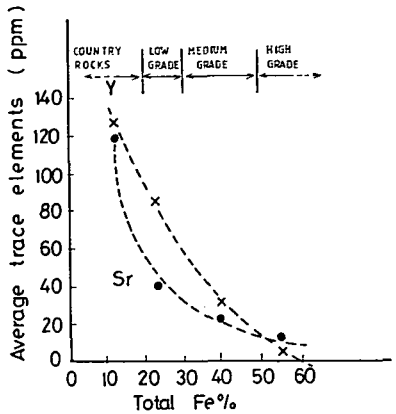

Fig. 7. Distribution of Sr and Y in the ores of different grades, Sr and Y content in ppm plotted *vs* total Fe content (in per cent)

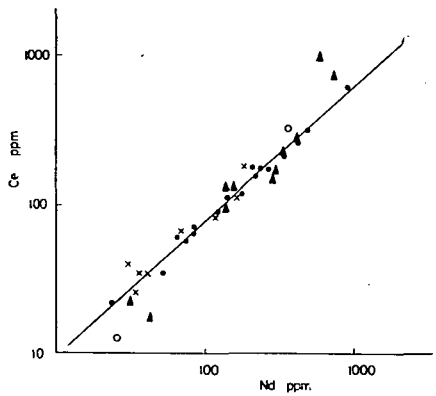

Fig. 8. Relationship between cerium and neodymium (denotation of grades as in Fig. 1.)

position. This indicated from the relative enrichment of Sr in the country rocks which contain most the alumino-silicates, and also from the sympathetic correlation between Sr and Al_2O_3.

Rare Earths: In the present work, three members of the rare earths (namely; La, Ce, and Nd, besides Y) were analysed. It is clear that La, Ce and Nd follow intimately each other (*Fig. 8).* Y is highly deviated from rare earths, and it shows some similarity to the behaviour of Sr and tends to concentrate in the country rocks as mentioned before. In agreement with FAIBRIDGE [1972]. Zr (0.79 Å) seems to be associated with the rare earths in the analysed samples.

The rare earths substitute for Ca^{2+} (0.99 Å) in the Ca bearing minerals (WEDEPOHL, 1972]. In the present study, Ca seems not to be responsible for the accumulation of the rare earths. They concentrate, however, in the high grade ore and deplate in the country rocks.

The highest concentrations of the analysed rare earths are 191 ppm La; 579 ppm Ce; and 909 ppm Nd. Such concentration magnitude may reflect an acidic composition of the primary deposits. Metamorphism has not influenced the composition of the rare earths [HASKIN, *et.al.,* 1966; SCHMIDT, *et al.,* 1963, 1964].

ACKNOWLEDGEMENT

The writers would like to thank PROF. DR. M. SHARKAWI, Geol. Dept., Cairo Univ., for his critical reading.

REFERENCES

BDELAZIZ, M. I. [1977]: Jebel Idsas iron ore. M. Sc. Thesis, Instit. App. Geol. King Abdelaziz Univ., Saudi Arabia.

BARTH, I. F. W. [1962]: Theoretical Petrology. Wiley, New York.

BASTA, E. Z. [1957]: Accurate determination of the cell dimensions of magnetite. Min. Mag., **31**, No. 237, pp. 431—442.

BASTA, E. Z. and GIRGIS, M. [1969]: Petrographical, mineralogical and geochemical studies on the magnetite-ilmenite-apatite ore (Nelsonits) from Kolmnab, South Eastern Desert, Egypt, Acad. Sci., **22**, pp. 145—157.

BUDDINGTON, A. F. and LINDSLEY, D. H. [1964]: Iron-titanium oxide minerals and synthetic equivalents. Jour. Pet., No. **2**, pp. 310—357.

CARSTENS, C. W. [1939]: Om titanholdige Jernmalmer. Norsk Geol. Tidskrift **19**.

CHIL-SUP So [1978]: Geochemistry and origin of amphibolite and magnetits from Yanyang iron deposit in the Gyeonggi metamorphic complex. Republic of Korea. Mineralium Deposita, **13**, No. 1, pp. 105—118.

DUNCAN, A. R. and TAYLOR, S. R. [1968]: Trace element analysis of magnetites from andesitic and dacitic lavas from Bay of Plenty, New Zealand, Contr. Mineral. Petrol., **29**, pp. 30—33.

EASTON, A. J. [1972]: Chemical Analysis of Silicate Rocks. Elsevier Pub. Comp., London.

FAIRBRIDGE, R. W. [1972]: The Encyclopedia of Geochemistry and Environmental Sciences, IV A. Van Nostrand Reinhold Company, New York, Toronto, London.

FRUTOS, J. J. and OYARZUM, J. M. [1975]: Tectonic and geochemical evidence concerning the genesis of El-Laco magnetite lava flow deposits, Chile. Econ. Geol., **70**, pp. 988—990.

GIRGIS, M. W. [1969]: Mineralogical studies on some titaniferous iron ores, South-Eastern Desert, Egypt. M. Sc. Thesis, Cairo University.

HASKIN L. A., WILDEMAN, T. R., FREY, F. A., COLLINS, K. A. KEEDY, C. R. and HASKIN, M. A. [1966]: Rare earths in sediments, J. Geophys. Res., **71**, pp. 6091—6105.

HUTCHISON, C. S. and JEACOCKE, J. E. [1971]: FORTRAN IV Computer programme for calculation of the Niggli Molecular Norm. Geol. Soc. Malaysia, Bull. **4**, 91—95.

LANDGREEN, S. [1948]: On the geochemistry of Swedish iron ores and associated rocks. Sveriges Geol. Undersig. **C 496**, p. 182.

LISTER, G. F. [1966]: The composition and origin of selected iron titanium deposits. Econ. Geol., **61**, pp. 275—310.

MASON, B. [1966]: Principles of Geochemistry, New York.

NORRISH, K. and CHAPPELL, S. W. [1966]: In: Physical Methods in Determinative Mineralogy. J. Zussman (ed), Acad. Press, pp 161—214.

SCHMITT, R. A., LASCH, J. E., MOSEN, A. W., OLEHY, D. A. and VASILEVOSKIS, J. [1963]: Abundance of the 14 rare earth elements, scandium and yttrium in meteoritic and terrestrial matter. Geochim. Cosmochim. Acta **27**, pp. 577—622.

SCHMITT, R. A. and OLEHY, D. A. [1964]: Rare earths, yttrium and scandium abundance in meteoritic and terrestrial matter, II. Geochim. Cosmochim. Acta **28**, pp. 67—86.

SHAOLAN, M. M. B.: [1970] Mineralogy of the iron titanium oxide minerals and their distribution in some volcanic rocks of Yemen and Aden. M. Sc. Thesis, Faculty of Science, Cairo Univ., Egypt.

TAYLOR, S. R. [1965]: The application of trace elements data to problems in petrology. In: Physics and Geochemistry of Earth, Pergamon Press, Oxford, **6**, pp. 133—213.

VAASJOKI, O. and HEIKKINEN, A. [1962]: On the significance of some textures and compositional properties of the magnetite of titaniferous iron ores. Bull. Comm. Geol. Finland, **34**, pp. 141—159.

VINCENT, E. A. and PHILLIPS, R. [1954]: Iron-titanium oxide minerals in layered gabbros of Skaergaard intrusion. East Greenland. Geochim. Cosmochim. Acta **6**, pp. 1—26.

WAGER, L. R. and MITCHEL, R. L. [1951]: The distribution of trace elements during strong fractionation of basic magma, a further study of the Skaergaard intrusion, East Greenland. Geochim. Cosmochim. Acta 1, pp. 129—208.
WEDEPOHL. K. H. [1972] Handbook of Geochemistry. Springer Verlag, Berlin, Heidelberg, New York.

Manuscript received, May 10, 1981

A. M. EL-KAMMAR
M. B. SHAALAN
Geol. Dept., Faculty of Science
Cairo Univ. Cairo, Egypt
and
H. M. OSMAN
Geol. Surv. Dept., Khartoum,
Sudan

CONTENTS

Felelős kiadó: Grasselly Gyula

Készült: monószedéssel, íves magasnyomással, 11,2 A/5 ív terjedelemben, az MSZ 5601—59 és 5602—55 szabvány szerint

Példányszám: 625

82-3181 — Szegedi Nyomda — Felelős vezető: Dobó József igazgató